İSTANBUL TECHNICAL UNIVERSITY ★ INSTITUTE OF SCIENCE AND TECHNOLOGY

THE EFFECTS OF DIFFERENT PRETREATMENTS ON DRYING RATE AND COLOR KINETICS OF CONVECTIVE AND MICROWAVE ASSISTED CONVECTIVE DRYING OF THOMPSON SEEDLESS GRAPES

Ph.D. Thesis by

Gökhan BİNGÖL, M.Sc.

(506012136)

Date of submission : 3 December 2007

Date of defence examination: 14 February 2008

Supervisor (Chairman): Prof. Dr. Y. Onur DEVRES

Members of the Examining Committee Prof.Dr. E. Özgül EVRANUZ (İ.T.Ü.)

Prof.Dr. Taner DERBENTLİ (İ.T.Ü.)

Prof.Dr. Mehmet DEMİRCİ (N.K.Ü.)

Assist. Prof.Dr. Ahmet KÜÇÜKÇETİN (A.Ü.)

FEBRUARY 2008

İSTANBUL TEKNİK ÜNİVERSİTESİ ★ FEN BİLİMLERİ ENSTİTÜSÜ

FARKLI ÖNİŞLEMLERİN THOMPSON ÇEKİRDEKSİZ ÜZÜMLERİNİN MİKRODALGA YARDIMLI KONVEKTİF VE YALNIZ KONVEKTİF KURUTULMASI SIRASINDA KURUTMA VE RENK KİNETİĞİ ÜZERİNE OLAN ETKİLERİNİN İNCELENMESİ

DOKTORA TEZİ

Y. Müh. Gökhan BİNGÖL
(506012136)

Tezin Enstitüye Verildiği Tarih : 3 Aralık 2007
Tezin Savunulduğu Tarih : 14 Şubat 2008

Tez Danışmanı : Prof. Dr. Y. Onur DEVRES
Diğer Jüri Üyeleri Prof.Dr. E. Özgül EVRANUZ (İ.T.Ü.)
Prof.Dr. Taner DERBENTLİ (İ.T.Ü.)
Prof.Dr. Mehmet DEMİRCİ (N.K.Ü.)
Yard. Doç.Dr. Ahmet KÜÇÜKÇETİN (A.Ü.)

ŞUBAT 2008

FOREWORD

Grapes are among the important export products of Turkey which not only take long time to dry into raisins but also get dark brownish final produce color. The purpose of this study was to evaluate the effects of several pretreatment methods and microwave assistance on drying rates and color kinetics of grapes. I hope this study will shed bright light on drying of grapes and contribute to Drying Technologies, which is an important part of Food Engineering Unit Operations in both academia and industry.

This thesis was a product of long and intensive study which, with regard to experimental investigation, was for the most part realized in United States of America. The long journey set out with the 5 months scholarship that was awarded by the Rectorate of Istanbul Technical University, Prof. Dr. Gülsün Sağlamer, to whom I am indebted many thanks. I would like to express my special thanks and sincere appreciation to Prof. Dr. Murat O. Balaban, who not only helped me to shape my dissertation, but also contributed to it in many ways. It was another milestone to meet Assist. Prof. John S. Roberts in Cornell University, who then moved to United States Department of Agriculture, under whose tutelage I had the chance to work on microwave technologies.

It is my privilege to express my special thanks and gratitude to my supervisor and mentor, with whom I worked with for many years and who helped me in countless ways to bring me up in the scientific realm, to Prof. Dr. Y. Onur Devres with whom the idea of drying had sparked and kindled into a struggle-driven thesis from which I appreciated the immense vastness of science and engineering. Many thanks to Prof. Dr. E. Ozgul Evranuz and Prof. Dr. Taner Derbentli with whom it was pleasure to work with and benefit from both the contributions and constructive concrete criticisms that helped to form this study.

I would like to thank to Ufuk Kındap, Canan Balaban, Yavuz Yagiz, Dr. Mustafa Can Ozturk, Ann Theodore Ballastris, Dr. Zhongli Pan, Dr. Tara McHugh, Dr. Roberto de Jesus Avena-Bustillos, Delilah Wood and Don Olson who helped me in various ways in realizing this study.

I would like to express my special thanks to my family who supported me patiently during this long-journey and give this thesis as a gift to my mother, who passed away in the year 2000, who would be proud of me for realizing this study.

November, 2007 **Gökhan BİNGÖL, M.Sc.**

CONTENTS

ABBREVIATIONS

a : Constant Equation (3.12) and Table 2.2
a_1 : Constant, (h^{-1}), in Wang and Singh Equation
a* : Chromatic Component Ranging from Green to Red
b_1 : Constant, (h^{-2}), in Wang and Singh Equation
b* : Chromatic Component Ranging from Blue to Yellow
BSMD : Bulk Scale Microwave Drying
c : Constant Equation (3.12) and Table 2.2
c_0 : Wave Velocity in Free Space, 3.0×10^8 (m/s)
C : Specific Heat of Material (J/kg°C)
C_0 : Initial Color Quantity
C_f : Final Color Quantity
CFT : Curve Fitting Tool
CIE : Comission Internationale d'Eclairage
CPR : Constant Power Ratio
D_0 : Reference Diffusion Coefficient (m^2/s)
d.b. : Dry Basis
D_{eff} : Effective Diffusivity (m^2/s)
df : Degrees of Freedom
div : Divergence of a Function
D_p : Penetration Depth (m)
E : Electric Field (V/m)
E_a : Activation Energy (kJ/mol)
E_{max} : Maximum Value of Electric Field (V/m)
E_{rms} : Root Mean Square Value of Electric Field
EPA : Environmental Protection Agency
f : Frequency (Hz) in Equation (2.6), constant in Equation (3.12)
grad : Gradient of a Function
h : Planck's Constant, 6.625×10^{-34} (J·s) in Equation (2.6), convective heat transfer coefficient ($W/m^2 \cdot °C$) elsewhere
H : Magnetic Field (A/m)
HHP : High Hydrostatic Pressure
IPR : Initial Power Ratio
k : Drying Constant (h^{-1}) in Table 2.2, Heat Conduction Coefficient in Equation (4.2)
k_1 : Drying Constant (h^{-1})
k_c : Color Constant (h^{-1})
L* : Lightness Component
M : Time Dependent Bulk Moisture Content (d.b.)
M_0 : Initial Moisture Ratio (d.b.)
M_{eq} : Equilibrium Moisture Content (d.b.)
MR : Unaccomplished Moisture Ratio (d.b.)
NBS : United States Department of Commerce's National Bureau Standards
P_{abs} : Absorbed Power (W)

PID : Proportional-Integral-Derivative Control
PPO : Polyphenol Oxidase
POTAS : Technical Potassium Carbonate
Rg : Universal Gas Constant (kJ/mol·K)
RMSE : Root Mean Square Error
SAR : Specific Absorption Rate
SEM : Scanning Electron Microscopy
SSE : Sum of Squares Due to Error
SSMD : Small Scale Microwave Drying
USB : Universal Serial Bus
w.b. : Wet Basis

TABLE LIST

FIGURE LIST

SYMBOL LIST

α : Attenuation Factor (Np/m) in Equation (2.10), Thermal Diffusivity (m^2/s) elsewhere
β_n : Bessel Function Roots of the First Kind and Zero Order
ΔE : Total Color Change
Δh_v : Specific Heat of Evaporation (J/kg)
ε : Complex Dielectric Constant
ε' : Relative Dielectric Constant
ε'' : Relative Dielectric Loss Factor
λ_0 : Free Space Wavelength (m)
π : PI Number, 3.14159265
δ : Dielectric Loss Angle
ρ : Density (kg/m^3)
μ : Permeability (W/A·m) only in Section 2.6.2.2, Viscosity (kg/m·s) elsewhere
μ_0 : Magnetic Permeability of Free Space, $4\pi\times10^{-7}$ (W/A·m)

THE EFFECTS OF DIFFERENT PRETREATMENTS ON DRYING RATE AND COLOR KINETICS OF CONVECTIVE AND MICROWAVE ASSISTED CONVECTIVE DRYING OF THOMPSON SEEDLESS GRAPES

SUMMARY

Grapes are important export product of Turkey and darken during drying due to the enzyme Polyphenol Oxidase (PPO). To prevent browning reactions, grapes are sulfited. Ingestion of sulfites can lead to asthmatic attacks, rashes and abdominal upset especially for elderly people and children. For these reasons in USA sulfites are either prohibited or subject to very low limit restrictions.

In this study, grapes were pressurized with high hydrostatic pressure, dipped into ethyl oleate and potassium carbonate solutions at different dipping times and dipping temperatures and blanched with steam at different temperatures. The aims of these pretreatments were to accelerate drying rate and to inactivate PPO without the use of sulphur dioxide. Pretreated grapes were dehydrated either in a convective dryer or in a microwave-assisted convective dryer.

It is known that pressures higher than 100 MPa causes irreversible cell permeabilization. Grapes were pressurized to 300 and 600 MPa for 10, 20 and 30 minutes in a High Hydrostatic Pressure vessel in order to both accelerate drying rate and inactivate grape PPO. It was observed that pressurization resulted in 1.5 to 3.4% moisture loss of grapes. The drying rate of pressurized grapes slightly increased compared to control. All of the applied thin-layer equations described the drying curves with an R^2 (regression coefficient) greater than 0.99, and RMSE (Root Mean Square Error) and SSE (Sum of Squares of Error) values smaller than 0.01. During drying shrinkage of pressurized grapes was linearly proportional with moisture content. Pressure treated grapes had higher effective diffusivity values than control. Pressurization increased the L*-values of grapes. It was observed that, even at ambient conditions browning took place after 2 hours. This clearly showed that pressurization at 600 MPa for 30 minutes did not inactive grape PPO on the contrary, 300 and 600 MPa pressurization activated PPO, which in turn accelearated browning reactions.

Heat is well known to inactivate enzymes or kill microorganisms. A simulation program was run to calculate 2-log inactivation time for PPO from the experimental temperature and time profiles of steam blanched of grapes. It was found that blanching grapes with steam at 80°, 90° and 100°C for 270, 140 and 90 seconds, respectively, would result in 2-log inactivation of grape PPO, which resides in the skin. It was observed that the center temperatures of 100°C and 90 seconds steam blanched grapes were the lowest, whereas the temperatures of nodes 1.1 mm from the skin were the highest, compared to 80° and 90°C steam blanching. All thin-layer

equations, except Wang and Singh, described the drying curves with an R^2 of 0.99, SSE and RMSE were close to zero, for all steam temperatures. The decrease in view area, thus the volume reduction, was linear with moisture content. If the maximum effective diffusivities were compared, values of steam blanched grapes were 320 times higher than that of control. Steam blanching had negligible effect on L*-value of grapes. Final color of steam blanched grapes was moderate yellowish brown.

Dipping in ethyl oleate emulsions is widely used for grape drying which both increases the drying rate and improves the final color quality of the raisins. Grapes were pretreated with 2% (volume/volume) ethyl oleate and 5% (mass/volume) potassium carbonate at 30°, 40°, 50° and 60°C for 1, 2 and 3 minutes. It was observed that at 30° and 40°C there was negligible difference between the drying rates of 1 and 2 minutes dipping time, whereas in 50° and 60°C this was between 2 and 3 minutes dipping time. It was found that as the temperature of the dipping solution increased the drying rate also increased and at all dipping temperatures the drying rates were greater than control. Midilli equation best described the thin-layer convective air drying of grapes where R^2 was greater than 0.99, SSE and RMSE values were smaller than 0.001 and 0.002, respectively, for all experiments. At 30° and 40°C dipping temperatures the volume reduction was linear with moisture content, whereas at 50° and 60°C this relationship was exponential. It was observed that at 30°, 40°, 50° and 60°C dipping temperature and 2 minutes dipping time hue values and L*-values of grapes dropped from 100° and 80 to 60° and 40, respectively, which would be perceived as brown raisins.

Grapes were also dried with an average air velocity of 1.8 m/s in a convective air dryer. It was found that 50°C air temperature drying of untreated grapes took 92.5 hours, whereas drying time was reduced to 37 hours at 60°C and to 17 hours at 70°C. However, the visual quality of raisins produced at 70°C air temperature was not satisfactory. Increasing the air temperature from 50° to 60°C halved the drying time of 40°C and 3 minutes dipped grapes and reduced the drying time of grapes that were blanched at 90°C steam temperature to one-third. There was no difference in drying time of peeled grapes at 50° and 60°C air temperatures.

Untreated grapes were dried in a microwave-assisted convective dryer at 1, 0.5 and 0.25 W/g initial or constant microwave power ratios with air velocity higher than 1.5 m/s and temperature at 60°C. Also blanched and chemically dipped grapes were microwave assisted dried at 0.25 W/g microwave power ratio. It was seen that at 0.25 W/g microwave power ratio there was no significant difference between the drying rates of dipped and untreated grapes, however the difference was considerable for steam blanched grapes. Microwave-assisted isothermal convective drying of grapes at 70°C took 7 hours, which is much shorter than the convective air drying which took 17 hours. Thin-layer modeling of microwave-assisted convective drying of grapes could be best described with Logarithmic equation. Applied microwave-power ratio did not significantly affected the L*,a*, b* values of raisins. In terms of color, it was visually observed that microwave-assisted convective drying of grapes resulted in better raisins than convective drying.

Mathematical modeling and simulation of temperature profiles of convective and microwave-assisted convective drying of untreated grapes, convective drying of steam blanched grapes and steam heating of grapes were performed by Matlab software. Except 90° and 100°C steam heating of grapes, all mathematical models were in good agreement with experimental data.

The pretreatment method's and drying technique's parameters had significant effect on the final color of raisins. Thus for a good quality end-product the parameters should be adjusted carefully according to physical properties of the raw material.

FARKLI ÖNİŞLEMLERİN THOMPSON ÇEKİRDEKSİZ ÜZÜMLERİNİN MİKRODALGA YARDIMLI KONVEKTİF VE YALNIZ KONVEKTİF KURUTULMASI SIRASINDA KURUTMA VE RENK KİNETİĞİ ÜZERİNE OLAN ETKİLERİNİN İNCELENMESİ

ÖZET

Türkiye'nin önemli ihraç ürünleri arasında olan üzüm, içeriğinde doğal olarak bulunan Polifenol Oksidaz (PPO) enziminden dolayı kuruma esnasında esmerleşmektedir. Üzümler, esmerleşme reaksiyonlarının önlenebilmesi amacıyla kükürtle muamele edilmektedirler. Kükürt, yaşlı ve çocuklarda astım krizleri, isilikler ve mide rahatsızlıkları gibi hastalıklara neden olabilmektedir. Bundan dolayı Amerika Birleşik Devletlerinde kükürt kullanımı ya yasaklanmış ya da kullanımına çok düşük oranlarda izin verilmektedir.

Bu çalışmada, üzümler i) yüksek basınç cihazı ile sıkıştırılmış, ii) farklı sıcaklıklarda etil oleat ve potasyum karbonat içeren çözeltiye farklı sürelerde daldırılmış ve iii) farklı sıcaklıklardaki su buharına farklı sürelerde maruz bırakılmışlardır. Yapılan önişlemlerin amacı hem kuruma hızını arttırmak hem de PPO enzimini kükürt kullanmadan inaktive ederek esmerleşme reaksiyonlarını engellemektir. Önişlemi takiben üzümler ya konvektif bir kurutucuda ya da mikrodalga yardımlı konvektif kurutucuda kurutulmuşlardır.

100 MPa ve üzerindeki basınçların hücrelerde tersinir olmayan geçirgenliğe neden olduğu bilinmektedir. Üzümler, 300 ve 600 MPa basınçta, kuruma hızını arttırmak ve PPO enzimini inaktive edebilmek amacıyla, yüksek hidrostatik basınç cihazında 10, 20 ve 30 dakika süre ile sıkıştırılmışlardır. Hidrostatik basınç ile sıkıştırma işleminin, üzümlerde %1.5'den %3.4'e varan oranlarda nem kaybına neden olduğu gözlenmiştir. Hidrostatik basınç ile sıkıştırılmış üzümlerin kuruma hızları önişleme tabi tutulmayan (kontrol) üzümler ile kıyaslandığında düşük miktarlarda artmıştır. Uygulanan tüm ince tabaka modelleri kuruma eğrilerini 0.99'dan daha büyük R^2 (regresyon katsayısı) ve 0.01'den küçük RMSE (Hataların karesinin ortalama karekökü) ve SSE (Hataların karesinin toplamı) ile tanımlamıştır. Sıkıştırılmış üzümlerin hacim azalmasının nem kaybı ile doğru orantılı olarak gerçekleştiği gözlenmiştir. Hidrostatik basınç ile muamele edilen üzümlerin efektif difüzivite değerleri kontrol örneklerinden daha yüksek çıkmıştır. Sıkıştırma işlemi üzümlerin L* değerini arttırmıştır. Ancak sıkıştırılmış üzümlerin ortam koşullarında bile, 2 saat sonra esmerleştiği gözlenmiştir. Bu ise açıkça, üzümdeki PPO enziminin 300 ve 600 MPa basınçlarda inaktive olmadığını, aksine belirtilen basınç değerlerinde PPO enziminin aktive olduğunu ve kararma reaksiyonlarını daha da hızlandırdığını göstermektedir.

Isı uygulamasının enzimleri inaktive ettiği ve mikroorganizmaları yok ettiği bilinmektedir. Bir simülasyon programı aracılığıyla buharla haşlamadan elde edilen

deneysel sıcaklık ve zaman değerleri kullanılarak, üzümdeki PPO enziminin 2-log inaktivasyon süresi hesaplanmıştır. Üzümün kabuğunda bulunan PPO enziminin 80°C'de 270 saniyede, 90°C'de 140 saniyede ve 100°C'de 90 saniyede 2-log inaktive edildiği hesaplanmıştır. Deneysel ve hesaplanan sıcaklık değerlerinden, 100°C'deki buhar uygulaması ile üzümün merkez sıcaklığının diğer sıcaklık ve sürelerdeki buhar uygulamalarına göre daha düşük, buna karşın yüzeyden 1.1 mm uzaklıkta seçilen düğüm noktasının ise daha yüksek sıcaklıkta olduğu gözlenmiştir. Wang ve Singh eşitliği dışındaki tüm ince tabaka modelleri, farklı sıcaklıklardaki buhar ile önişlenmiş üzümün kuruma eğrilerini 0.99'dan daha yüksek R^2 ve sıfıra yakın SSE ve RMSE değerleri ile tanımlamıştır. Üzümlerin görüntü alanı, dolayısıyla hacimlerinin, nem kaybı ile doğru orantılı olarak azaldığı gözlenmiştir. Buhar ile önişlem gören üzümlerin maksimum noktadaki efektif difüzivite değeri kontrolden 320 kat daha yüksek çıkmıştır. Buhar ile haşlamanın üzümlerin L* değeri üzerinde ihmal edilebilir bir etkisi vardır. Buhar ile muamele edildikten sonra kurutulan üzümlerin sarımsı bir son renge sahip olduğu görülmüştür.

Üzümleri, hem kuruma hızını arttırmak hem de son ürün renk değerini iyileştirmek amacıyla, etil oleat ve potasyum karbonat çözeltisine daldırdıktan sonra kurutmak sıkça uygulanan bir işlemdir. Bu çalışmada üzümler, 30°, 40°, 50° ve 60°C sıcaklıkta hacimsel olarak %2 etil oleat ve %5 potasyum karbonat (kütle/hacim) içeren çözeltiye, 1, 2 ve 3 dakika süreyle daldırılmışlardır. 30° ve 40°C sıcaklıktaki çözeltiye 1 ve 2 dakika daldırmanın; 50° ve 60°C sıcaklıktaki çözeltiye ise 2 ve 3 dakika daldırmanın kuruma hızı üzerindeki etkisinin aynı olduğu gözlenmiştir. Farklı sıcaklıklardaki çözeltiye farklı sürelerde daldırılan üzümlerin kuruma hızının kontrole göre belirgin miktarda arttığı görülmüş ve çözelti sıcaklığı arttıkça kuruma hızının da arttığı gözlemlenmiştir. Midilli eşitliği, farklı sıcaklıktaki çözeltilere farklı sürelerde daldırılan üzümlerin kuruma eğrilerini 0.99'dan daha yüksek R^2 ve 0.001'den daha düşük SSE ve 0.002'den daha düşük RMSE değerleri ile tanımlamıştır. 30° ve 40°C sıcaklıktaki çözeltiye daldırılan üzümlerin hacim azalması nem kaybı ile doğrusal olurken, 50° ve 60°C sıcaklıktaki çözeltiye daldırılan üzümlerin hacim azalması ile nem kaybı arasındaki ilişki üstel ("eksponansiyel") çıkmıştır. 30°, 40°, 50° ve 60°C sıcaklıktaki çözeltilere 2 dakika süre ile daldırılan üzümlerin L* ve "hue" renk değerleri sırasıyla 80 ve 100°'den kuruma sonunda 40 ve 60°'ye düştüğünden, kuru üzümler kahverengi olarak algılanmaktadır.

Üzümler ayrıca ortalama hava hızı 1.8 m/s olan konvektif bir kurutucuda da kurutulmuşlardır. 50°C hava sıcaklığında, önişleme tabi tutulmayan üzümler, 92.5 saatte kururken bu süre 60°C'de 37 saate ve 70°C'de ise 17 saate inmiştir. Fakat 70°C'de kurutulan üzümlerin görsel kalitesi tatmin edici bulunmamıştır. Hava sıcaklığını 50°C'den 60°C'ye arttırmak, 40°C sıcaklığındaki çözeltiye 3 dakika süreyle daldırılan üzümlerin kuruma süresini yarıya, 90°C sıcaklıktaki buhar ile haşlanmış üzümlerin kuruma süresini ise üçte birine indirmiş fakat kabuğu soyulan üzümlerin kuruma sürelerinde bir fark gözlenmemiştir.

Önişleme tabi tutulmayan üzümler, mikrodalga yardımlı konvektif kurutucuda 1.5 m/s'den yüksek ortalama hava hızı ve 60°C hava sıcaklığında, 1, 0.5 ve 0.25 W/g oranında başlangıç ve sabit mikrodalga güç verilerek kurutulmuşlardır. Ayrıca buharla haşlanmış veya kimyasal çözeltiye daldırılmış üzümler, başlangıç 0.25 W/g oranında mikrodalga güç uygulanarak konvektif kurutucuda kurutulmuşlardır. 0.25 W/g oranındaki başlangıç mikrodalga gücü uygulanarak konvektif kurutulan önişleme tabi tutulmamış ve çözeltiye daldırılmış üzümlerin kuruma hızında belirgin

bir fark olmazken, buhar ile haşlanmış üzümlerin kuruma hızında önemli bir artış görülmüştür. Üzümlerin 70°C'de mikrodalga yardımlı konvektif izotermal kurutulması 7 saat sürerken, 70°C yalnız konvektif kurutulması 17 saat sürmüştür. Üzümlerin mikrodalga yardımlı konvektif kurutulması sırasındaki kuruma eğrileri Logaritmik eşitlik ile en iyi şekilde tanımlanabilmektedir. Uygulanan mikrodalga güç oranı üzümlerin L*, a* ve b* değerlerinde belirgin bir fark oluşturmamıştır. Renk kalitesi açısından mikrodalga yardımlı konvektif olarak kurutulan üzümlerden, yalnız konvektif olarak kurutulan üzümlere göre daha iyi son ürün elde edilmiştir.

Mikrodalga yardımlı konvektif veya sadece hava ile kurutulan önişleme tabi tutulmamış üzümlerin kurutulması sırasındaki; ayrıca buhar ile ön haşlanarak konvektif olarak kurutulan üzümlerin, kuruma ve haşlama esnasındaki sıcaklık profilleri matematiksel olarak modellenmiş ve Matlab yazılımı kullanılarak simüle edilmiştir. 90° ve 100°C'deki buhar ile haşlanan üzümler hariç, diğer tüm matematiksel modeller, deneysel veriler ile uyum içinde çıkmıştır.

Önişleme ve kurutma tekniğinin kuru üzüm kalitesi üzerinde önemli bir etkisi vardır. İyi bir kalitede son ürün elde edebilmek için hammaddenin özelliklerine göre, önişleme ve kurutma yönteminin parametreleri dikkatli bir şekilde seçilmelidir.

1. INTRODUCTION

Drying of fruits and vegetables is one of the most time consuming and energy intensive processes in the modern food industry. For accelerating the drying process in order to reduce the processing time, a number of complications must be overcome. The main problem in drying of grapes is the skin which impedes water transport from the interior to its surface, decreasing the drying rate. A number of pretreatments can be applied either to grape skin or to the interior of grape prior to drying for either accelerating the drying process or improving the final quality of the dried produce.

Grabowski and Marcotte (2003) divided all pretreatments into two main groups: chemical (inorganic and organic) and non-chemical (heating, blanching, freezing, etc.). According to the authors, the main advantages of pretreatments are reduction in drying time, denaturation or inactivation of surface enzymes, removal of intracellular air and softening of texture.

The main problem in grape drying has been slow drying rate due to waxy layer at skin and the browning reactions that took place due to polyphenol oxidase (PPO) enzyme. Sulphuration is the most common commercially applicable method for preventing enzymatic and non-enzymatic browning and also microbial activity. However sulphites can cause asthmatic attacks, rashes and abdominal upset in sensitive individuals (Karabulut et al., 2007; Warner et al., 2000). Hence, grape drying should facilitate from pretreatment methods either by removal of waxy layer or by inactivation of PPO or by both ways. Also the drying method should not cause any undesirable physical, chemical and microbiological changes that can affect the desired final quality of raisins.

In Turkey, pretreatment method of grapes prior to drying has been to dip into a mixture of 5% (w/w) POTAS (technical potassium carbonate) and 0.5-0.7% (v/v) olive oil. There has been no predefined dipping time and the dipping is performed by immersing grapes into solution and then taking out. This procedure is repeated for 10 to 12 times. It is reported that the raisins produced in this way obtains yellow color (Kismali and Altindisli, 2007). Currently, there is no report of other pretreatment

applications such as steam blanching or application of high hydrostatic pressure prior to grape drying.

In Turkey, drying of grapes has been accomplished mainly by sun drying and to a lesser extent by convective drying. Sun drying of grapes has been performed by spreading grapes onto concrete slabs covered with paper, fine canvas or a similar material (Petrucci and Clary, 2002). Sun drying is strongly dependent on weather conditions and the product may suffer from overheating, insect infestations or contamination from the environment.

In convective drying heated air acts as the heat and moisture carrier and drying takes place in the falling rate period where the drying rate is controlled by diffusion of water from interior of the product to the surface. The drying rate is higher at the beginning of drying and gradually falls as the evaporation front recedes resulting in a longer drying time. The temperature is the highest at the surface and lowers to the interior. The drying process relies solely on conduction of heat from the surface to the interior which may result in case hardening of grapes. Apart from reduced final raisin quality, hot air drying suffers from high-energy consumption due to lengthy drying times and inefficient heat transfer mechanism.

Microwave-assisted drying of fruits and vegetables has drawn considerable attention due to high mass transfer coefficients and occasionally better end-product quality. In microwave, the volumetric heat generation in moist samples due to directly absorbed electromagnetic energy by the water molecules, results in higher interior temperature and thus the water removal rate is faster than convective drying (Sanga et al., 2002).

In the literature, currently there are two different ways of using microwave energy to produce raisins: (1) application of microwave energy throughout drying (Tulasidas, 1995) and (2) application of microwave as a pretreatment method (Dev et al., 2007). Both authors reported that good quality raisins in terms of color could be obtained by these ways of application. Moreover, it is reported that microwave pretreated grapes had superior appearance and market quality than untreated grapes. Tulasidas et al., (1995) reported that grapes that were not sulfated and dried by microwave-assisted drying had color quality comparable to that of sulfated grapes.

In this study prior to drying, as a chemical pretreatment grapes were dipped into ethyl oleate/potassium carbonate mixture and as a non-chemical pretreatment grapes

were steam blanched or pressurized with high hydrostatic pressure. After the pretreatments drying was carried out either in a convective air dryer or in a microwave-assisted convective dryer. Drying curves were described by thin-layer equations and effective diffusivity values during drying were calculated. Color kinetics of grapes that were pretreated and then convective dried were calculated and final color values of microwave-assisted convective dried grapes were obtained. Temperature profiles during convective drying and microwave-assisted convective drying were obtained and were mathematically modeled and simulated.

2. LITERATURE REVIEW

2.1 Raisin Outlook

Grapes are one of the fruit crops most widely (8,026,000 tonnes) grown throughout the world (Baydar et al., 2004). There are two basic types of grapes, American and European (Anon., 2005a). Table grapes are derived from a single European species, *Vitis vinifera*. Thompson Seedless grapes, bred especially for raisins (Anon., 2005b), are oval, amber green and are the most popular fresh variety grown in the United States (Anon., 2005a). Approximately 15.5% of the weight of Thompson seedless grapes is sugars which is composed of 46% of glucose and 52% of fructose. Grapes have 0.18% fat which can be neglected. A serving size of grape (151 g) can meet the 27 and 28% of daily value of Vitamins C and K therefore grapes can be regarded as a good source of Vitamins C and K (Anon., 2005c). Their water activity is around 0.98 and moisture content is around 82% (w.b.).

Figure 2.1: Thompson Seedless Grapes (adapted from www.sinnettsmp.com)

The domestic equivalent for Thompson seedless grapes is "Sultani çekirdeksiz" which is the same variety grown in California. In Turkey, "Sultani çekirdeksiz" is known as a variation of "Yuvarlak çekirdeksiz" and is acknowledged as the best known and extensively grown variety for raisin production in the world (Petrucci and Clary, 2002).

Seedless grapes are harvested between August and September in northern hemisphere and between March and April in southern hemisphere (Ozden, 2007).

The primary areas for raisin production in Turkey are the provinces of Izmir, Manisa and Denizli in Aegean region and to a lesser extent in the southeastern Anatolia, eastern Anatolia and Mediterranean region (Petrucci and Clary, 2002). Generally, grapes are harvested when their Brix content reach around 23 °Bx. By this way, approximately 26 kg raisins can be obtained from 100 kg of grapes (Kismali and Altindisli, 2007).

There are two terms used interchangeably to refer to dried grapes: raisins and sultanas. Raisins generally refer to the natural sun-dried product of California Thompson Seedless grapes or Australia Muscat Gordo Blanco and Waltham Cross grapes, and sultanas refer to the product treated with various dipping solutions and then dried (Petrucci and Clary, 2002). Since the delightfulness of the raisins produced worth eating of Ottoman Sultans, the raisins were given the name "sultana" (Ozden, 2007) which is a type of white, seedless grape of Turkish origin and also the name given to the raisin made from it. Sultana raisins are often called simply sultanas or sultanis and are smaller than raisins (Anon., 2007a).

Grapes are grown on six continents in 62 different countries, with a total of 7.93 million hectar in production supplying grapes to commercial trade (Petrucci and Clary, 2002; Anon., 2007b). Table 2.1 shows the important countries in raisin production.

Table 2.1: Major Raisin Producers (Amounts are given in tonnes) (Ozden, 2007).

Rank	Country	2003	2004	2005
1	Turkey	338,400	329,000	343,100
2	United States	300,900	310,500	320,000
3	Iran	145,000	145,000	145,500
4	Greece	69,656	73,269	71,194
5	Chili	40,000	53,700	64,000
6	South Africa	36,727	39,500	40,000
7	Uzbekistan	30,000	37,500	37,500
8	Afghanistan	33,750	33,750	33,750
9	Australia	20,462	28,500	30,000
10	Syria	12,000	12,000	12,000
	Miscellaneous	10,695	10,000	10,000
	TOTAL	**1,074,413**	**1,106,817**	**1,142,052**

Turkey and the United States are the world's largest raisin producers. Combined, these two countries account for more than 74 percent of production among the major northern hemisphere producing countries (Anon., 2004), and generally, about 65 percent of global production.

Turkey is the top raisin exporter in the world, with an average total of more than 234,000 tons between 1995 and 2006. Figure 2.2 shows Turkey's raisin production and export from 1995 to 2006 (Ozden, 2007).

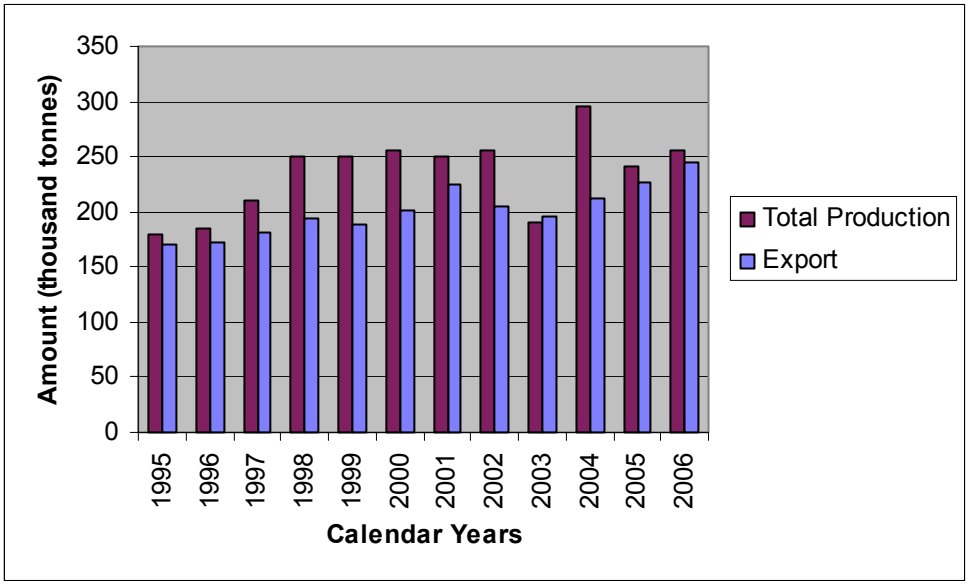

Figure 2.2: Turkey's Raisin Production and Export between 1995 and 2006

Generally 20-28% of raisins produced have been domestically consumed and the rest have been exported. According to Undersecretariat of The Prime Ministry for Foreign Trade Export Promotion Center's report, England, Germany and Netherlands were the top raisin exported countries in 2005 and 2006 calendar years with an average total of 264.47 million USD.

2.2 Drying of Biological Materials

A better understanding of heat and mass transfer phenomena is required to better design and optimize many industrial unit operations. Common unit operations which involve heat and mass transfer include drying, evaporation, and distillation. (Geankoplis, 1993).

It is not known when the preservation of foods by drying began, but history does show that our ancestors learned how to dry foods by trial and error. Food drying

eventually evolved within a scientific based environment and made possible the establishment of a world-wide industry, capable of providing a convenient food supply (Barbosa-Canovas and Vega-Mercado, 1996).

Drying or dehydration is a process where volatile liquid such as water, is removed from solid materials to halt or slow down the growth of spoilage microorganisms as well as the occurrence of chemical reactions. A dried food product offers the advantage of decreased weight, which has the potential for savings in the cost of transporting the product. (Geankoplis, 1993; Cohen and Yang, 1995).

2.2.1 Characteristics of drying curves

The process of drying can be divided into a "constant-rate" period and one or two "falling-rate" periods (Fortes and Okos, 1980) as seen in Figure 2.3.

Points A' and A represents either a hot or a cold material, respectively. Point B shows an equilibrium condition of the product surface. The period between points A (or A') and B is usually short, and is often ignored in the analysis of drying times (Barbosa-Canovas and Vega-Mercado, 1996). Stages of a typical drying operation can be explained as given below:

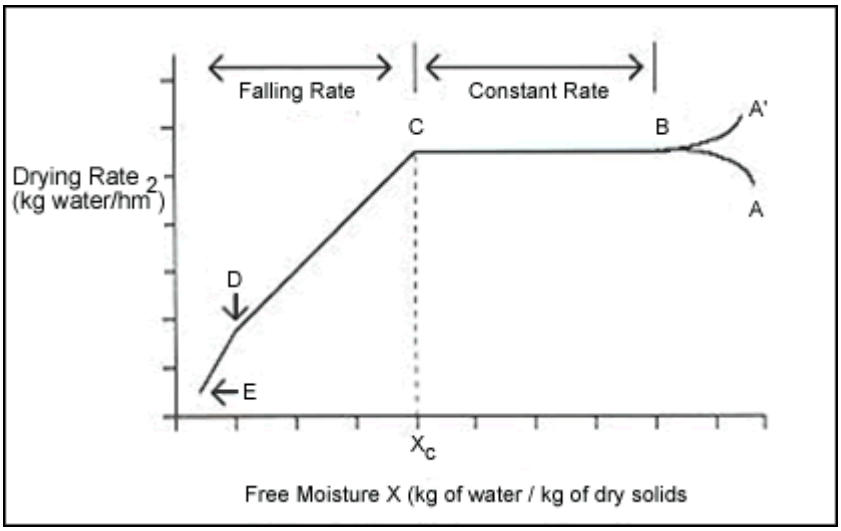

Figure 2.3: Characteristics of a Drying Curve (adapted from Barbosa-Canovas and Vega-Mercado, 1996)

1. *Constant-rate drying period (B-C):* If, at the start of drying, the material is completely wet, liquid flow may occur under hydraulic gradient. Moisture is unbound, exerting its full vapor pressure and held on the surface and the largest capillaries. The surface temperature is approximately at the wet-bulb temperature.

2. *First drying period (C-D):* The moisture still exerts its full vapor pressure and is transferred mainly by capillarity. The temperature rises above the wet-bulb temperature and it is common to assume that water moves by diffusion.

3. *Second drying period (D-E):* The drying rate decreases sharply. Moisture is held in the finest capillaries and can migrate by creeping along the capillary walls. The partial pressure of water vapor decreases sharply.

4. *Third drying period:* It is the period that an equilibrium is attained when the amount of water that vaporizes equals the amount that condenses (Barbosa-Canovas and Vega-Mercado, 1996).

2.2.2 Mathematical modeling of drying curves

The thin-layer drying models, describing the drying process, can be distinguished in three main categories, namely the *theoretical*, the *semi-theoretical* and the fully *empirical* ones (Sharaf-Eldeen and Hamdy, 1979). The major difference between these groups is that the theoretical models suggest that the moisture transport is controlled mainly by internal resistance mechanisms, while the other two consider only external resistance (Babalis et al., 2006).

The semi-theoretical models are derived directly from the general solution of Fick's law by simplification. The empirical models are derived from statistical relations and they directly correlate moisture content with time, having no physical connection with the drying process itself (Babalis et al., 2006).

The basic equation is similar to the Newton's law for cooling, incorporating a single layer drying constant (k) for the combined effect of various transport phenomena existing which was first suggested by Lewis (1921)

$$\frac{dM}{dt} = -k \cdot (M - M_{eq}) \qquad \textbf{(2.1)}$$

Assuming that the bulk moisture content (M) depends only on time, the solution of equation (2.1) is obtained by integration as follows:

$$MR = \frac{M - M_{eq}}{M_0 - M_{eq}} = \exp(-k \cdot t) \quad \textbf{(2.2)}$$

The moisture ratio (MR) determines the unaccomplished moisture change, defined as the ratio of the free water still to be removed at time t over the initial total free water (Babalis et al., 2006).

To model drying curves, approaches reported by different authors in literature are given in Table 2.2, which are used to model the drying curves of different drying methods in this study.

Table 2.2: Thin-layer Models Fitted to Experimental Data

Model	Mathematical expression	References
Lewis	$MR = \exp(-k \cdot t)$	(Lewis, 1921)
Page	$MR = \exp(-k_1 \cdot t^n)$	(Page, 1949)
Henderson and Pabis	$MR = a \cdot \exp(-k \cdot t)$	(Henderson and Pabis, 1961)
Logarithmic	$MR = a \cdot \exp(-k \cdot t) + c$	(Yaldiz et al., 2001)
Approximation of Diffusion	$MR = a \cdot \exp(-k \cdot t) + (1-a)\exp(-k \cdot b \cdot t)$	(Yaldiz and Ertekin, 2001)
Wang and Singh	$MR = 1 + a_1 \cdot t + b_1 \cdot t^2$	(Wang and Singh, 1978)
Midilli et al.	$MR = a \cdot \exp(-k_1 \cdot t^n) + b \cdot t$	(Midilli et al., 2002)

2.2.3 Diffusion theory

Diffusion takes place within the solid and within the capillaries, pores and small voids filled with liquid water. This liquid water diffuses outward until, at the open end of a capillary, it is carried away in the air stream. Unfortunately, the diffusion theory does not take into account shrinkage, case hardening or sorption isotherms. The modified Fick's Law, applied to a one-dimensional cylinder can be expressed as:

$$\frac{\partial M(r,t)}{\partial t} = \frac{1}{r}\left(r \cdot D_{eff} \cdot \frac{\partial^2 M}{\partial r^2} \right) \quad \textbf{(2.3)}$$

where r (m) is the radius of the cylinder and D_{eff} (m^2/s) is the effective diffusion coefficient.

Geometrically, Thompson seedless grapes can be approximated to a cylinder. If radius and effective diffusivity are taken as constant, the solution of the modified Fick's Law for an infinite cylinder is given below:

$$MR = \frac{M - M_{eq}}{M_0 - M_{eq}} = \sum_{n=1}^{\infty} \frac{4}{\beta_n^2} \cdot \exp\left(- \frac{\beta_n^2 \cdot D_{eff} \cdot t}{r^2} \right) \quad \textbf{(2.4)}$$

where β_n is the Bessel function roots of the first kind and zero order (Barbosa-Canovas and Vega-Mercado, 1996).

For n>1, the values of β_n increase drastically thus for long drying times the value of exponential in equation (2.4) can be taken as zero. For three digit accuracy the value of β_1 is equal to 2.404 thus equation (2.4) can be reduced to,

$$MR = \frac{M - M_{eq}}{M_0 - M_{eq}} = 0.692 \cdot \exp\left(- \frac{5.78 \cdot D_{eff} \cdot t}{r^2} \right) \quad \textbf{(2.5)}$$

From equation (2.5), effective diffusivity, D_{eff} (m^2/s), can be calculated at any time t (s) if radius, r (m), and moisture content, M (d.b.), is known. The underlying assumptions required to accurately determine the diffusivity using the procedure outlined above are: (1) isothermal drying conditions; (2) constant effective diffusivity; (3) negligible shrinkage occurs; (4) uniform initial moisture content; (5) negligible external resistance (Srikiatden and Roberts, 2006).

In order to correct deviations resulting from the second and third hypotheses, the method described by Azzouz et al. (2002) was used. The authors supposed that values of D_{eff} and r were constant for only short intervals of time. During the drying process and between successive intervals of time, an instantaneous value of D_{eff} could be estimated based on the determination of r from the corresponding average moisture content. The value of r was calculated from the variation of shrinkage of the grape during the drying process. The analysis continued until the end of drying in order to obtain the effective diffusion coefficient, D_{eff}, as a function of the water content of the product.

2.3 Dipping of Biological Materials in Chemical Solutions

The cuticle or cuticular membrane plays an integral part in extending shelf life of many different kinds of post-harvest produce. The cuticle forms a continuous extracellular membrane over the epidermal cells of leaves and fruits. The primary functions of the cuticle are as follows (Glenn et al., 2005):

1. Minimize water loss by mediating the moisture vapor permeability,
2. Prevent the loss of solutes by leaching,
3. Provide the first line defense against pathogen invasion,
4. Act as a shield against mechanical impact, provide some protection from exposure to pesticide and fertilizer chemicals, reduce damage from solar irradiation,
5. Facilitate the efficient exchange of gases.

The cuticle is not simply a homogenous membrane that covers the epidermal cell layer in plants but rather it contains a layered structure. In addition, the cuticle structure and composition varies among plants and among different organs of the same plant and changes as the tissue grows and matures. The young tissue is covered with a highly water-repellent wax layer called the procuticle. As the leaf develops, the cuticle thickens and adds to the wax layer (Glenn et al., 2005).

This cuticle, if it has not been damaged, has little permeability to moisture. It includes two types of compounds: natural waxes and cutin. Wax is soluble in solvent and is made of heterogeneous mixture of lipids that vary considerable among different plants. Waxes are a complex mixture of alcohols, alkanes, aldehyds, ketones, and esters made from long-chain fatty acids. These $C_{16:1}$ and $C_{18:1}$ fatty acids are first produced in cell plastids and the waxes deposit as a thin, amorphous layer known as epicuticular wax layer on the cuticle surface. The structure and shape of the wax crystals depend on wax composition, which is influenced by environmental and developmental factors (Glenn et al., 2005). All of these compounds have high molecular weights and similar physical properties, especially insolubility in water and a melting point between 40 and 100°C. The second layer of the fruit skin (cutin) is poorly soluble in most organic solvents, as the chains of constituents are firmly fixed by cross-polymerization in the membrane (Grabowski and Marcotte, 2003; Suarez et al., 1984; Mazliak, 1970).

Dipping in hot water or the use of chemicals such as sulphur, NaOH, and ethyl or methyl oleate emulsions are some pretreatments widely used for grape drying (Doymaz and Pala, 2002). The dipping pretreatment not only reduces the drying time, in some cases it also improves the quality (lighter color, sweeter flavor, nutritional quality and better sanitation) of the raisins produced (Pangavhane et al., 1999). The most effective dipping materials for increasing the drying rate were found to be the ethyl esters of fatty acids in C_{10}-C_{18} range. Among these, ethyl oleate and ethyl linolenate are found to be most effective for grapes (Ponting and McBean, 1970).

Drying rates increase and drying times decrease with increasing ethyl oleate concentration. However, ethyl oleate can add a noticeable flavor, thus the optimum dip concentration is 2% for grapes (Ponting and McBean, 1970). Tarhan (2007) dipped plums in 4% of ethyl oleate solution for 60 seconds before drying however the author did not report the taste of produced prunes. Ethyl oleate acts on the grape skin by dissolving the waxy components which offer a high resistance to moisture transfer (Saravacos and Marousis, 1988). Alkaline substances such as K_2CO_3 or NaOH along with ethyl oleate facilitate the moisture removal from grapes. Dipping grapes in a solution of 0.5% NaOH or 2.5% K_2CO_3 breaks the skin and facilitates the moisture transfer (Saravacos and Marousis, 1988). Ponting and McBean (1970) mentioned that Grncarevic (1963) found an effect of potassium carbonate alone, but Radler (1964) found it to be no better than water for increasing drying rate. Doymaz and Pala (2002) studied the effect of K_2CO_3 amount in a solution of 2% ethyl oleate on red peppers which also have wax on the skin. They reported that increasing the amount of K_2CO_3 from 4% to 5% decreased the drying time from 21 to 19 hours, but an increase from 4% to 6% decreased drying time for just half an hour. Doymaz (2006) investigated the effect of three different solutions at ambient temperature each containing 2% ethyl oleate and 2.5% K_2CO_3 or 2.5% KOH or 2.5% Na_2CO_3 on drying kinetics of black grapes and the author reported that the drying times were 25, 30 and 33 hours, respectively whereas control's was 65 hours. It can be concluded that the best combination of ethyl oleate with K_2CO_3 solution thus far acts much more on grape skin and facilitates the mass transfer.

With respect to the temperature of the solution Pangavhane et al. (1999) classified dipping solutions into two categories:

1. Cold dipping: Temperatures are generally considered to be around ambient temperature or slightly higher.
2. Hot dipping: Temperature of the solution is higher than that of cold dipping.

Although the author classified solutions at ambient temperature as cold and at 93°C as hot and made no classifications within this temperature range, in this study 30°C dipping temperature was considered as cold, 40°C was considered as moderately hot and, 50° and 60°C dipping temperatures were considered as hot. Pangavhane (1999) states that hot dipping causes cracking and perforation in the waxy cuticle thus increasing the drying rate while cold dipping increases the drying rate less than that of hot dipping however the raisins produced get an attractive color without any cracks on the berries.

2.4 Blanching of Biological Materials

Enzymatic activity in food products is inhibited at water activities lower than 0.75. Short heat treatments, such as blanching of raw vegetable, are used to inactivate enzymes. Improvement of sensory properties of foods may be achieved by enzymatic activity, such as the production of glucose from starch while processing domestic animal feed. In other cases, enzymatic activity is not desirable because it affects the amount of nutrients in food, such as in the hydrolysis of lecithin by phospolipase. Enzymatic browning of food products causes dark pigment formation, production of gases, and the reduction in fruit volumes (Barbosa-Canovas and Vega-Mercado, 1996).

Browning occurs due to the oxidation and dehydrogenation of colorless polyphenols present in the plants. The initial reaction is catalyzed by polyphenoloxidase (PPO) and produces reddish-brown quinones (Busch, 1999). Oxidative browning is an important problem, especially in fruits such as peaches, apples, bananas, cherries, nectarines, apricots, grapes and persimmons (Ramaswamy, 2004). PPO is a copper-containing enzyme which is also known as catechol oxidase, diphenol oxidase, phenolase and tyrosinase (Kim et al., 2005). PPO's are found in almost all higher plants, including wheat, tea, potato, cucumber, artichoke, lettuce, pear, papaya,

grape, peach, mango, apples as well as seeds such as cocoa (Martinez and Whitaker, 1995).

There are several ways to inactivate PPO in fruits and vegetables. Kim et al. (2005) used hot onion extracts, 500 g onion homogonized with 500 ml water for 3 minutes, at 100°C to inhibit the browning of pear and found that onion extract contains potential inhibitors of pear PPO. The authors reported that inactivation of PPO could be due to both effect of temperature of onion extract and the effect of thiol compounds which are found in onion that also inhibits PPO activity. Gomez-Lopez (2002) studied the effect of different chemical inhibitors, namely L-cysteine, ascorbic acid, NaCl, glycine and resorcinol on avocado PPO and found that L-cysteine was the most effective inhibitor closely followed by ascorbic acid. Robert et al. (1996) studied L-cysteine inhibition of palmito PPO and reported an inverse relationship between L-cysteine concentration and PPO activity such that, increase in L-cysteine concentration decreased PPO activity.

The reducing compound sulfite is used by the food industry by placing fruit slices in controlled-atmosphere chambers with burning sulfur, which reacts with oxygen to produce bisulfite (Martinez and Whitaker, 1995). However sulfites can lead to asthmatic attacks, rashes and abdominal upset. For table grapes the use of sulfur dioxide as a fumigant is officially defined as a pesticide and is required by the U.S. Environmental Protection Agency (EPA) to be less than 10 ppm (Warner et al., 2000). For processed foods, FDA requires the amounts higher than 10 ppm to be listed on the product's package.

Blanching serves a variety of functions, such as destruction of enzymatic activity in vegetables and some fruits prior to further processing, and may be applied either by immersing food in hot water or by spraying steam onto the food (Fellows, 2000). In literature blanching has been applied prior to processing to several foods: apricot (Piga et al., 2004), banana puree (Palou et al., 1999), green pepper (Thomas and Gopalakrishnan, 1991), potato (Yemencioglu, 2002), sugar beet cossettes (Leblebici and Koksel, 1999).

Browning reactions, initialized by PPO, occur mainly under post-harvest conditions when tissues are exposed either to stress conditions or deterioration (Robert et al., 1996). PPO can be inactivated by steam blanching. Under-blanching may cause more

damage to food than not blanching, because heat is sufficient to disrupt tissues and release enzymes. Inadequate heating does not inactivate PPO, and causes accelerated damage by mixing the enzyme and substrates (Fellows, 2000). Since color is one of the most important visual attributes influencing consumer acceptability (Maskan, 2001) it is important as a quality and its prevention is a priority in the food industry (Kim et al., 2005).

2.5 High Hydrostatic Pressure (HHP) Treatment of Biological Materials

2.5.1 Evolution and history of high pressure processing

The early development of high pressure technology was driven, not by food technologists, but by the needs of the military to improve the cannon. The early development of cannon designs aimed to contain higher pressures in order to allow gunpowder charges to project heavier and heavier missiles further and further. This work led to vessel designs that much later became available for laboratory-scale experiments, including experiments with foods. The first experiments with microorganisms were reported at the end of the 19^{th} century by Hite (1899) and effects of pressure on the physical properties of foods were reported soon after (Gould, 2001).

High pressure processing has advanced further than the other alternative new technologies (such as Electroporation, Manothermosonication, High-Intensity Light, High-Strength Magnetic Fields) except for irradiation. To some extent, this is because of the efficacy of high pressure processing. It inactivates all vegetative and spore forms of microorganisms if the applied pressure is high enough. In addition, the engineering aspects of high pressure processing have advanced to such an extent that commercially economic processes have become practical within the last decade or so, at least for high-value market products (Gould, 2001).

2.5.2 HHP equipment

There are two major types of high pressure processing of food products: the (conventional) batch systems, derived from cold isostatic processing, and the semicontinous systems. Batch systems can process both liquid and solid products, but these have to be prepacked. In-line systems can be applied only to pumpable products (Berg et al., 2001).

Equipment for high pressure batch processing consists of three main parts: the vessel, its surrounding yoke, and the hydraulics. The actual pressure treatment takes place in the pressure vessel, which is considered to be the heart of the equipment. The volume of the vessel may vary from less than a liter (for laboratory-scale applications operating at 1000 MPa) up to 500 liters (for processing units operating at 600 MPa. In many cases the pressure vessel is forged cylinder constructed in low-alloy steel of high-tensile strength. The wall thickness of these vessels is determined by the maximum working pressure, the vessel diameter and the number of cycles for which the vessel is designed. The use of industrial-scale monobloc vessels is limited to working pressures up to 600 MPa (Berg et al., 2001).

Treatment of foods with high pressure is generally accomplished by compressing the medium (usually water mixed with lubricating oil) surrounding prepackaged foods in flexible or semi-rigid vacuum-sealed containers. The liquid is pressurized using hydraulic pumps, which have a typical power of 100 to 200 kW for production-scale units. In this manner, HHP for food processing in the range of 100 to 1000 MPa is generated through direct or indirect compression. In the case of *direct or internal compression*, the system is pressurized by a piston driven at its larger diameter by a low-pressure pump. The advantage of direct compression is that it achieves fast pressurization rates. Its main disadvantage is that it requires a dynamic high pressure seal between piston and inner core. Pressurization by means of *indirect or external compression* takes place through an external high pressure intensifier that pumps liquid into the vessel under high pressure. The main advantage of this technique is that static seals can be used. In practice, for operating pressures up to 600 MPa, external pressurization is common. However for higher pressures, internal pressurization is more efficient than external pressurization (Berg et al., 2001; Barbosa, 2003).

Capacity of an HHP system is closely related to the cycle time of the process. For batch systems, the cycle time may be broken into a number of steps: (1) Fill the vessel with the product, (2) Close the vessel, (3) Pressurize the system, (4) Holding time, (5) Release pressure, (6) Open the vessel, (7) Empty the vessel.

The time needed for each of these steps is related to mechanical limitations, except step 4, which is related to microbiological and food quality considerations. A combination of high temperature and high pressure may reduce holding time

significantly. A disadvantage is that higher working pressures result in increasing costs due to higher demands from the high pressure system. A second disadvantage is that at higher temperatures product quality might be degraded. Filling, closing, opening and emptying of the vessel can be speeded up by automation of the system. The time needed for pressurizing the vessel is closely related to the power of the high pressure generator, the final pressure required, and the type of hydraulics (internal/external intensifier) (Berg et al., 2001).

2.5.3 Effect of HHP on biological materials

The effects of high pressure derive from Le Chatelier principle. Pressure favors any physical or chemical reaction in which there is a net volume decrease and suppresses any reaction in which there is a net volume increase. With reference to biological systems, the most important volume-decrease reactions include the denaturation of proteins, gelation, hydrophobic interactions, phase change in lipids and increases in the ionization of dissociable molecules. Small molecules are less affected than macromolecules so that low molecular weight flavor and odor compounds in foods tend to survive with consequent retention of high organoleptic quality of some types of foods. On the other hand, the high molecular weight components of some foods (e.g., proteins in meat, fish and eggs) change greatly on pressurization, and the changes that occur, particularly in texture, may or may not be desirable (Gould, 2000).

At pressures around 100 MPa the nuclear membrane of yeast was affected, and at more than 400-600 MPa further alteration occurred in the mitochondria and the cytoplasm. In particular, metal ions are released at pressures over 300 MPa. Although it is not yet known whether pressure can enhance resistance to physical treatment, cells subjected to stress other than pressure become more resistant to pressure. Enzymes of extreme thermophiles are not only more heat resistant but also more pressure resistant than mesophilic microorganisms. In general, heat-resistant microorganisms are also more resistant to pressure, but there are numerous exceptions. Gram-positive bacteria are more pressure resistant to heat and pressure than Gram-negative bacteria. Most spores and yeasts easily inactivated by pressures of nearly 400 MPa (Smelt, 1998).

In view of the specificity of enzymatic reactions, enzymes may be affected by pressure in several ways: (1) Pressurization at room temperature may bring about reversible or irreversible, partial or complete enzyme inactivation resulting from conformational changes in the protein structure. These changes depend on the type of enzyme, micro-environmental conditions, pressure, temperature, and processing time. (2) Enzymatic reactions may be enhanced or inhibited by pressure, depending on the volume change (positive or negative) associated with the reaction. (3) A macromolecular substrate (protein, starch) may become more sensitive to enzymatic action once it has been unfolded or gelatinized by pressurization (Ludikhuyze et al., 2001).

Polyphenoloxidase (PPO) which causes browning reactions in damaged fruits and vegetables can be either activated or inactivated by pressurization depending on the pressure level. Ludikhuyze et al. (2001) concluded that the pressure level needed for PPO inactivation at ambient temperature is strongly dependent on its origin and the pH of the medium. Research by Castellari et al. (1997) and Weemaes et al. (1998) showed that in order to inactive grape PPO around ambient temperatures, the pressure level should begin from 600 MPa. Matser et al. (2000) pressurized mushrooms at 600, 800 and 950 MPa and reported an increase in activity of PPO at 600 MPa. Although it is reported that higher pressures resulted in inactivation, there was still residual activity of PPO. It is concluded that in order to inactivate PPO completely in mushrooms, higher pressures at longer holding times and/or temperatures above 50-60°C should be performed.

HHP affects cell wall structures of fruits and vegetables thus leaving the cells more permeable which leads to reversible or irreversible changes in tissue structure depending on applied pressure. Ade-Omowaye et al. (2001) pressurized sliced red paprika at 400 MPa for 10 min at 25°C. It is reported that drying time during the falling rate period of HHP pretreated samples was comparable with 3 minute boiling water-blanched samples. Similarly Rastogi et al. (2000) applied 200 and 400 MPa hydrostatic pressures before osmotic dehydration of sliced potato samples, which increased effective diffusion coefficient of water proportional to applied pressure level (0.45×10^{-9} at 200 MPa, 0.84×10^{-9} at 400 MPa) thus reducing the drying time.

2.6 Microwave Processing of Biological Materials

2.6.1 The electromagnetic spectrum

Microwaves, or hyper-frequency waves, constitute the 300 MHz to 300 GHz range of electromagnetic spectrum (Figure 2.4), corresponding to wavelengths ranging from about 1 m to 1 mm (Saltiel and Datta, 1998).

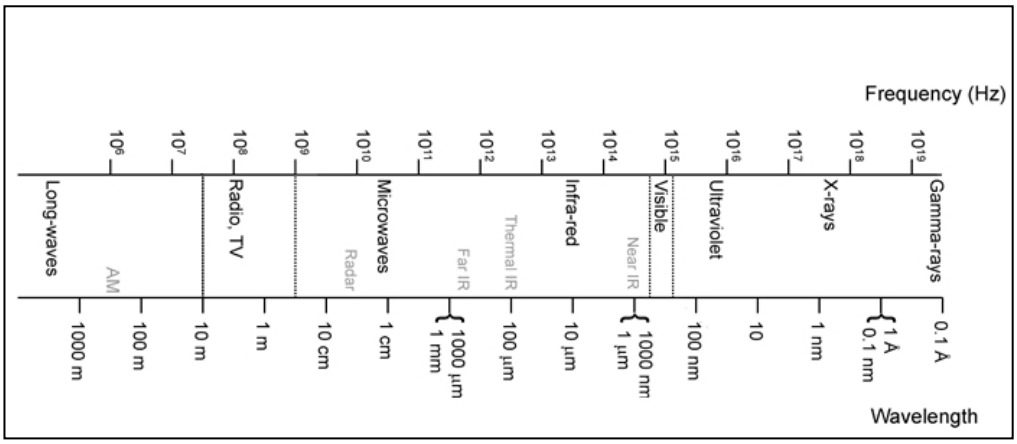

Figure 2.4: Electromagnetic Spectrum (adapted from http://www.answers.com)

2.6.1.1 Electromagnetic waves

Energy transfer by electromagnetic waves is by radiation and can be considered as a collection of discrete packets of energy called photons or quanta where each photon of frequency f is considered to have an energy of

$$e = h \cdot f \tag{2.6}$$

where $h=6.625\times10^{-34}$ J.s is Planck's constant (Çengel, 1998). Photons of microwaves correspond to an energy range of 1μeV to 1 meV and are incapable of ionization (Ehlerman, 2002).

A propagating electromagnetic wave has two components; an electric field (E; unit V/m) and a magnetic field (H; unit A/m). They are always perpendicular to each other. In free space the propagating wave has a velocity (c_0) of about 3.0×10^8 m/s, and this is the maximum speed at which energy can travel. Frequency and wavelength (λ) are linked with the equation (2.7) (Ryynanen, 2002):

$$c = \lambda \cdot f \tag{2.7}$$

2.6.1.2 Definition and regulations

Microwaves, or hyper-frequency waves, form a continuous electromagnetic spectrum that extends from low-frequency alternating currents to cosmic rays. Traditionally the microwave domain is subdivided into bands designated by the letters P, L, S, X, K, Q, V and W is shown in Table 2.3. (Thuery, 1992).

Table 2.3: Microwave Bands

Designation	Frequency Limits, GHz
P	0.225 – 0.39
L	0.39 – 1.55
S	1.55 – 5.20
X	5.20 – 10.90
K	10.90 – 36.00
Q	36.00 – 46.00
V	46.00 – 56.00
W	56.00 – 100.00

The frequency range of microwaves adjoins the range of radio frequencies used for broadcasting which is also used for telecommunications such as mobile phones and radar transmissions. In order to prevent interference problems, special frequency bands are reserved for industrial, scientific and medical (so-called ISM) applications, where a certain radiation level has to be tolerated by other applications such as communication devices. In the range of microwaves the ISM bands are located at 433 MHz, 915 MHz and 2450 MHz (which are in the L-S band); the first is not commonly used and the second is not generally permitted in continental Europe. Outside the frequency range leakage is very restricted. Although 915 MHz has some considerable advantages for industrial applications, for microwave ovens at home the only frequency used is 2450 MHz (Regier and Schubert, 2005).

Apart from interference regulations, there also exist two other types of safety regulations:

1) The regulation concerning the maximum exposure or absorption of a human working with a microwave equipment. This is based on estimation of thermal effects on sensitive organs, which limits human exposure to 1 mW/cm^2. Also the specific

absorption rate (SAR) which is defined as quotient of incident power to body weight and should have a maximum value of 0.4 W/kg.

2) The regulation concerning maximum emission or leakage of the microwave equipment which is limited to a value of 5 mW/cm^2 measured at a distance of 5 cm from the point where the leakage has the maximum level (Regier and Schubert, 2005).

2.6.1.3 Microwave oven history and its major components

The introduction of the magnetron during Second World War presented engineers and scientists in industry, universities and government with a unique challenge to put such a device for generating microwaves into profitable use. During late forties and early fifties, a pioneering work was made to obtain reliable data on material properties, led by von Hippel and his co-workers at MIT on the properties of many organic and inorganic materials in the frequency region $100\text{-}10^{10}$ Hz (Metaxas and Meredith, 1988).

The use of microwaves for heating food was first conceptualized by Percy Spenser at the Raytheon Manufacturing Laboratories in Waltham, Massachusetts in late 1945 (Saltiel and Datta, 1998). The microwave oven was a by-product of a radar-related research project around 1946 that Dr. Percy Spencer noticed something very unusual while he was testing a new vacuum tube, called a magnetron, when he discovered that the candy bar in his pocket had melted (Anon., 2006). The first commercial microwave oven the Radarange was first demonstrated by Raytheon in 1947. Microwave ovens were first introduced on a large scale in 1965, with considerable growth taking place in the 1970s and 1980s (Saltiel and Datta, 1998).

Microwave appliances have three major components:

1) A magnetron: It is a diode-type electronic tube which converts electrical voltage to microwave radiation. Magnetrons allow either continuous or pulsed microwave generation with powers up to megawatts and frequencies between 1 and 40 GHz. Efficiencies are around 80% and lifetimes about 5000 hours (Vollmer, 2004).

2) A waveguide: For guiding an electromagnetic wave, transmission lines such as coaxial cable and waveguides can be used (Regier and Schubert, 2005).

Microwave waveguides rely on high-reflectivity of metallic walls for microwave propagation. The open end of the waveguide, the horn, acts as a feed to the oven section of the microwave (Saltiel and Datta, 1998). Inner dimension of the waveguide should be at least $\lambda_{max}/2$ to be able to transmit the wave (Vollmer, 2004).

3) An applicator: Common applicators can be classified by type of field configuration into three types: near-field, single-mode and multi-mode applicators.

a. Near field applicator: The microwaves originating from a horn antenna or slot arrays directly hit the product to be heated (Regier and Schubert, 2005).

b. Single-mode applicators: This type of applicators has a single resonance near the operating frequency. Their use for food industry is extremely limited. The volume and dielectric loss properties of the food material have to be extremely small (Dibben, 2001).

c. Multi-mode applicators: The majority of food heating applications use a multimode resonant cavity applicator (Dibben, 2001) to process larger samples (Saltiel and Datta, 1998) which have larger dimensions compared to single-mode applicators (Regier and Schubert, 2005). Uniformity is maintained by using mode stirrers which perturbs electrical field within the applicator (Saltiel and Datta, 1998).

2.6.2 The electromagnetic properties of materials

2.6.2.1 Polarization of dielectric materials

When two opposite charges are separated by a distance, they constitute an electric dipole. Molecules with non-zero permanent electric dipole moments are called polar molecules. Non-polar molecules may obtain a dipole moment in an electric field as a result of the distortion of their electronic distributions and nuclear positions. The relative permittivity, ε, is a measure of the polarizing effect from an external field, that is, how easily a medium is polarized (Ryynanen, 2002).

Metaxas and Meredith (1998) list four types of polarization: electronic, atomic, orientation and Maxwell-Wagner. *Electronic polarization* arises mainly from the displacement of electrons around the nuclei whereas *atomic polarization* occurs due

to the relative displacement of atomic nuclei because of the unequal distribution of charge in molecule formation. Polar dielectrics contain permanent dipoles due to the asymmetric charge distribution of unlike charge partners in a molecule which tend to reorientate under the influence of a changing electric field which gives rise to *orientation polarization*. Polarization, which arises from charge build-up in interface between components in heterogeneous systems, termed interfacial, space charge or *Maxwell-Wagner polarization*. Ions within a material, such as dissolved salt, move within the material as a result of the alternating field. The movement of ions, termed direct current conduction, also contributes to heat generation and is similar to ohmic heating (Srikiatden and Roberts, 2006)

Of all the possible forms of loss mechanisms, orientation polarization is perhaps the most significant in microwave heating applications at frequencies above 1 GHz (Ryynanen, 2002) where as electronic and atomic polarization plays an important role at lower frequencies (below 200 MHz) (Wang et al, 2003).

2.6.2.2 Dielectric properties of materials

Dielectric properties are the most important physical properties associated with radio frequency (RF) and microwave heating (Tang, 2005) and describe how materials interact with electromagnetic radiation (Ryynanen, 2002). It is critical to have knowledge of the dielectric properties of materials in product and process development (Tang, 2005).

The interaction of microwaves and the material can be characterized by the complex permittivity, ε, and the permeability, μ, which determine the storage and dissipation of electric and magnetic energy, respectively (Dibben, 2001). Complex permittivity or complex dielectric constants of materials are given by equation (2.8):

$$\varepsilon = \varepsilon' - j\varepsilon'' = |\varepsilon| e^{-j\delta} \qquad \textbf{(2.8)}$$

where ε'= the relative dielectric constant,

ε''= the relative dielectric loss factor

δ = dielectric loss angle (tan δ= ε''/ ε')

j = $\sqrt{-1}$

ε' is related to the material's ability to store electric energy (for vacuum ε'=1) while ε" indicates dissipation of electric energy into heat (Metaxas and Meredith, 1988; Tang et al, 2002). The relative dielectric constant of most biological materials is in the range of 40 to 70 whereas relative dielectric loss factor is 10 to 17 at 2.45 GHz microwave frequency. For example, dielectric constant and dielectric loss of whey protein gels and liquid whey protein mixture which were investigated by Wang et al. (2003), at a frequency range of 27 to 1800 MHz by using an Agilent 4291B Impedance analyzer, was found to be 57.17 ± 0.60, 23.30 ± 1.25 and 58.90 ± 0.57, 23.10 ± 0.14, respectively, at 20°C and 1800 MHz. A similar study by Garcia et al. (2004) at 3 GHz revealed the dielectric constant and dielectric loss of grape juice as 65.358 and 19.976, respectively.

The magnetic permeability for most biological materials is the same as that of free space ($\mu_0=4\pi\times10^{-7}$ W/Am). Therefore, these materials absorb only the electric part of the electromagnetic field. Food materials are practically non-magnetic; as they contain only trace amounts of magnetic material, such as iron and cobalt. Magnetic materials such as ferrite, often used in susceptors and browning dishes, interact with the magnetic field, which results in substantial heating (Ryynanen, 2002; Tang et al, 2002).

Equation (2.9) shows the decrease in the impinging electric field strength (E_0) with distance from the entry surface of a large dielectric material:

$$E = E_0 \cdot e^{-\alpha \cdot z} \tag{2.9}$$

The degree of decay is determined by an attenuation factor (equation (2.10)), which in turn is a function of the material (von Hippel, 1954):

$$\alpha = \frac{2\pi}{\lambda_0} \cdot \left[\frac{1}{2} \cdot \varepsilon' \cdot \left(\sqrt{1 + \left(\frac{\varepsilon''}{\varepsilon'} \right)^2} - 1 \right) \right]^{\frac{1}{2}} \tag{2.10}$$

where λ_0 is the free space wavelength.

The penetration depth of microwaves is defined as the depth where the dissipated power is reduced to 1/e (Euler's number e≈2.718) of the power entering the surface

and can be calculated in meters by equation (2.11) (Metaxas and Meredith, 1988; Tang, 2005):

$$d_p = \frac{1}{2\alpha} \tag{2.11}$$

It is seen that as the frequency of the electromagnetic waves increases, attenuation factor increases thus penetration depth decreases. Also higher the relative dielectric loss factor of the material, lower the penetration depth of the electromagnetic wave.

2.6.2.3 Microwave heating of materials

The conversion of microwave energy into heat is explained by basically two phenomena:

1. Molecules, with a permanent dipolar moment, rotate in the rapidly changing electric field. Molecules rotate in a field that changes polarity at a frequency of many millions of times per second. However, in practice because of frictional effect that is interaction with the electrical field of neighboring molecules, oscillation of molecules is retarded and heat is imparted to medium. This means that at very low electromagnetic frequencies no energy is imparted because the water molecules can rotate and reorientate themselves quickly enough to follow the field of wave and at very high frequencies (approaching 1000 GHz) molecules are too inert to follow the field of the wave (Nijhuis et al., 1998; Ehlerman, 2002).
2. Charge drift under the action of the field (*ionic conduction*). When the ions drift, due to the electric field, they collide with other molecules in a billiard ball fashion and heat is evolved because of friction (Nijhuis et al., 1998).

When exposed to an electromagnetic field, the amount of thermal energy converted in food is proportional to the value of the loss factor ε". The increase in temperature (ΔT), without consideration of heat transfer, can be calculated from equation (2.12) (Nelson, 1996):

$$\rho \cdot C \cdot \frac{\Delta T}{\Delta t} = 5.563 \times 10^{-11} f \cdot E^2 \cdot \varepsilon'' \qquad \textbf{(2.12)}$$

where C (J/kg°C) is the specific heat of heated material, ρ (kg/m^3) is the density, E (V/m) is electric field intensity, f (Hz) is frequency, Δt (s) is time increment, and ΔT (°C) is the temperature rise. It should be noted that the right part of the equation is equal to volumetric heating rate or microwave energy deposition. Equation (2.12) is only based on sensible heat and does not take heat transfer into account. An energy conservation equation was proposed by Bilbao-Sainz et al. (2006) where dissipated microwave power was equal to the sum of sensible heat, latent heat and convection heat.

An in-depth approach made by Datta (2001) considers the governing energy conservation equation for microwave heating which uses the rate of heat generation as a source term as shown in the following one-dimensional equation (2.13):

$$\underbrace{\rho \cdot C \cdot \frac{\partial T}{\partial t}}_{\substack{\text{rate of} \\ \text{energy} \\ \text{accumulation}}} + \underbrace{\rho \cdot C \cdot u \cdot \frac{\partial T}{\partial x}}_{\substack{\text{convective} \\ \text{energy flow}}} = \underbrace{k \cdot \frac{\partial^2 T}{\partial x^2}}_{\substack{\text{diffusive} \\ \text{energy}}} + \underbrace{\dot{Q}}_{\substack{\text{microwave} \\ \text{heat generation}}} - \underbrace{m_w \cdot h_{fg}}_{\substack{\text{energy used} \\ \text{in internal} \\ \text{evaporation}}} \qquad \textbf{(2.13)}$$

where Q (W/m^3) is the volumetric heat generation, T is the temperature at position x and time t, u is the velocity m/s and k is thermal conductivity W/m·°C.

Zhang and Datta (2001) list the factors that affect microwave heating of foods inside the oven as follows:

1. Strength and distribution of electromagnetic fields where the food is placed,
2. Reflection of electromagnetic waves from the food, as characterized by its property and geometry,
3. Propagation of the waves inside the food, also characterized by the food properties and geometry.

From the viewpoint of the material, Srikiatden and Roberts (2006) list 3 important properties that play an important role in microwave heating:

1. *Moisture content* is the most important parameter affecting loss factor. The more water present, the higher the dielectric loss factor and thus the better the heating rate (Tong, 1988). However, a low moisture product may heat very well because its specific heat is low, so it does not require as much energy to increase its temperature which is shown in equation (2.12).
2. *Temperature* of the material affects its dielectric properties depending on the material. The loss factor and dielectric constant decrease slowly with temperature in the range 2000-2800 MHz.
3. The dielectric constant increases linearly with increasing *density*. Materials with air pockets, such as porous materials, are able to have microwave energy penetrate deeply. Thus, porous materials are able to heat uniformly (Schiffmann, 1986).

Similar to every emerging technology, microwave heating has some drawbacks which should be taken in consideration during processing of biological materials. Nijhuis et al. (1998) summarizes some of them as follows:

1. Uneven heating. Although the ability of microwave radiation to penetrate materials can lead to controlled and precise heating, too high temperature in edges and corners of products may lead to overheating and irreversible drying out.
2. Input power should be controlled as too rapid mass transport may cause damage to the food texture by puffing,
3. Operational costs were considerable.

The future of microwave heating in food processing applications is promising, but successful application of microwave heating rely on a complete understanding of the interaction between microwaves and foods, and on the ability to predict and provide a desired heating pattern in foods for specific applications (Tang et al, 2002).

2.6.3 Microwave-assisted drying of biological materials

Microwave-assisted drying of fruits and vegetables has drawn considerable attention due to high mass transfer coefficients and occasionally better end-product quality. A search in popular search engines, Google and Yahoo, returned 76,400 and 22,000 results for the keyword of “microwave drying”. However in terms of scholarly

articles, the search in Scholar Google, Science Direct and Blackwell Synergy returned 3200, 194 and 2223 results, respectively, for the same keyword.

2.6.3.1 Heating pattern of biological materials during drying

Microwave heating does not depend on the transfer of heat through a surface. The existence of volumetric heat source enables the rapid transfer of energy throughout the body of the moist solid and alters the physical characteristics of drying. Considering the heating profile shown in Figure 2.5 Perkins (1979) describes three categories for radio frequency and microwave drying:

1. The solid is rapidly heated to the moisture's boiling point temperature, thereafter $\partial T / \partial t \cong 0$. Applicable to preheated materials which are not temperature sensitive.
2. The temperature increases throughout the drying operation which may occur when the boiling point of the liquid is not reached.
3. The solid is heated to a critical temperature below the boiling point temperature of the liquid phase and the material is force cooled. Applicable to heat sensitive materials (Metaxas and Meredith, 1988).

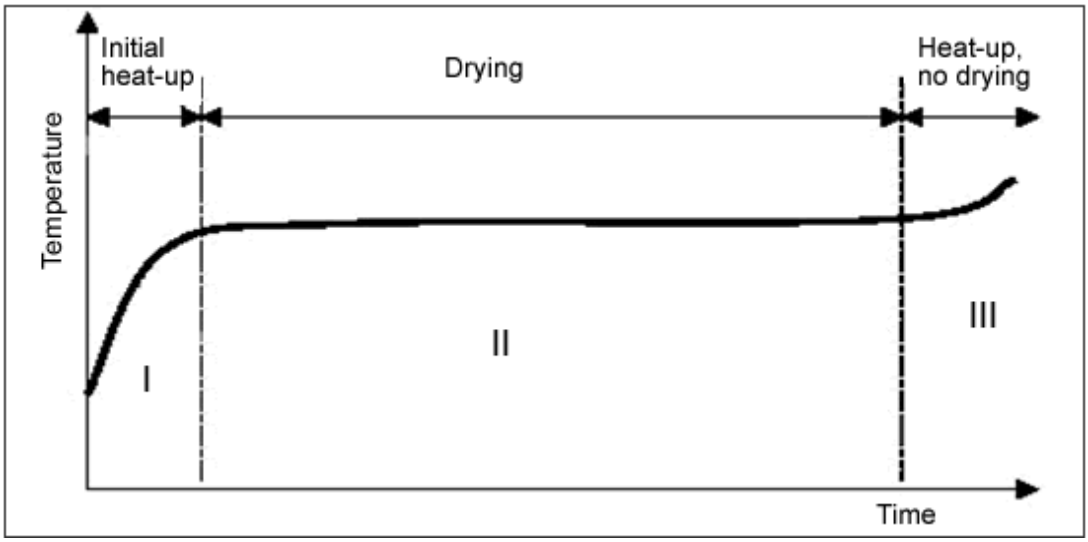

Figure 2.5: Rate of Rise of Temperature during High Frequency Drying

Boldor et al (2005) assumes the second region to be the constant drying region, where most of the liquid is being vaporized within the sample and removed with pressure gradients.

Since only a limited amount of water is available in third region, the final stage of drying, material temperature can easily rise to a level that might cause scorching. The final product temperature is difficult to control as compared to that in hot air drying in which product temperature never rises beyond air temperature (Zhange et al., 2006).

2.6.3.2 Combined use of microwave energy

Combination of microwaves with other modes of heating is seen as a practical solution to improve uniformity of microwave heating and provide more control on the moisture transport while simultaneously increasing the speed of heating (Datta et al., 2005).

Two particular combinations that are being cited in literature for drying are microwaves combined with convective air flow and microwaves combined with infrared radiation and to a lesser extent combination with vacuum.

Schiffmann (2001) proposed using microwave energy for drying in three different ways:

1. Applying microwave in the falling rate where hot air drying of foods has low energy efficiency and drying time is long. Since microwave penetration depth increases with decreasing moisture content (Datta and Ni, 2002), application of microwave in the last stages of drying will facilitate microwave interaction with water. Maskan (2000) first air-dried banana samples to an intermediate moisture of 1.25 kg H_2O/kg dry solids. Subsequent application of 350 W microwave power to reach the final desired moisture content provided 64.3% reduction in total drying time.
2. Application of microwaves throughout the drying process at low levels. Ren and Chen (1998) used combined microwave-hot air to dry fresh American Ginseng roots. The authors applied 60 W microwave power to 100 g of roots which reduced drying time by 28.7 and 55.2% for small and large roots, respectively, compared to hot air drying.
3. Applying microwave prior to hot air drying, thereby pre-heating the product to the drying temperature. Wang and Sastry (2000) pre-heated cylindrical samples

of carrot, potato and yam to 50° or 80°C by using microwave. The authors reported that drying rate increased with microwave pretreatment.

In addition to Schiffmann's (2001) second proposal, microwave energy can also be delivered intermittently throughout drying. Chua and Chou (2005) investigated intermittent microwave and infrared drying of potatoes and carrots. Microwave energy was delivered with an intermittency of 1/9 and 1/5 where intermittency was defined as the ratio of power on cycle to total elapsed time (power on cycle + power off cycle). Compared to convective drying, intermittent delivery of microwave power shortened drying time by 42% for potato and 31% for carrot samples, respectively, and prevented samples getting charred while reducing the change in color.

Contrary to Chua and Chou (2005), Wang and Xi (2005) proposed a two-stage microwave-convective drying of carrots where the microwave energy was delivered continuously but in varying powers. There were two falling-rate periods in microwave-convective drying of carrots and microwave power was higher or lower in the second-stage than the first-stage. It was found that first-stage power significantly affected rehydration ratio whereas second-stage power affected both rehydration ratio and β-carotene content of carrots.

Infrared heating provides heat flux on the surface (Datta et al., 2005) and can be used alone in drying of biological materials. However Wang and Sheng (2006) found that at the same power level the drying of peaches with far infrared radiation is far lower than microwave drying. Within the same media, penetration depth of microwave is very much longer compared to infrared radiation. Combination of optimized microwave and infrared heating provides higher surface temperatures needed to prevent sogginess and improve browning (Datta et al., 2005). Sumnu et al. (2005) reported to dry carrot slices by halogen lamp-microwave combination as fast as microwave only drying. However, the total power input in halogen lamp-microwave combination was 706 W (only 280W microwave power) whereas in microwave only was 560 W. Although penetration depth of near infrared radiation is lower in this case, than it was in Wang and Sheng, 2006, where they used far-infrared radiation while drying peaches, the energy consumption in both cases to achieve the same amount of drying rate was higher than microwave drying. Thus microwave-infrared combination method could give better results than the only usage of infrared radiation.

In conventional drying methods, heat and mass transfer are in the opposite direction, however in microwave vacuum drying they are in the same direction thus moisture transfer conditions can be greatly improved (Hu et al., 2005). The material to be dried can be either put directly into microwave cavity (Hue et al., 2005) or into a microwave transparent container (Giri and Prasad, 2007), generally glass, which is also placed in the cavity and the vacuum is provided by a vacuum pump which is attached to the cavity or the container. Decreasing the pressure also decreases the saturation temperature of the water, thus suitable for heat sensitive materials which can be, by this method, dried with low microwave power. Moreover, the absence of air during drying may avoid oxidative reactions and therefore effectively preserve food color and nutrients.

Giri and Prasad (2007) reported that increasing the vacuum has negligible effect on drying time of mushrooms however rehydration properties were improved. Similar findings were reported by Cui et al. (2004) on drying kinetics of carrot slices.

2.7 Color Analysis of Biological Materials

2.7.1 Importance of color measurement

A consumer first judges the visual appearance of foods hence visual attributes play an important role in the foods' market value. Color is one of the most important visual attribute due to its influence on consumer acceptability (Maskan, 2001). Pangborn (1967) stated that "In foods, colors are identified with previously experienced quality and serve as instant indicators of good or bad, according to the product and its intended use. A perceived inferior color quality or a color variation from unit to unit of a branded product are factors that are not well appreciated by the consumer. The manufacturer, therefore, has the difficult task of providing a product of the expected color quality at perhaps three different times of judgment: at purchase point if the product is packed in a transparent container; at the unpacking point in the kitchen; and at the consumer's plate after preparation and serving" (Brimelow and Joshi, 2001).

2.7.2 Color measurement of foods

The food industry uses color measurement for a number of reasons, all aimed at reducing the variability caused by subjective analysis and providing numerical

specification (Brimelow and Joshi, 2001). However color is a psychological phenomenon, its measurement is based on human color perception. Hence, photoelectric instruments must be corrected for both lightning and human visual response, while visual techniques must use observers with normal color vision under defined lighting (MacDougall, 2001).

It is essential that the source of illumination for visual color examinations be standardized in order to get reproducible results. In 1931, the CIE (Commission Internationale d'Eclairage) approved three "standard" illuminants. Illuminant A represents lights from an incandescent lamp. Illuminant B represents direct sunlight. Illuminant C represents average daylight from the entire sky. In 1966, the CIE proposed a fourth series, the D illuminants. This series represented daylight more completely and defined the energy spectra down to 300 nm as opposed to the A, B, C series which cut off at 400 nm. (Francis, 2005). The D_{65} is the most commonly-used daylight illuminant and represents the average or noon daylight all over the world. Illuminants are formulas used for mathematical manipulation of color data. They are not realizable physical light sources (HunterLab, 2000).

Photoelectric color-measuring instruments can be divided into two classes, trichromatic colorimeters and spectrophotometers. The most successful of the early trichromatic colorimeters was developed in the 1940s by Hunter (1958). It comprised a light source and three wideband red, green and blue filters to approximate CIE standard illuminant C and the 2° observer. The tristimulus value obtained were transformed into Hunter L, a, b color space. Until the beginning of computer era such instruments were much less expensive than spectrophotometers and, although absolute accuracy may have been poor, they were very good at measuring the small color differences demanded for industrial process control (Patterson, 1987; MacDougall, 2001). Objective measurement of color can be done by colorimeters. Barreiro et al. (1997) studied the effect of thermal treatment on kinetics of color change of double concentrated tomato paste using a tristimulus colorimeter. Ochoa et al. (2001) investigated the effect of room temperature and light on kinetics of color change of raspberry, sweet and sour cherries preserves that are packed in glass containers using a spectrophotometer at 527 nm.

2.7.3 L*,a*,b* color space

L*, a*, b* is an international standard adopted by CIE. Here L* is the luminance or lightness component which ranges from 0 for black and 100 for perfect white, a* is the chromatic component indicating green for negative a* and red for positive a* values, and b* is the other chromatic component indicating blue for negative b* and yellow for positive b*. Hunter L,a,b and CIE L*,a*,b* are both mathematically derived from tristimulus values. Neither scale is visually uniform and Hunter L,a,b is over expanded in the blue region whereas CIE L*, a*, b* is over expanded in the yellow region. The current CIE recommendation is to use CIE L*, a*, b* color space (Hunter, 2001). Both scale is widely used to quantify the colors of foodstuffs: Maskan (2001) quantified the color kinetics of kiwifruits during hot air and microwave drying; and Nisha et al. (2004) studied the degradation kinetics of visual green color in spinach and the effect of salt in terms of Hunter L, a, b color space. Pedreschi et al. (2005) studied the kinetics of browning during deep-fat frying of blanched and unblanched potato chips using CIE L*, a*, b* color space.

2.7.4 Computer imaging

Computer imaging can be defined as the acquisition and processing of visual information by computer. The importance of computer imaging is derived from the fact that our primary sense is our visual sense and the information that can be conveyed in images has been known throughout the centuries to be extraordinary-one picture is worth a thousand words.

Computer imaging systems are comprised of two primary component types: hardware and software. The hardware components can be divided into the image acquisition subsystem, the computer itself, and the display devices. The software allows manipulating the image and performing any desired processing on the image data (Umbaugh, 1998).

In food engineering research, it is often necessary to analyze the surface color of food samples both qualitatively and quantitatively. Qualitative analysis may involve visual inspection and comparison of the food samples such as lighter, darker and more appealing in color. Quantitative analysis may involve obtaining color distribution and averages (Yam and Papadakis, 2004). Computer vision has been widely used to automate quality evaluation (Luzuriaga et al., 1997) using the

difference in L*, a*, b* values. Luzuriaga et al. (1997) studied the melanosis levels and developed predictive relationships of view area versus weight of white shrimps using a machine vision system. Image processing software used in Luzuriaga et al.'s study analyzes the images pixel by pixel and returns the values in L*a*b* coordinates. Yam and Papadakis (2004) investigated measurement and analysis of microwaved pizza. Measurement of color was done by a digital camera and analysis was done by Adobe Photoshop.

2.7.5 Color kinetics

There have been several studies on the rate of color change. Majority of these studies indicate either zero-order (equation (2.14)) or first-order (equation (2.15)) degradation reaction kinetics.

$$C = C_0 \pm k \cdot t \tag{2.14}$$

$$C = C_0 \cdot \exp(\pm k \cdot t) \tag{2.15}$$

where (+) and (-) shows formation or degradation of any color quantity. Also color kinetics can be expressed with fractional conversion (equation (2.16)) as follows:

$$\frac{C - C_f}{C_0 - C_f} = \exp(\pm k \cdot t) \tag{2.16}$$

where C_0 and C_f are the initial and final color quantity, respectively. Maskan (2001) reported that kinetics of color change of kiwifruits can be either expressed by zero-order or first order reactions. Nisha et al. (2004) reported that the visual green color in spinach can be inspected by a-value which followed first-order degradation kinetics. Chen and Ramaswamy (2002) used fractional conversion equation to fit the color data of ripening bananas and found an R^2 greater than 0.95 for L, a, b and ΔE values.

3. MATERIALS AND METHOD

3.1 Grapes

Thompson Seedless grapes (*Vitis vinifera*) were bought from a local store and were stored in plastic bags in a refrigerator at 4°C until pretreatments or drying without pretreatments. Individual berries were graded using a caliper. The average diameter of the grape along the long axis was measured, and only the ones that fell in the range of 17.5-18.5 mm were selected. However for microwave bulk drying, grape diameters were in the range of 16-22 mm. Grapes were washed with tap water and their surfaces were dried with a paper towel. Initial moisture content of grapes was measured using an infrared Moisture Balance (CSC Scientific Company, Inc.) or infrared Moisture Determination Balance (FD-620 Kett Electric Laboratory, Japan). Infrared determination of moisture content method was used by Bilbao-Sainz et al. (2006) for apple cylinder and by Togrul and Pehlivan (2003) for apricot. The moisture content of grapes ranged between 78% and 82.6% wet basis. Grapes that were not pretreated were referred as control or untreated.

On the average Thompson seedless grapes contained 80.54% water, 18.10% carbohydrate, 0.72% protein, 0.48% ash and 0.16% fat. Since the physical properties of Thompson seedless grapes were approximately known, density, specific heat capacity (C), thermal conductivity (k) and thermal diffusivity (α) were calculated using the descriptive equations:

Density of grape was calculated using equation (3.1) and found as 1077.932 kg/m^3.

$$\rho = \frac{1}{\sum \frac{x_i}{\rho_i}} = \frac{1}{\frac{x_C}{1600} + \frac{x_P}{1320} + \frac{x_F}{920} + \frac{x_A}{2420} + \frac{x_W}{1000}} \quad \textbf{(3.1)}$$

Here, ρ_i is the density of the ith component. For an unfrozen food specific heat is calculated using equation (3.2),

$$C_{grape} = 1.6x_C + 2.0x_P + 2.0x_F + 1.1x_A + 4.2x_W \quad \textbf{(3.2)}$$

where C_{grape} is the specific heat of the grape. Both in equation (3.1) and (3.2), x is the weight fraction and the subscripts C, P, F, A, W denotes carbohydrate, protein, fat, ash and water, respectively. C_{grape} was calculated as 3.395 kJ/kg°C.

A general equation to find thermal conductivity of biological materials based on specific heat capacity is given in equation (3.3) where k_{water} is the thermal conductivity of water and C_{water} and C_{grape} is the specific heat capacity of water and grape, respectively.

$$k_{grape} = k_{water} \cdot \frac{C_{grape}}{C_{water}} \quad \textbf{(3.3)}$$

Using equation (3.3) grape's thermal conductivity was calculated as 0.479 W/m·°C. Thermal diffusivity was found using equation (3.4),

$$\alpha_{grape} = \frac{k_{grape}}{\rho_{grape} \cdot C_{grape}} \quad \textbf{(3.4)}$$

where α_{grape} was calculated as 1.203×10^{-7} m^2/s.

The equilibrium moisture content (M_{eq}) was obtained by extending the drying time until no measurable weight loss was observed. The equilibrium moisture content was also confirmed with respect to the psychrometric properties of hot air conditions and moisture isotherms for grapes proposed by Ertekin and Gedik (2004). The inlet properties, namely the relative humidity, temperature and pressure (51%, 21°C and 1 atm) were known. Then for the corresponding drying temperature, 50°, 60° and 70°C the relative humidity of air was found which was, in equilibrium conditions, equal to the water activity of grapes. Using sorption isotherms from Ertekin and Gedik (2004) equilibrium moisture content was calculated to be 0.100, 0.080 and 0.073 dry basis (d.b.) for 50°, 60° and 70°C drying temperatures, respectively. The equilibrium moisture content was assumed to be zero for microwave drying (McMinn, 2006; Soysal, 2004; Maskan, 2000).

3.2 Convective Drying Equipment

Grapes were put in a tray dehydrator (Excalibur, Sacramento, California) which operated in the range of 29.45°-62.78°C (85°-145°F). The temperature of the dehydrator was set to 60°C, considered as a safe temperature for grape drying. Velocity and temperature of blowing air in the dehydrator was measured using a hot wire anemometer/thermometer (Fisher Scientific, Texas, USA) and was around 0.6 m/s. Samples were taken out of the dryer and weight loss was measured using an analytical balance (Mettler-Toledo, PG 603-S).

Also drying of grapes was performed in a Fischer Scientific oven with an average air velocity of 1.8 m/s (Figure 3.1a). Weight was measured online every 5 minute using an analytic balance (Mettler-Toledo, PG 603-S) which is connected to a desktop computer via RS-232 port.

3.2.1 Convective temperature profiles

Single grape was put in Fischer Scientific oven that operated with an average air velocity of 1.8 m/s. Surface temperature of grape was measured using an infrared sensor (RAYIT1CFSW, Raytek Inc., USA). Center and ambient temperature was measured using a T-type and K-type thermocouple, respectively. DAQ-56 (Omega, USA) which was connected to USB (Universal Serial Bus) port of a computer was used to collect data from thermocouples and transfer to MS Excel. The schematic is shown in Figure 3.1b.

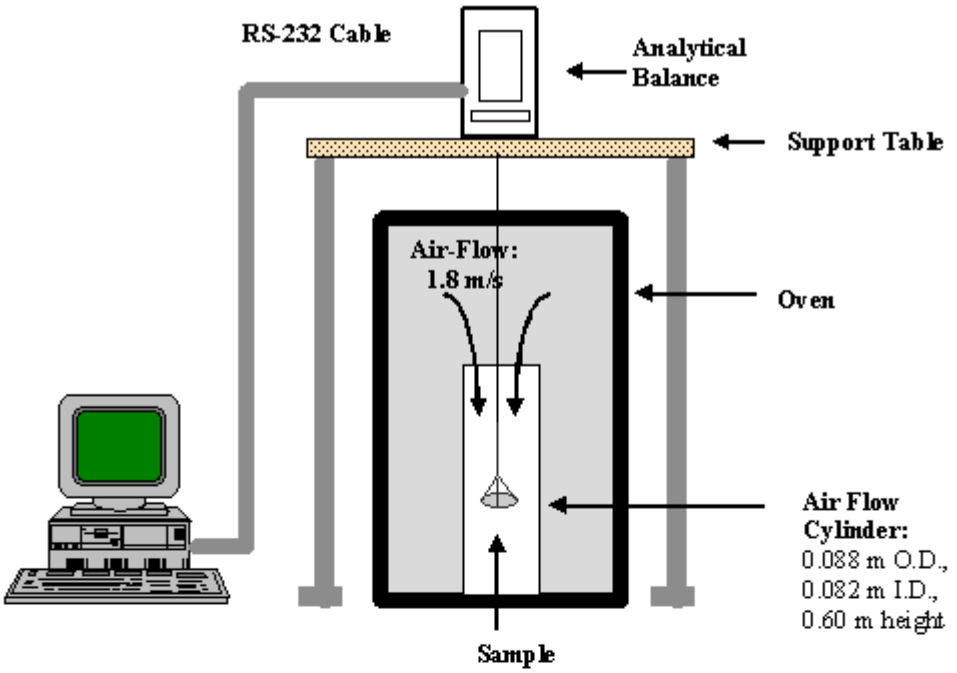

a)

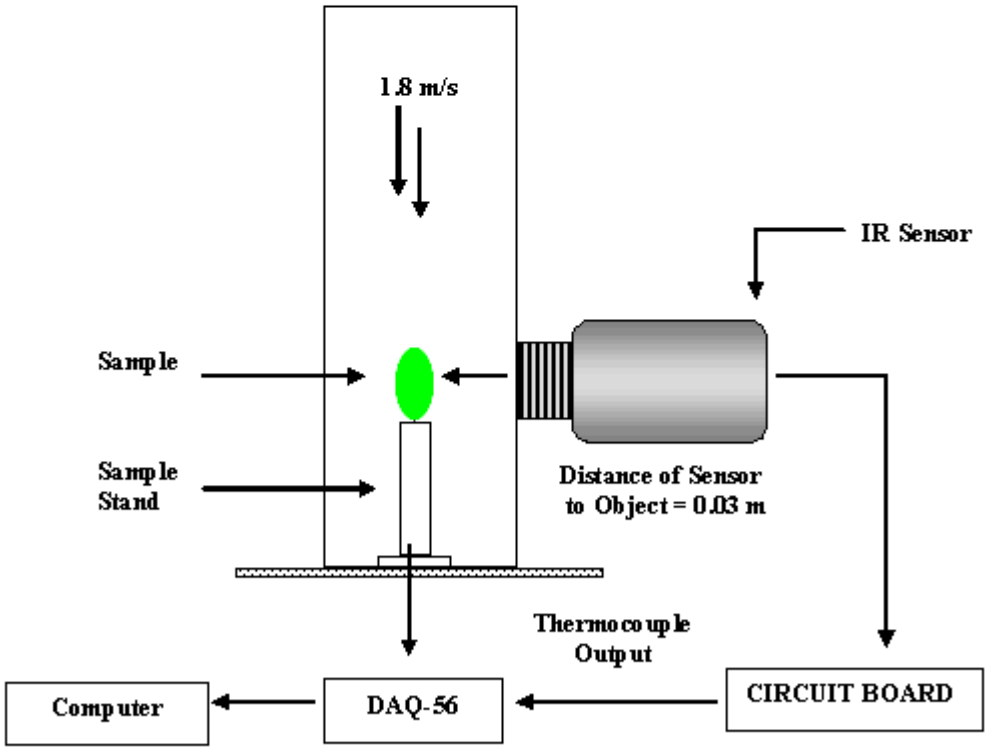

b)

Figure 3.1: a) Convective Drying, **b)** Temperature Measurement of Grapes

3.3 Dipping of Grapes in Chemical Solutions

About 50 g grapes were dipped in a beaker containing 250 ml of solution of 12.5 g (w/v) K_2CO_3 (SigmaUltra, minimum 99.0%, Sigma-Aldrich, Inc., USA) and 5 ml (v/v) ethyl oleate (mixture of isomers 98%, $C_{20}H_{38}O_2$, Acros Ogranics, USA) at 30°, 40°, 50° and 60°C for 60, 120 and 180 seconds. The solution was heated using a stirrer/hot plate (Corning, model PC-420, USA). A thermometer was dipped into solution in order to follow solutions temperature. Each experiment was done twice.

3.4 Steam Blanching of Grapes

Steam blanching was performed using a continuous steam blancher (Laitram Machinery, Inc., Model DFC-001, Harahan, Louisiana, USA). The temperature of the steam can be set to a desired temperature by mixing with air, and the blanching time is controlled by the speed of the conveyor belt. The blancher was allowed to reach steady-state conditions and then grapes were steam blanched at 80°C for 270 sec, at 90°C for 140 sec and at 100°C for 90 seconds. These blanching times corresponded to the 2-log reduction of PPO at 80, 90 and 100°C steam temperatures (see Section 3.4.2).

Immediately after steam blanching grapes could be cooled either by spraying water onto them or by leaving them in ambient air and let them cool naturally. The latter case was selected because cooling is slower and there could be further PPO inactivation. Since in industrial practice, soon after blanching grapes will be dried, there was no need to wet them by water spraying to cool them. Since the surface was wetted with steam during blanching, some evaporative cooling took place in ambient air, which explains the convective heat transfer coefficient higher than the usual.

3.4.1 Determination of thermo-physical properties of grapes

To determine the heating and cooling characteristics of grapes in the continuous steam blancher (Laitram Machinery, Inc.) the following experiment was performed:

Copper-Constantan thermocouples (36 gauge) were placed in the center of five grapes of the same size, and time-temperature data were collected at every second at 80°, 90° and 100°C steam temperature using a data acquisition system (Omega, DAQ-55 Stamford, Connecticut; Engineering and Cyber Solutions, Inc., Gainesville,

Florida). The slowest heating-cooling curve was selected for analysis. This represented the thermocouple that was placed closest to the center. Thermal Processing Simulation software (Engineering and Cyber Solutions Inc., Gainesville, Florida, USA) was used to determine the thermophysical properties of grapes. Grapes were assumed to be cylindrical objects and diameter and length of the grape for the selected heating-cooling curve was given as an input to the program. Temperature versus time profiles for grape center and steam blancher were also given as inputs. Grape radius and length were divided into 10 nodes and temperatures at all nodes were calculated during heating and cooling. Thermal properties of grapes (Table 3.1) namely the thermal diffusivity, outside heat transfer coefficient and thermal conductivity were estimated by a trial-and-error procedure, shown in Figure 3.2, by minimizing the difference between the experimental and predicted temperature profiles.

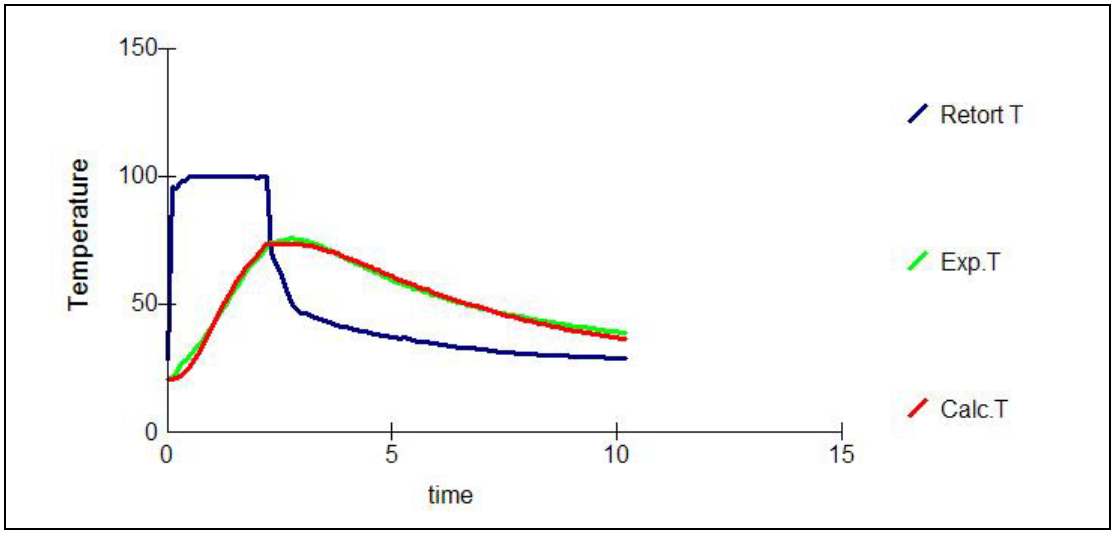

Figure 3.2: Trial and Error Fitting of Calculated Heating Curve to Experimentally Found Curve

Table 3.1: Thermal Properties of Grapes and Environment during Steam Blanching Found by Simulation Software

Grape	Steam
$\alpha_{heating}=1.49\times10^{-7}$ m^2/s	$h_{heating}=68000$ W/m$^2\cdot$°C
$\alpha_{cooling}=1.39\times10^{-7}$ m^2/s	$h_{cooling}=800$ W/m$^2\cdot$°C
k=0.40 W/m·°C	

3.4.2 PPO inactivation kinetics

Preliminary drying experiments with peeled grapes revealed that without skin there was no browning during drying. Thus the objective was to inactivate PPO residing in the skin. The kinetics parameters for thermal inactivation of PPO (z-value=13°C and D-value=600 seconds at 66°C) in grapes were taken from Weemaes et al. (1998).

Grape radius was divided into 10 nodes, and the node closest to the skin was chosen for PPO thermal inactivation calculations. The average grape diameter used in simulations for all steam temperatures was 19.76 ± 0.05 mm thus the distance between the chosen node and surface was 1.1 mm. Since the enzyme resides in the skin, choosing this node will ensure thermal inactivation of PPO at different steam temperatures (80°, 90°, and 100°C). Using the thermophysical data of grapes and the Thermal Processing Simulation software, the residual PPO in the selected node at various steam temperatures was calculated using an iterative procedure. The blanching time resulting in 2-log reduction of PPO at each steam temperature was found.

3.5 High Hydrostatic Pressure Processing

Before pressurizing, grapes were vacuum packed in polyethylene bags using a vacuum packager (Koch Multivac, Kansas City, Missouri). The bags were then put into polyethylene jars which was 100% filled with tap water and mouth of which was tightly wrapped with Teflon tape in order to prevent any leakage of water from the lid into the pressurization chamber wherein the jar was put.

The high-pressure equipment consisted of a Stansted laboratory scale unit (Stansted Fluid Power, Stansted, Essex, United Kingdom) with a pressurization chamber of 114 mm diameter and 243 mm height, providing a usable volume of approximately 2,480 ml. The pressure containment comprised a triplex pressure barrel having stainless steel inner liner, top and bottom flanged end caps that delimit the working chamber, a nickel alloy steel main vessel body, and a ductile steel outer member, which provided protection and an annular cavity for heating or cooling capability. The pressure was applied to the yoke type closure indirectly by the use of twin pressure intensifiers, operating in opposite phase, driven by twin radial pumps that injected the working fluid into the pressurized chamber.

The intensifiers were sequentially recharged with working fluid by a pre-charge pump which also performed the chamber pre-fill and first stage pressurization functions. The pressure controller allowed the high-pressure pumping system to step ramp to simulate any programmed ramp rate less than, or equal to, the maximum rate which the pumping system could achieve. The system could reach pressures up to 600 MPa, at rapid compression rates as well as programmable pressurization and decompression cycle through a computerized PLC controller. The equipment was designed to operate with several pressure transmission fluids, including water; however, for the present investigation it was operated with a mixture of ethanol and castor oil in 9:1 ratio.

The operation of the system was straightforward: by entering compression and decompression cycles setup parameters into the PLC controller with a computer program interface. The system allowed setup operating parameters to be chosen by software interface SCADA-SCAN 1000 (Hexatec Systems, Hexham, Nortumberland, United Kingdom). The pressure profile settings were divided into six segments, each one comprised of a compression or decompression rate (1 to 350 MPa min^{-1}), a hold level or the pressure set point (up to 600 MPa), and dwell duration (1 to several hours). For the present investigation ramp rate was chosen between 120 MPa and 180 MPa, dwell time was 10, 20, 30 minutes and hold level was 300 and 600 MPa. A process including compression, holding and decompression is shown in Figure 3.3 where dwell time was 20 minutes and hold level was 300 MPa.

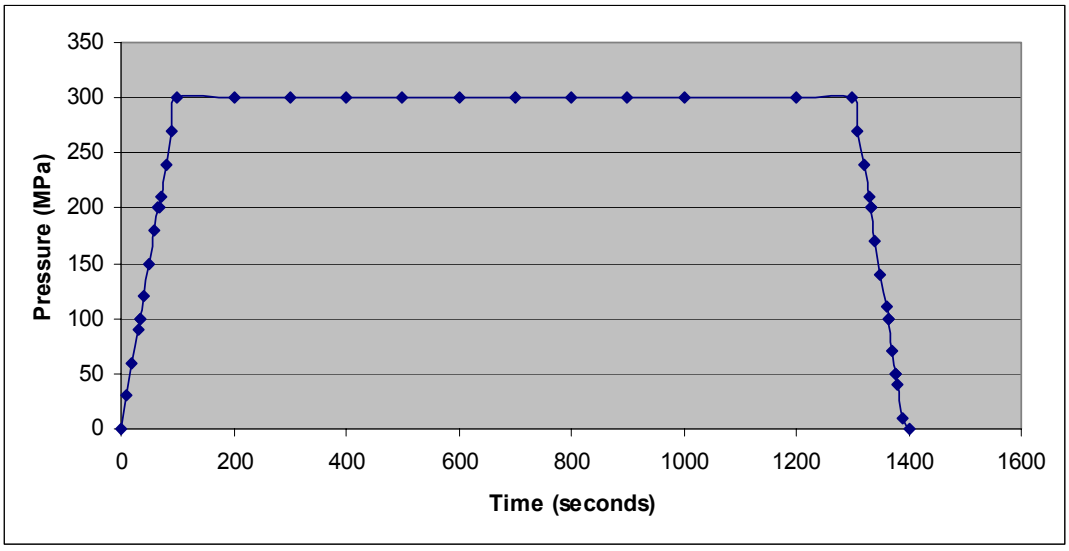

Figure 3.3: 300 MPa and 20 minute Compression of Grapes

3.6 Microwave-Assisted Drying

3.6.1 Constant or adjustable power drying

The schematic of the combined hot air microwave drying system is given in Figure 3.4.

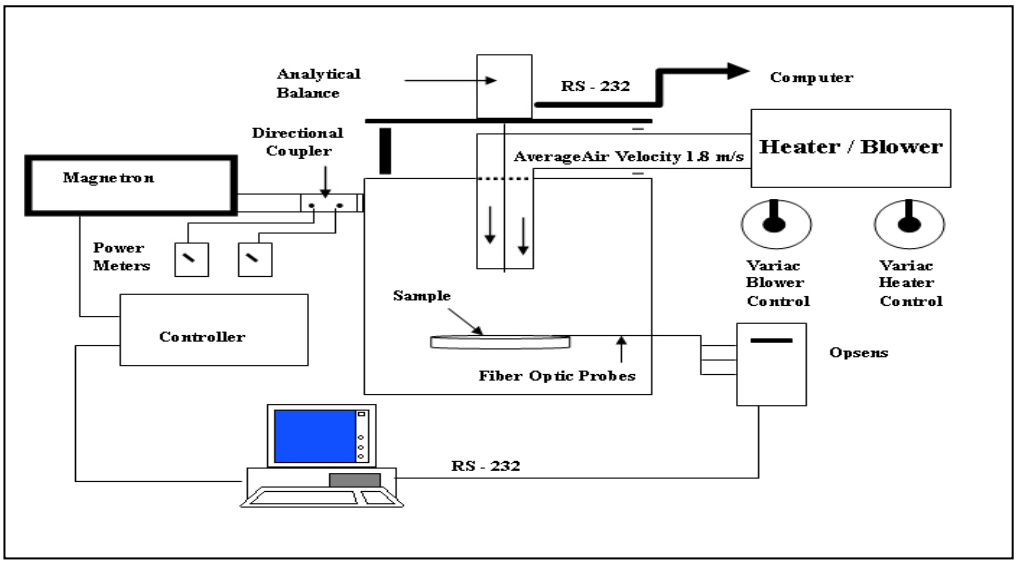

Figure 3.4: Microwave Hot Air Drying Equipment

The microwave oven was powered by a 2450 MHz magnetron with continuously variable power control from 0-2,500 W (GAE Inc., Modesto, California). The magnetron was connected to the oven cavity using WR-284 waveguide components. The oven cavity measured 0.88 m × 0.88 m × 0.88 m and had two-mode stirrers operating at 30 and 35 rpm. Both the cavity and mode stirrers were made of aluminum. Input and reflected power were measured using power meters (Model 435B, Helwett Packard Corp., Santa Clara, California) connected to a directional coupler in the waveguide. The microwave oven was designed to insure uniform heating within the cavity. Gentry and Roberts (2005) placed 1 l of water at nine different locations within the cavity that was used in this study and measured the absorbed power. They reported no significant difference ($P \leq 0.05$) in absorbed power with respect to levels and position within the cavity. The constant input power was 200, 100, and 50 W for small scale drying (SSMD) where the amount of grapes ranged between 31.4 and 36.3 g.

For bulk scale microwave drying (BSMD) applied microwave power was adjusted according to mass of grapes to be dried. Power ratio was calculated according to equation (3.5).

$$\text{Power Ratio} = \frac{\text{Applied microwave power}}{\text{Weight of grapes}} \quad \textbf{(3.5)}$$

Power ratio was 1, 0.5 and 0.25 W/g for BSMD experiments where 300 or 600 g grapes were used. The power ratios were both an initial starter; where 600 g of grapes were subjected to 600 W for 1 W/g power ratio and then the applied microwave power was kept constant at 600 W throughout. Power ratios were also kept constant; where 600 g of grapes were initially subjected to 600 W microwave power, but then according to weight loss, applied microwave power was also decreased and 1 W/g power ratio was kept constant throughout. Equation (3.5) was named as power intensity (Hu et al., 2006), as power density (Sanga et al., 2002) or as power level (Zhang et al., 2006). However intensity for a wave (mechanical, sound or electromagnetic) is the ratio of power of wave to cross-sectional area of the material that the wave interacts with; the density is wave power divided by volume and power level could be attributed to quantity of applied microwave power. Thus the term power ratio was chosen in this study to describe the ratio of applied microwave power to weight of grapes. The temperature of convective air was 40°, 50° and 60°C and its velocity was between 2 m/s (around center) and 1.8 m/s (around edges).

Grapes were pretreated either by chemical dipping or steam blanching. The chemical composition of the dipping solution was kept as same as the "Dipping of Grapes in Chemical Solutions" section where dipping temperature was 40°C and dipping time was 3 minutes. Steam Blanching of grapes was performed at 90°C for 140 seconds. Dipping at 40°C for 3 minutes dipping slightly accelerated the convective drying of grapes and 90°C and 140 seconds considerably reduced the convective drying time. Thus the objective was to see the response of microwave-assisted convective drying to pretreatments that slightly or considerably reduced convective drying time.

Three fiber optic probes (Model 790 Thermometry System, Luxtron Corporation, Santa Clara, California) were used to monitor center and surface temperature of

grapes and the entering air temperature. For SSMD, weight loss was monitored every 15 seconds using an analytical balance (Mettler-Toledo, PG 603-S) however for BSMD, weight loss was monitored every 15 minutes to 30 minutes using a balance (Mettler TE).

3.6.2 Isothermal drying

The isothermal drying apparatus used a PID controller to adjust the power to the oven cavity. This design was first introduced by Roberts and Tong (2003) where the temperature of the sample was controlled by an on/off system. This controller was upgraded to a PID controller to allow continuous power supply to the cavity. Isothermal microwave drying was only applied to SSMD.

3.7 Freezing of Grapes

Freezing of grapes were carried out by placing grapes in cold storage room at -2° and -23°C, and by putting in a freezer at -86°C (Forma Scientific, Thermo Fisher Scientific, Inc., Massachusetts, USA) for 1 day. After taking out from the cold storage and the freezer, grapes' surfaces were cleaned with a paper towel and were directly put in dryer.

3.8 Peeling of Grapes

Grapes' skin was scratched by using a very sharp razor blade which was then carefully removed by using tweezers.

3.9 Color and View Area

Color and view area measurement and analysis of grapes and resulting raisins were mainly done by a machine vision system which comprised two parts: 1) Computer vision hardware, 2) Image Processing Software. The details of both parts can be found in Luzuriaga et al. (1997). Here, the term measurement means a digital camera (Sony 1394 DFW-V500, Sony Electronics Inc., USA) was used to obtain color values of grape's and raisin's surface. The term analyze means that Color Analysis Version 7.0.1 image processing software (Engineering and Cyber Solutions Inc., Florida) was used to manipulate those color values to obtain color distribution,

averages and also the view area of grapes and raisins. Color measurement of microwave bulk dried grapes was done using a Minolta Chroma Meter (Ramsey, New Jersey).

Color was expressed in CIE values as L* (whiteness/darkness), a* (redness/greenness) and b* (yellowness/blueness). Total color change, chroma and hue angle was calculated using equation (3.6), (3.7) and (3.8), respectively:

$$\Delta E = \sqrt{(L_g - L_r)^2 + (a_g - a_r)^2 + (b_g - b_r)^2} \tag{3.6}$$

$$Chroma = \sqrt{(a^2 + b^2)} \tag{3.7}$$

$$hue° = \begin{cases} \tan^{-1}\left(\frac{b*}{a*}\right)\cdot\frac{180}{\pi}, & a*>0, b*>0 \\ \tan^{-1}\left(\frac{b*}{a*}\right)\cdot\frac{180}{\pi}+180, & a*<0, b*>0 \end{cases} \tag{3.8}$$

where subscript "g" and "r" refer to the color of the fresh grapes and raisins, respectively. The larger the ΔE value the larger the color change from the original reference state. Color kinetics can also be expressed with fractional conversion (equation (3.9)) as follows:

$$\frac{C - C_f}{C_0 - C_f} = \exp(\pm k \cdot t) \tag{3.9}$$

where C_0 and C_f are the initial and final color quantity, respectively

3.10 Scanning Electron Microscopy (SEM) Images

Prior to preparing the samples, the Alto 2500 Cryo Preparation System (Gatan, Pleasanton, CA; previously Oxford, Inc., UK) was set up according to the manufacturer's specifications. A copper specimen holder was placed onto the end of the rod of the vacuum transfer device which was held in its room temperature wooden holder to keep the specimen stable during mounting. A fresh grape berry

was cut into small pieces using an ethanol-cleaned, sharp razor blade. A single piece of sample was mounted onto the brass specimen holder using Tissue-Tek O.C.T. Compound (Miles Scientific, Naperville, IL). The end of the vacuum transfer device with the specimen on the holder were plunged directly into a styrofoam container containing slushed liquid nitrogen. A slight vacuum was drawn on the specimen allowing the liquid nitrogen to chill to slightly below -192°C. The holder containing the specimen was pulled up into the small, isolated chamber of the vacuum transfer device. The chamber was closed, the vacuum was released, and the specimen was transferred to the preparation chamber of the cryo preparation system. Thus, the specimen remained frozen and under vacuum during the transfer minimizing the possibility of water condensing onto the sample surface.

Samples were fractured in the preparation chamber using the chilled knife for observation of the grape interior. Both unfractured (skin) or fractured (interior) samples were heated to -85°C for 5 to 10 min to sublimate water from the sample surface since water is opaque to electrons. The samples were subsequently chilled to below -130°C and coated with gold-palladium inside the preparation chamber. The coated samples were transferred to the specimen cryo stage in the chamber of a Hitachi S-4700 field emission SEM (Hitachi, Japan) where they were viewed and photographed at 2 kV. Digital images were captured at 2560x1960.

3.11 Statistical Analysis

Using curve fitting tool (CFT) of Matlab software (Natick, Massachusetts) non-linear regression analyses were performed to thin-layer models (Table 2.2). Three criteria were adopted to evaluate the goodness of fit in each model: the R^2 (regression coefficient), SSE (Sum of Squares Due to Error) and RMSE (Root Mean Square Error). SSE and RMSE was calculated using equation (3.10) and (3.11), respectively.

$$SSE = \sum_{i=1}^{N} \left(MR_{\exp,i} - MR_{predict,i} \right)^2 \quad \textbf{(3.10)}$$

$$RMSE = \left[\frac{1}{N} \cdot \sum_{i=1}^{N} \left(MR_{\exp,i} - MR_{predict,i} \right)^2 \right]^{1/2} \quad \textbf{(3.11)}$$

where $MR_{exp,i}$ is the experimental moisture ratio; $MR_{predict,i}$ is the predicted moisture ratio; N is the number of experimental points.

Moisture ratio was calculated with left side of equation (2.2). An R^2 closer to 1 and an SSE or RMSE a value closer to 0 indicates a better fit.

3.12 Numerical Simulations of Temperature Profiles

Numerical simulations were conducted for temperature profiles of convective drying of untreated and steam blanched grapes, for steam heating of grapes during blanching and for microwave drying of untreated grapes. The main assumptions for all cases were:

1. The initial temperature of grape was uniform.
2. The initial moisture content of grape was uniform.
3. Both heat and moisture flows were considered in radial direction.
4. Heat losses due to radiation were not considered.

For simulations Partial Differential Equation Toolbox of Matlab was used. In this toolbox Generic Scalar type of equation was selected and the partial differential equation was specified to be parabolic type (equation (3.12)).

$$d \cdot u' + div(c \cdot grad(u)) + a \cdot u = f \quad \textbf{(3.12)}$$

Here u is a quantity that changes with time and space. The general equation for transient heat conduction in cylindrical coordinates is as follows:

$$\frac{1}{r}\cdot\frac{\partial}{\partial r}\left(k\cdot r\cdot\frac{\partial T}{\partial r}\right)+\dot{q}=\rho\cdot C\cdot\frac{\partial T}{\partial t} \quad \textbf{(3.13)}$$

Here T is temperature, t is time (seconds), r is radius (m), k is thermal conductivity (W/m·°C), ρ is density (kg/m^3), C is specific heat (J/kg·°C) and $\dot{q}$ is the heat generation (W/m^3). For all cases grapes were assumed to be cylinders thus differential equations were solved in cylindrical coordinates. The constants d, c, a and f in equation (3.12) was taken as ρ·C, k·r, zero and $\dot{q}$, respectively, to solve equation (3.13) in accordance with equation (3.12). It should be also noted that the constant f in equation (3.12) can be replaced both by internal heat generation or heat loss due to evaporation or some other means.

Matlab requires boundary conditions to be specified to solve equation (3.12). There are two types of boundary conditions that can be specified: (1) Dirichlet condition, where the boundary is at constant temperature, (2) Neumann condition, where there is constant heat flux to the boundary. In this study the boundary was exposed either to steam or to convective air, thus Neumann boundary condition was selected. Matlab specifies Neumann boundary condition as follows:

$$n\cdot c\cdot grad(u)+q\cdot u=g \quad \textbf{(3.14)}$$

The boundary condition in cylindrical coordinates was:

$$k\cdot\frac{\partial T}{\partial r}=h\cdot\left(T-T_{\infty}\right) \quad \textbf{(3.15)}$$

Since the constant c in equation (3.14) was already specified as k·r, equation (3.15) was multiplied by r. To solve boundary conditions specified in equation (3.15) with equation (3.14) the constants c, q and g was taken as k·r, h·r and $h\cdot T_{\infty}\cdot r$ where h and T_{∞} were outside convective heat transfer coefficient (W/m^2·°C) and temperature, respectively.

4. RESULTS AND DISCUSSION

4.1 Dipping of Grapes Into Chemical Solutions

Dipping in ethyl oleate emulsions is widely used for grape drying which not only reduces the drying time but in some cases also improves the color quality of the raisins produced (Doymaz and Pala, 2002; Pangavhane et al., 1999). In this section the effect of dipping in ethyl oleate and potassium carbonate solution on grape's drying rate and color kinetics is investigated.

4.1.1 Drying kinetics

4.1.1.1 Effect of dipping temperature

Effect of temperature on 180 seconds dipping time is shown in Figure 4.1. As the temperature of the solution increased drying rate also increased. There is significant increase in drying rate of grapes at 60°C compared to 30°, 40° and 50°C. Below 1.0 moisture content (d.b.) (approximately MR=0.2) the beneficial effect of solution temperature decreased as seen in Figure 4.1. It took 15, 14.5, 13, 12 hours for 30°, 40°, 50° and 60°C, respectively, to decrease from 1.0 to 0.15 moisture content (d.b.) (from MR=0.2 to MR=0.015). However, from over 4.0 to 1.0 moisture content (d.b.) (from over MR=0.85 to MR=0.2) the difference in drying time was 13 hours between 30° and 60°C.

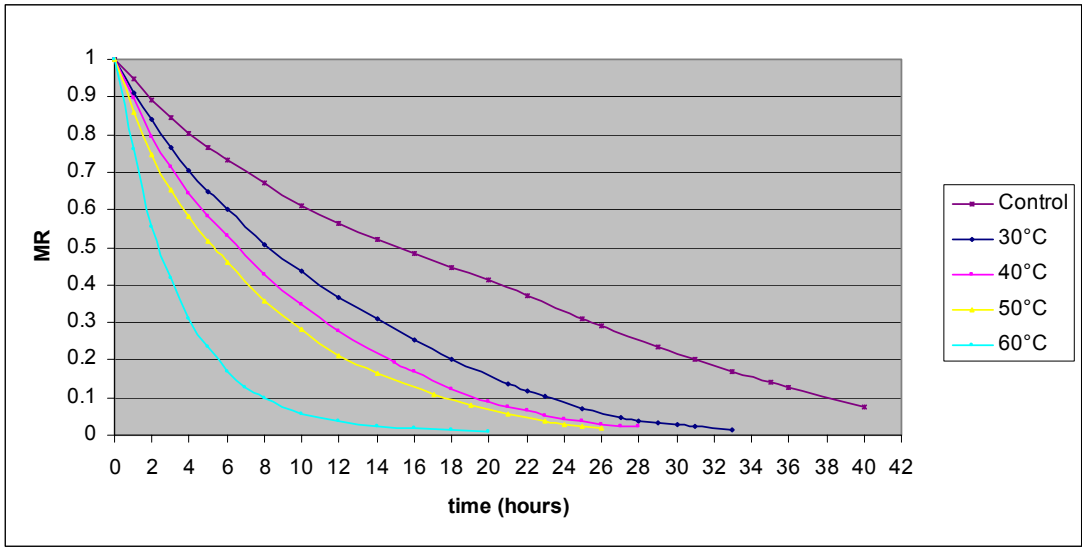

Figure 4.1: Effect of Dipping at 30°, 40°, 50° and 60°C for 180 seconds on the Drying Rate of Grapes

Effect of temperature on 120 seconds dipping time is shown in Figure 4.2. Similarly, as the temperature increased the drying rate also increased. From moisture content (d.b.) over 4 to moisture content (d.b.) 1.0 (from over MR=0.85 to MR=0.2) the difference in total drying time was 20 hours between 30° and 60°C. Below 1.0 moisture content (d.b.) (MR=0.2), to reach a moisture content (d.b.) of 0.15 (MR=0.015), drying times at all temperatures were around 14 hours.

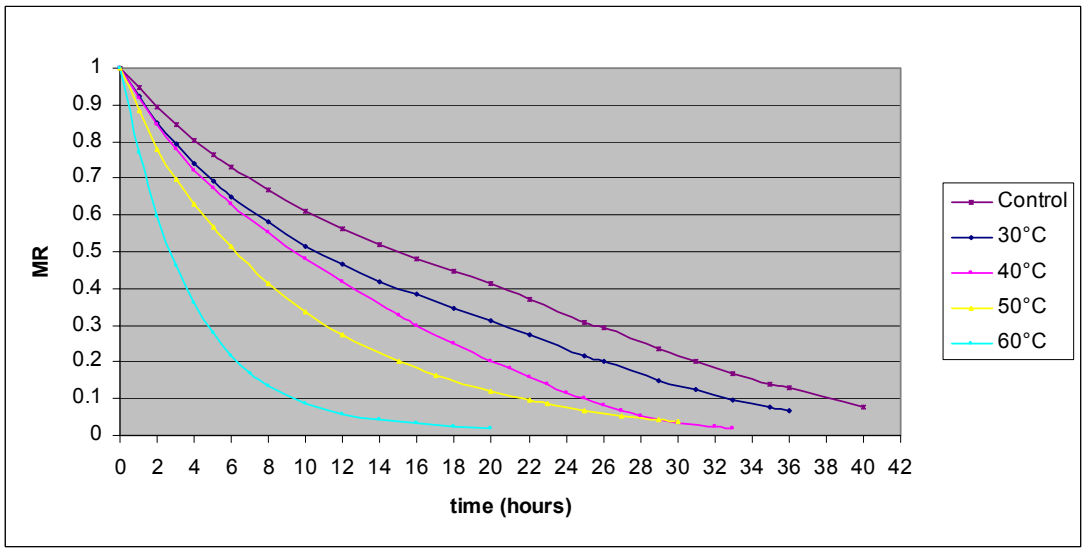

Figure 4.2: Effect of Dipping at 30°, 40°, 50° and 60°C for 120 seconds on Drying Rate of Grapes

Figure 4.3 shows the grapes dipped for 1 min at 30°, 40°, 50° and 60°C. At all temperatures the drying rate was higher than that of control. This is in agreement

with Tarhan (2007) who dipped plums in 4% ethyl oleate solution at 60°C for 60 seconds and reported acceleration in drying rate compared to that of control. However, the author reported a negative effect of addition of ethyl oleate on drying rate. In the author's study hot water dipping (no chemical solutions) for the same temperature and time combination accelerated the drying rate further. From Figure 4.3 it is seen that there was no clear distinction between drying curves of 30°, 40° and 50°C until 0.5 moisture ratio except 60°C. Thus it can be concluded that dipping temperatures lower than 60°C, affected the drying rate in the later stages of drying (below 0.5 moisture ratio) for 60 seconds dipping time.

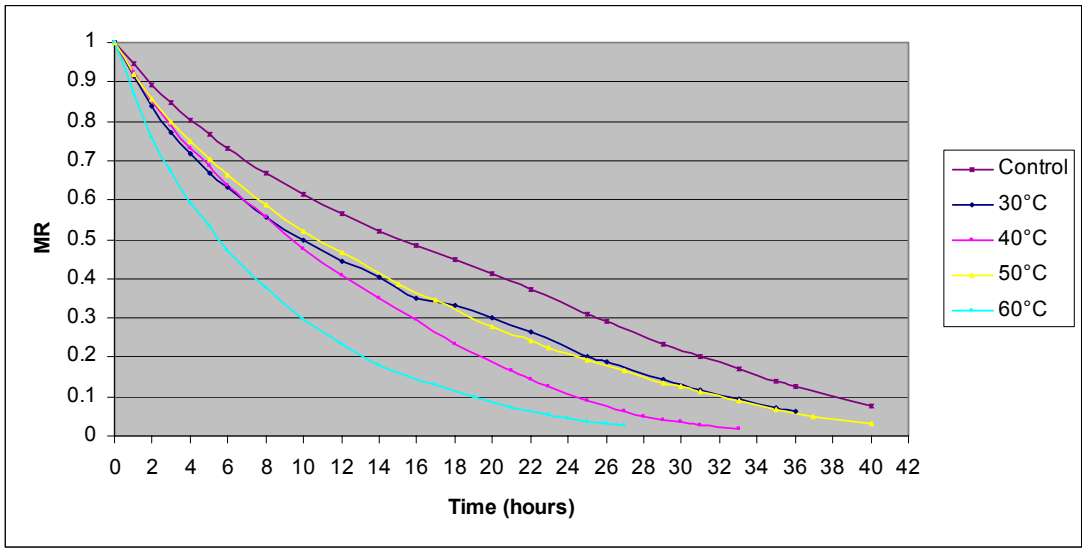

Figure 4.3: Effect of Dipping at 30°, 40°, 50° and 60°C for 60 seconds on Drying Rate of Grapes

4.1.1.2 Effect of dipping time

Figure 4.4 shows the drying rate of grapes that were dipped in 30°C solution for 60, 120 and 180 seconds. The change in drying rates was not statistically significant ($P>0.05$) as the holding time increased from 60 to 120 seconds. However there was 10 hours of reduction in total drying time as the holding time increased from 60 to 180 seconds. The result for 180 seconds holding time was in close agreement with Pangavhane et al. (1999) who also dipped grapes in 2% ethyl oleate and 2.5% K_2CO_3 solution at ambient temperature for 180 seconds and reported a significant reduction in drying time compared to control although the temperature of the dipping solution was lower than 30°C. On the contrary, Ponting and McBean (1970) dipped grapes in 2% ethyl oleate solution at ambient temperatures from 10 seconds to 180 seconds

and reported that just wetting the grapes in dipping solution was enough to accelerate drying rate and that the dipping time had no effect on drying rate. However as can be seen from Figure 4.4 to reach the moisture content of 0.5 kg/kg solids (MR=0.09) it took nearly 33 hours for 60 seconds dipping and nearly 24 hours for 180 seconds dipping. Thus dipping time had indeed affected the drying rate. However it is seen from Figure 4.1, Figure 4.2 and Figure 4.3 that the effect of dipping time became more significant as the solution temperature increased which might explain the discordance with Ponting and McBean (1970).

It is seen from Figure 4.4 that the effect of dipping time was not pronounced in the first stages of drying and the curves of 60, 120 and 180 seconds almost overlapped. However when the moisture ratio reached to 0.6, dipping time at 30°C affected the drying rate. In all stages of drying, dipping into solution at 30°C regardless of dipping time had a higher drying rate than that of control. This is not in well agreement with Doymaz (2004) who dipped plums into 2% ethyl oleate (v/v) solution at ambient temperature for 60 seconds and reported that until 0.6 moisture ratio dipping had no effect on drying rate. This might be due to the fact that, revealed by Ponting and McBean (1970), at the same drying temperature and ethyl oleate concentration, plums dry into prunes slower than does the grapes into raisins.

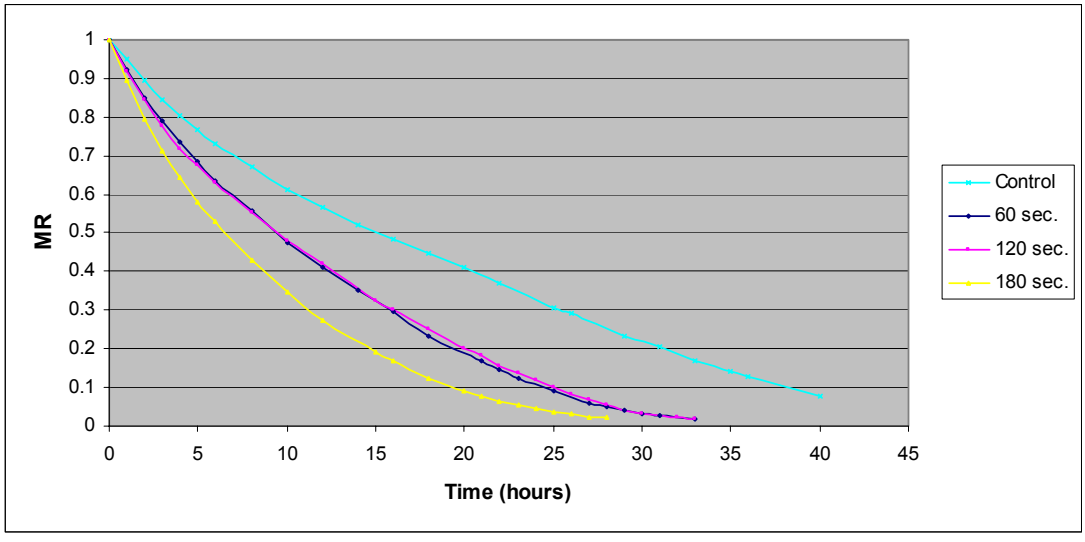

Figure 4.4: Effect of Dipping at 30°C for 60, 120 and 180 seconds on Drying Rate of Grapes

At 40°C, the drying curves of 60 and 120 seconds overlapped (Figure A.2) and there was no statistically significant (P>0.05) difference in drying rate. Although the changes at 30° and 40°C were not statistically significant, it is seen from Figure 4.4

and Figure A.2 that at both temperatures, 60 seconds holding time gave slightly better drying rates compared to 120 seconds. Increasing the holding time to 180 seconds at 30° and 40°C reduced the total drying time for 11 and 5 hours, respectively, compared to 60 and 120 seconds. It is seen from Figure A.2 that for 180 seconds holding time, there was 37.5% reduction in drying time to dry the grapes to 0.5 moisture content (d.b.) (MR=0.09) compared to control. This is in agreement with Matteo et al. (2000) who also dipped grapes in 2% (v/v) ethyl oleate and 2.5% (v/v) K_2CO_3 solution at 40°C for 180 seconds and reduced the drying time about one third of the time required to dry the untreated seedless white grapes (var. *Nevado*).

At 30° and 40°C (Figure 4.4, Figure A.2), the drying curves of 60 and 120 seconds of holding time were very close but at 50° and 60°C the drying curves of 120 and 180 seconds became closer (Figure A.3, Figure 4.5). At 50° and 60°C dipping temperatures, increasing the dipping time increased the drying rate. Increasing dipping time from 120 to 180 seconds reduced total drying time 6 and 4 hours at 50° and 60°C, respectively.

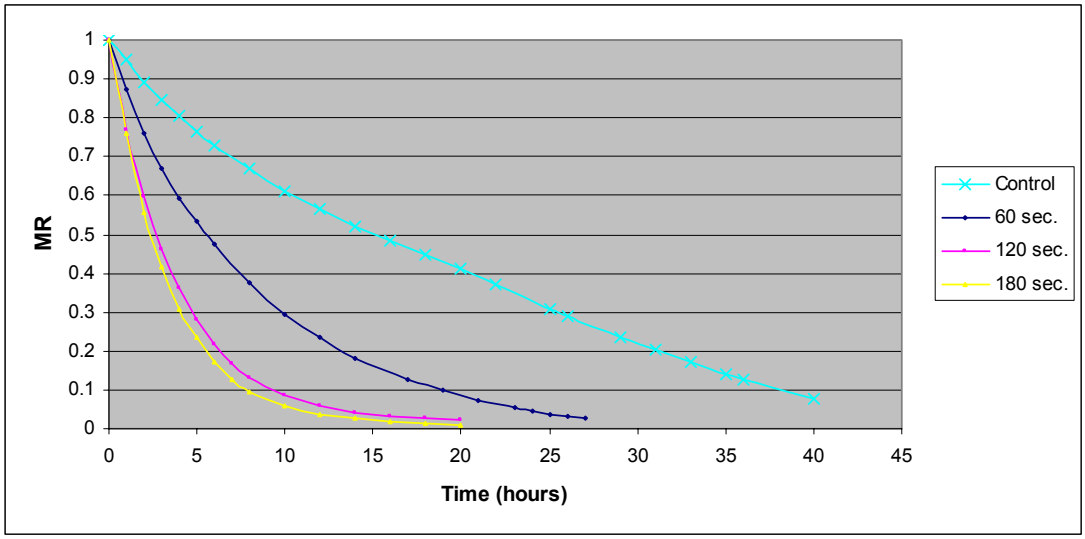

Figure 4.5: Effect of Dipping at 60°C for 60, 120 and 180 seconds on Drying Rate of Grapes

At all dipping temperatures and dipping times, 2% ethyl oleate (v/v) and 5% K_2CO_3 (m/v) increased the drying of grapes. Doymaz and Pala (2002) dipped *Sultana* grapes in 2% ethyl oleate (v/v) and 5% K_2CO_3 (m/v) for 60 seconds at ambient temperature and reported more than 134.1% reduction in drying time at 60°C drying temperature compared to untreated grapes. Although in this study it was observed that as the temperature of dipping solution increased the drying rate of grapes increased, even at

30°C dipping temperature and 60 seconds dipping time the reduction in total drying time was 15%. This might be due to difference in grape size where Sultanas have smaller diameter than the grapes that were used in this study.

4.1.2 Thin-layer modeling

Thin-layer models available in literature (Table 2.2) were fitted to moisture ratios calculated using the normalization part of equation (2.2). For all dipping times and temperatures the thin-layer models were fitted to experimental data with an R^2 greater than 0.950. Among the models tested, Midilli et al. (2002) best described the thin-layer convective air drying of grapes pretreated with 2% ethyl oleate (v/v) and 5% K_2CO_3 (m/v). R^2 was greater than 0.99, SSE and RMSE values were smaller than 0.001 and 0.02, respectively, for all experiments, statistics of which are given in Table B.5 and Table B.6. Constants of the thin-layer models (Table 2.2) for 30° and 60°C dipping temperature are given in Table 4.1 and for 40° and 50°C are given in Table B.4.

Table 4.1: Constants of Thin-layer models Applied to 30° and 60°C Dipping Temperatures Obtained by Using Non-linear Regression Analysis

Model	Dipping Temperature					
	30°C			60°C		
	Dipping Time					
	60 sec.	120 sec.	180 sec.	60 sec.	120 sec.	180 sec.
Lewis	k=0.068	k=0.064	k=0.091	k=0.125	k=0.253	k=0.290
Page	k_1=0.088 n=0.905	k_1=0.076 n=0.943	k_1=0.071 n=1.095	k_1=0.134 n=0.970	k_1=0.269 n=0.960	k_1=0.289 n=1.003
Henderson and Pabis	a=0.960 k=0.065	a=0.972 k=0.062	a=1.017 k=0.093	a=0.986 k=0.123	a=0.993 k=0.251	a=1.003 k=0.292
Logarithmic	a=0.979 k=0.061 c=-0.026	a=1.018 k=0.054 c=-0.058	a=1.083 k=0.073 c=-0.096	a=0.989 k=0.121 c=-0.006	a=0.983 k=0.264 c=-0.017	a=0.998 k=0.298 c=0.008
Approximation of Diffusion	a=0.078 k=0.677 b=0.091	a=0.049 k=0.841 b=0.072	a=-9.25 k=0.135 b=0.957	a=0.010 k=-0.004 b=-32.98	a=0.983 k=0.265 b=0.008	a=0.999 k=0.293s b=-0.341
Wang and Singh	a_1=0.001 b_1=-0.054	a_1=0.001 b_1=-0.052	a_1=0.001 b_1=-0.066	a_1=0.002 b_1=-0.091	a_1=0.006 b_1=-0.155	a_1=0.006 b_1=-0.164
Midilli et al.	a=1.011 k_1=0.115 n=0.728 b_2=-0.001	a=1.010 k_1=0.101 n=0.749 b_2=-0.001	a=0.995 k_1=0.084 n=0.973 b_2=-0.003	a=1.001 k_1=0.142 n=0.921 b_2=-0.001	a=0.999 k_1=0.262 n=0.990 b_2=0.001	a=1.002 k_1=0.286 n=1.020 b_2=0.001

4.1.3 Shrinkage

During drying of grapes into raisins, due to moisture loss, the view area and therefore the volume of the grapes decreased. Depending on the dipping temperature and dipping time grapes lost their 30-50% volume within the first 9 hours as can be seen in Figure 4.6. After then volume reduction slowed and for some cases such as 50 and 60°C for 120 and 180 seconds change in volume could be ignored.

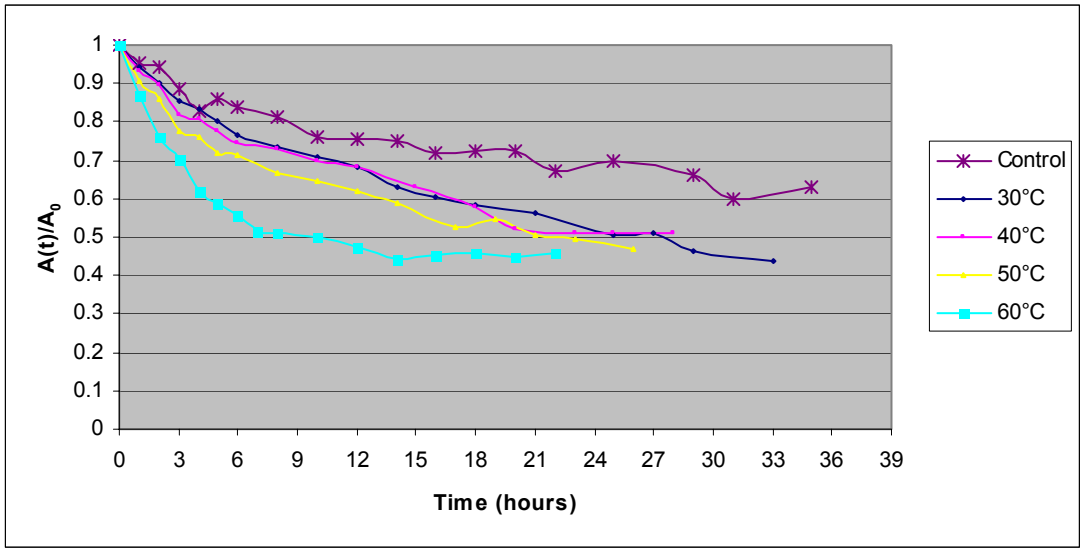

Figure 4.6: Normalized View Area of 180 seconds Dipped Grapes

At all dipping times of 30° and 40°C dipping temperatures, the volume reduction was linear with moisture content with a regression coefficient greater than 0.9 which is given in Figure 4.7.

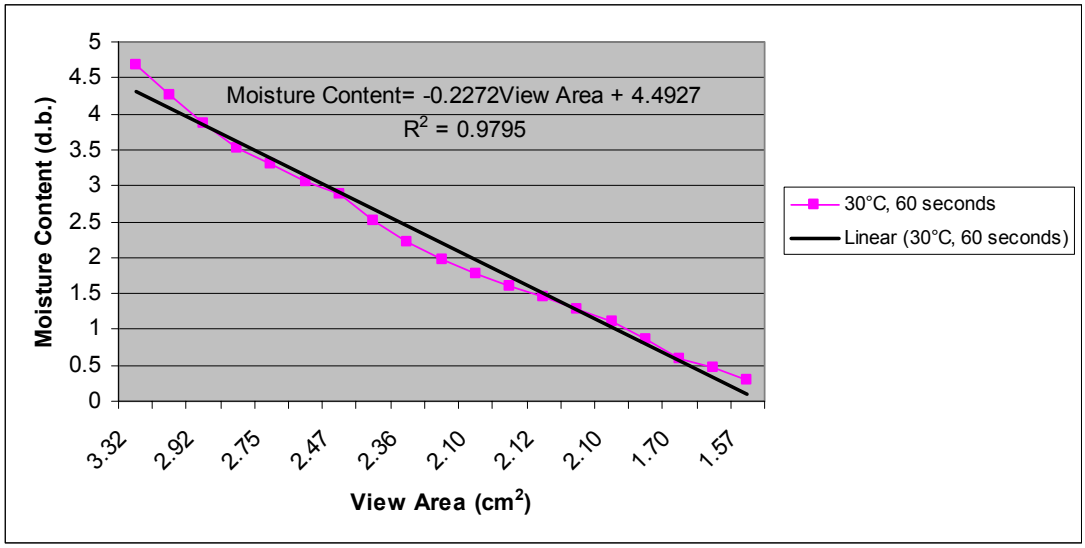

Figure 4.7: Moisture Content (d.b.) versus View Area (cm^2) of 30°C and 60 seconds Dipped Grapes

However, for 50° and 60°C dipping temperatures this relationship was exponential except 50°C and 60 seconds case which was linear. Figure 4.8 shows the exponential relationship of 60°C dipping temperature and 180 seconds dipping time case.

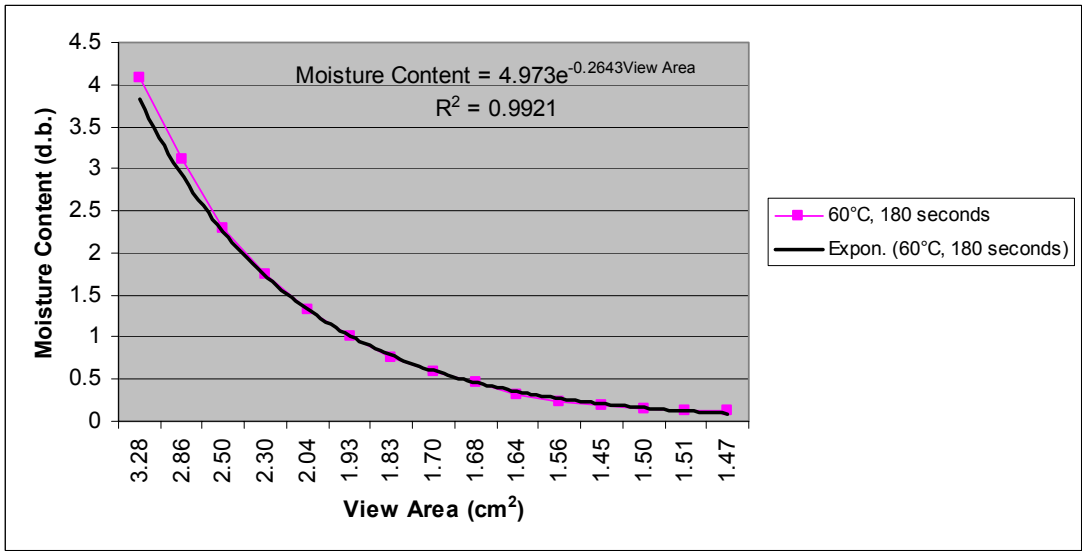

Figure 4.8: Moisture Content (d.b.) versus View Area (cm^2) of 60°C and 180 seconds Dipped Grapes

Since mass transfer rate and drying rate is proportional, from Figure 4.7 and Figure 4.8 it could be inferred that if drying rate was high, then shrinkage was less due to high radial outward vapor pressure which helped the tissue to collapse less during drying.

4.1.4 Effective diffusivities

For all dipping temperatures and dipping times effective diffusivity was calculated using equation (2.5) and the values for 30° and 60°C dipping temperature are given in Figure 4.9 and for 40° and 50°C are presented in Figure 4.10.

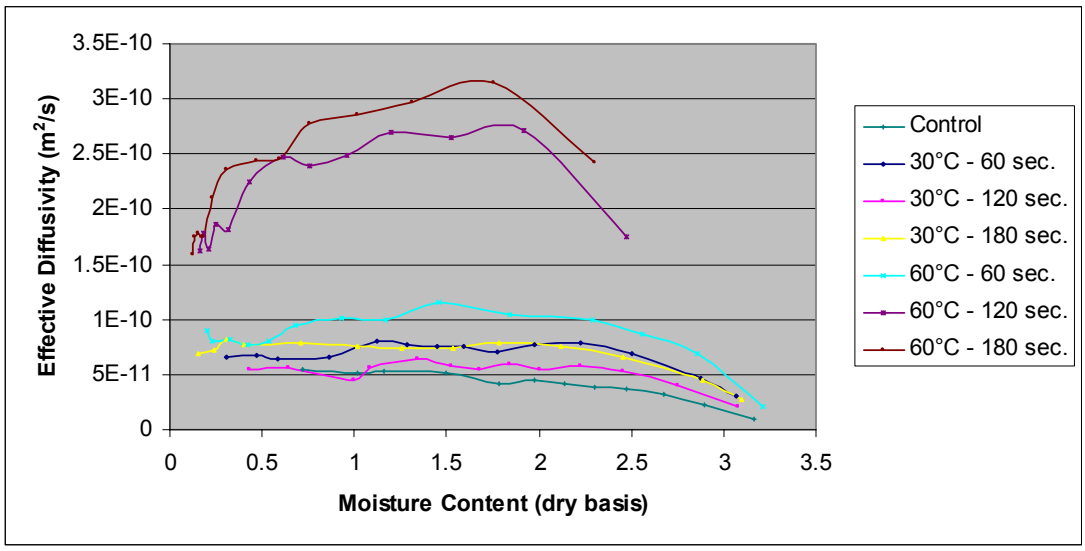

Figure 4.9: Effective Diffusivity of 30° and 60°C Dipped Grapes

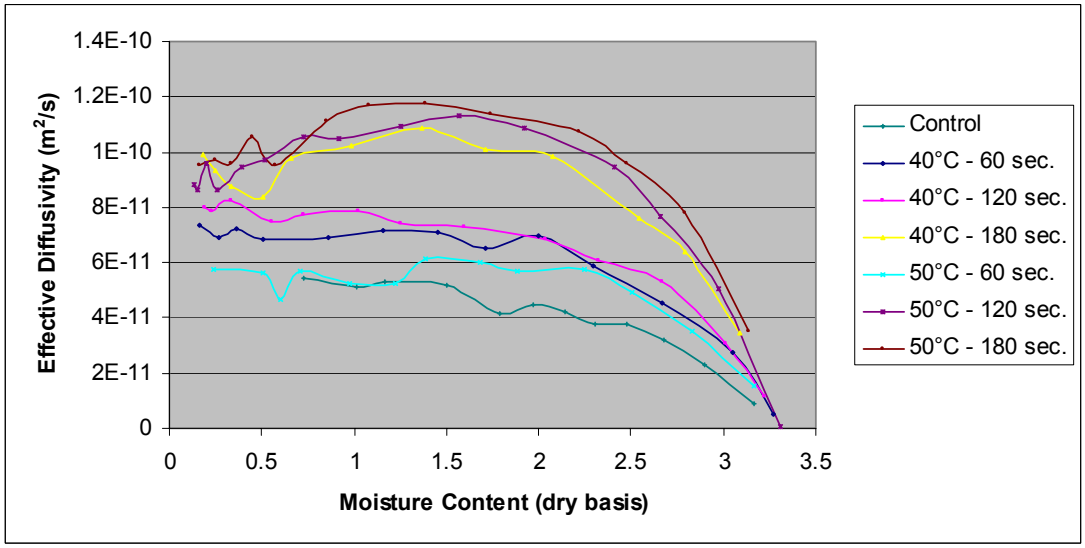

Figure 4.10: Effective Diffusivity of 40° and 50°C Dipped Grapes

As cited in the literature all of the dipped and untreated grapes showed the same characteristic effective diffusivity values which reached a maximum and then decreased as the drying progressed (Azzouz et al., 2002). All of the dipping temperatures and dipping times had effective diffusivities that were greater than that of control throughout drying except 30°C, 120 seconds and 50°C, 60 seconds dipping

combinations which showed close effective diffusivity values with control after 1 kg/kg (d.b.) moisture content as the drying progressed. This clearly suggested that regardless of dipping temperature and dipping time, pretreatment with 2% ethyl oleate and 5% K_2CO_3 accelerated the total drying process. Except 60 seconds dipping time, increasing the dipping temperature had increased the effective diffusivity. At 50° and 60°C dipping temperatures, increasing the dipping time increased the effective diffusivity values however this was not observed at 30° and 40°C dipping temperatures.

4.1.5 Color analysis

Equation (3.9) is used to normalize the b*, chroma and total color change values at all temperatures and dipping times. Kinetic parameters for 30° and 60°C dipping temperatures are given in Table 4.2 and for 40° and 50°C are given in Table C.3. ΔE, chroma and b-values followed a first-order degradation kinetics. It should be noted the C_0 in equation (3.9) for ΔE is zero. The R^2 for chroma and b*-values for all dipping temperatures and dipping times was greater than 0.92, except at 30°C dipping temperature and 60 seconds dipping time it was 0.85. Total color change data fitted in equation (3.9) with an R^2 greater than 0.94 for all cases.

Table 4.2: Non-linear Regression Coefficients of Fractional Conversion Equation to Selected Dipping Temperatures and Color Values

Constants		**Temperature**					
		30°C			*60°C*		
		Dipping time (sec.)					
		60	*120*	*180*	*60*	*120*	*180*
ΔE	C_f	58.99	62.26	56.41	61.70	46.38	38.39
	k_c (h^{-1})	-0.14	-0.12	-0.10	-0.15	-0.22	-0.37
Chroma	C_0	44.98	46.97	49.55	49.26	46.41	44.22
	C_f	7.84	7.39	13.63	10.13	19.02	22.40
	k_c (h^{-1})	-0.10	-0.12	-0.09	-0.16	-0.24	-0.46
b*	C_0	43.35	45.74	47.37	46.20	45.38	43.59
	C_f	7.35	6.99	12.68	9.43	17.45	20.59
	k_c (h^{-1})	-0.11	-0.12	-0.09	-0.16	-0.23	-0.39

Plots of total color changes for 30°C is given in Figure 4.11. If the temperature of the dipping solution is 30°C total color change of grapes steeply increases within the first ten hours and then the steepness of the curve decreases.

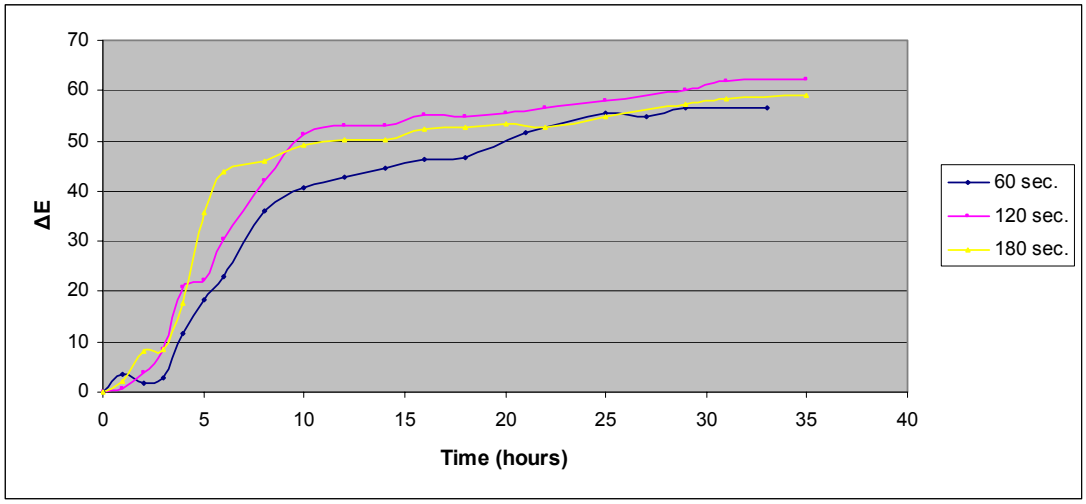

Figure 4.11: Effect of 30°C Dipping Temperature on Total Color Change at Different Dipping Times

Doubling the temperature however halved the time of steep increase of color change to five hours which is seen in Figure 4.12.

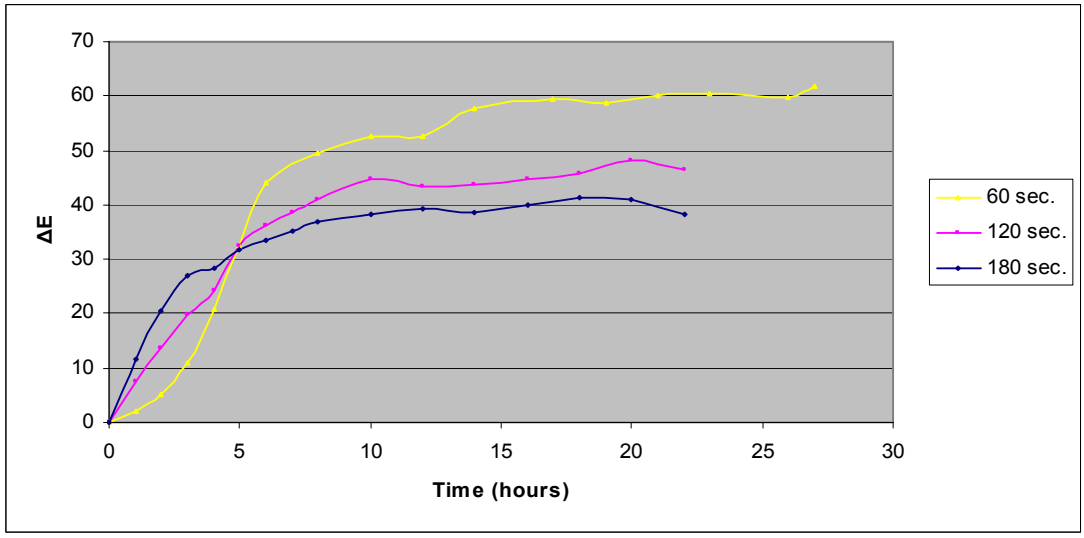

Figure 4.12: Effect of 60°C Dipping Temperature on Total Color Change at Different Dipping Times

This might be caused from under-blanching of grapes at 60°C dipping temperature and 120 and 180 seconds dipping time, where tissues were damaged because of heat and substrates became available for browning causing enzyme polyphenol oxidase. At 60°C dipping temperature and 60 seconds dipping time the total color change curve was much the same as 30°C dipping solution temperatures dipping time. It might be due to shorter dipping time at 60 seconds dipping time at 60°C dipping temperature and due to lower dipping temperature at 30°C dipping temperature and

180 seconds dipping time which could not cause tissue disrupture. It is also worth mentioning that as the drying time increased the total color change of grapes increased.

Chroma, sometimes called saturation, is the purity or strength of the color. It has two components: a*- and b*-values. There was no significant difference (P>0.05) between chroma and b*-values of the grapes for all dipping temperatures and dipping times. This may indicate the strength of yellow color forming pigments in the grapes.

From Figure 4.13 it is seen that grapes started with a hue angle of approximately between 100-110° and an L*-value of 80 which indicated a light yellow-green. After dipping in ethyl oleate and potassium carbonate at 30, 40, 50 and 60°C for 120 seconds hue angles dropped to 60° and L*-value dropped below 40 which would be a very dark orange and would be perceived as brown (Bartleson, 1976). Also the visual color change of grapes for each treatment is given in Table C.6.

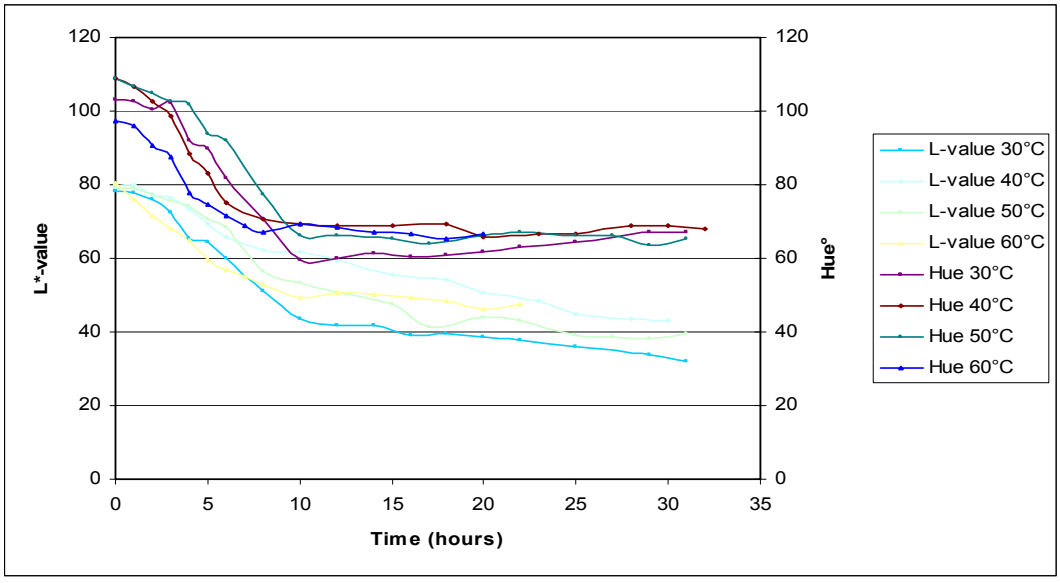

Figure 4.13: Hue Angles and L*-values of Grapes Dipped at 30°, 40°, 50° and 60°C for 120 seconds.

4.2 Steam Blanching of Grapes

Blanching serves a variety of functions, one of the main one is to destroy enzymatic activity in vegetables and some fruits, prior to further processing (Fellows, 2000). This assumption was utilized in this study to enhance mass transfer rates during drying of grapes into raisins and to inactivate browning causing enzyme, polyphenol oxidase, by blanching the grapes at different steam temperatures.

4.2.1 Drying kinetics

There was no constant-drying period in convective drying of steam blanched grapes. The drying took place in falling-rate period which is in agreement with Yaldiz et al. (2001) who used a solar dryer for Sultana grapes. The drying curves of steam blanched grapes at different steam temperatures are shown in Figure 4.14.

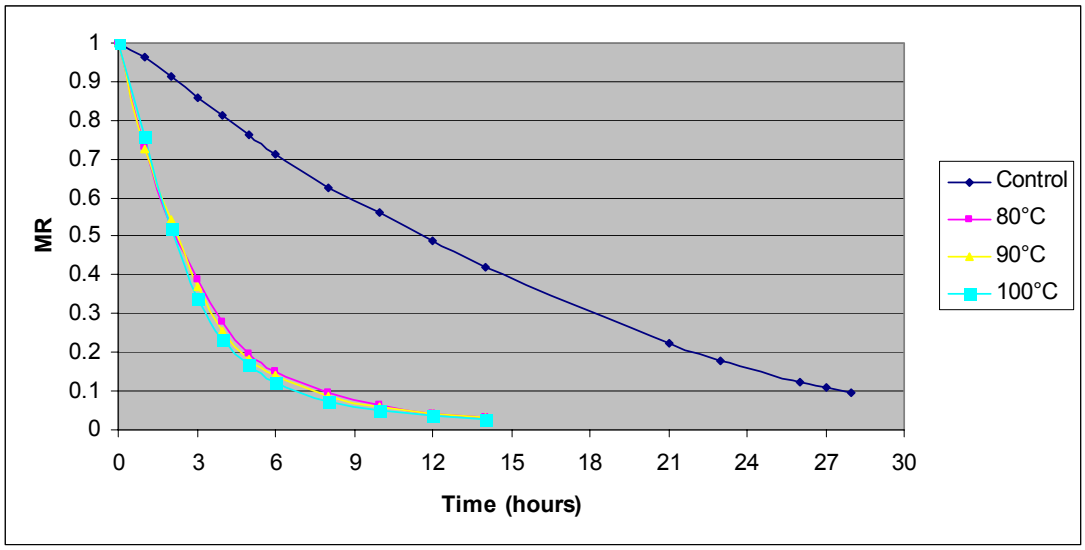

Figure 4.14: Drying Curves of Grapes Treated at Different Steam Temperatures

As the temperature of the steam increased the drying rate increased slightly, however, application of T-test revealed that there were no significant differences ($P>0.01$) between the drying curves for 80˚, 90˚ and 100˚C. Within the first 8 hours, grapes lost nearly 65% of their initial moisture, drying slowed in the next 6 hours and only 14% of the initial moisture was lost.

4.2.2 Thin-layer modeling

Thin-layer drying models were applied to describe the drying data. All thin-layer equations, except Wang and Singh (1978), described the drying curve with an R^2 of 0.99 for all steam temperatures. In the Wang and Sing equation, the constant 1 that was forced by the equation reduced the R^2 for the fit. Trials by letting this constant to become another parameter resulted in much improved R^2 values. The constants of all equations of Table 2.2 were found by fitting the experimental data to the respective equation for each blanching temperature using CFT. These constants are given in Table 4.3. Statistics of non-linear regression analysis of thin layer models (Table 2.2) are given in Table B.3.

Table 4.3: Constants of Thin-layer Models Obtained Using Non-linear Regression Analysis

Model	80°C	90°C	100°C
Lewis	k=0.315	k=0.324	k=0.341
Page	k_1=0.331 n=0.960	k_1=0.327 n=0.995	k_1=0.312 n=1.078
Henderson and Pabis	a=0.996 k=0.314	a=1.003 k=0.325	a=1.020 k=0.349
Logarithmic	a=0.980 k=0.336 c=0.024	a=0.987 k=0.346 c=0.022	a=1.008 k=0.365 c=0.017
Approximation of Diffusion	a=0.987 k=0.329 b=-0.131	a=0.997 k=0.329 b=-0.504	a=-0.999 k=0.345 b=-0.747
Wang and Singh	a_1=-0.206 b_1=0.010	a_1=-0.210 b_1=0.010	a_1=-0.216 b_1=0.011
Midilli et al.	a=1.001 k_1=0.321 n=1.011 b_2=0.002	a=0.999 k_1=0.312 n=1.064 b_2=0.003	a=1.005 k_1=0.302 n=1.147s b_2=0.003

4.2.3 Shrinkage

During drying the grapes into raisins the view area and therefore the volume of the grapes decreased. Just after blanching, approximately 6% reduction occurred in view area of grapes for all blanching temperatures, as determined by machine vision. View area of grapes throughout the drying operation is given in Figure 4.15.

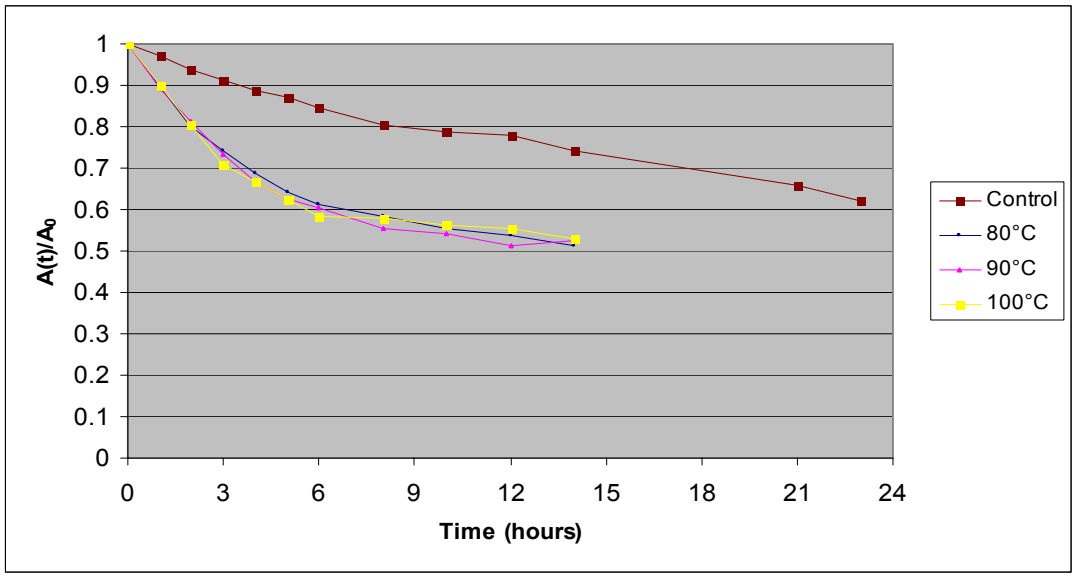

Figure 4.15: Normalized View Area of Blanched and Control Grapes during Drying

Similar to drying curves, the view area curves of blanched grapes also have a decreasing slope throughout drying. When drying was complete, grapes shrunk to 50% of their initial view area.

Change of moisture content of steam blanched grapes with view area is seen in Figure 4.16. It was seen (Figure 4.8) that at 60°C dipping temperature and 3 minutes dipping time the change of moisture content with view area could be fitted exponentially however a linear fit in steam blanching case gave better regression coefficient. Since according to Fellows (2000) one of the purposes of blanching is to soften the texture of fruits or vegetables to facilitate filling into containers prior to canning, although the outward vapor pressure was as high as in 60°C dipping temperature and 3 minutes, steam exposure might have soften the outer layers of the grape and these layers might have collapsed easier compared to dipping pretreatment which might thus have a linear relationship between moisture content and view area.

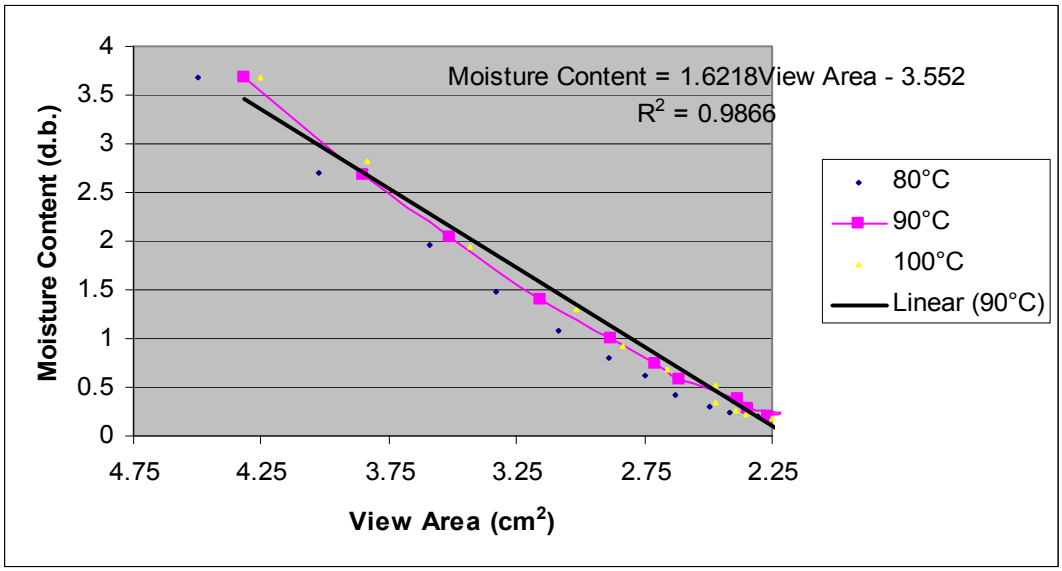

Figure 4.16: Change of Moisture Content with View Area

4.2.4 Effective diffusivities

The change in effective diffusivity of steam blanched and untreated grapes are given in Figure 4.17. Characteristic to effective diffusivity curves that were reported in the literature, both for steam blanched and untreated grapes, effective diffusivity values reached maximum and then decreased as the drying progressed which was also observed for dipped grapes. For all steam temperatures, the effective diffusivity values of steam blanched grapes were considerable higher than untreated grapes (320

times higher if maximum effective diffusivity values were compared) throughout the drying.

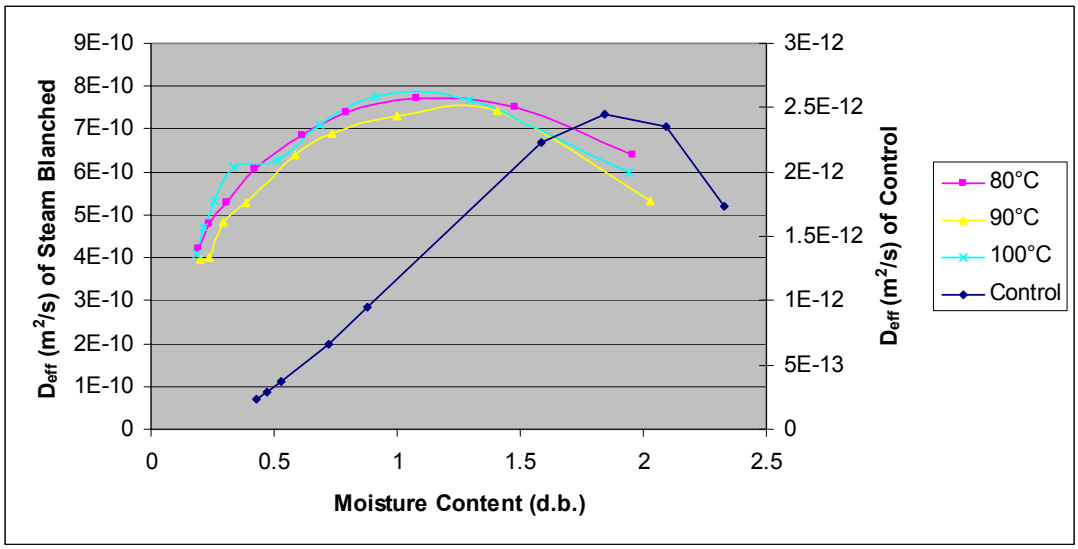

Figure 4.17: Effective Diffusivity of Untreated and Blanched Grapes

4.2.5 Color analysis

The L*-value of control grapes were 73.4 and immediately after steam treatment the L*-values were 72.7, 73.6, 72.7 for 80°C, 90°C and 100°C, respectively, which could be considered as same as the control. Therefore, steam blanching had negligible effect on the lightness of grapes. The a*- and b*-value of control grapes were around -11.0 and 38.8, respectively, but directly after blanching, a*-value of the grapes increased to around -1.7 and b*-value decreased to around 35.5 for all temperatures, which shows that the blanching itself caused a slight browning in the green color of grapes. The overall color changed from green to grayish olive green after steam treatment which might be due to conversion of chlorophyll to pheophytin and pyropheophytin.

The ΔE value measures the overall color change and is a good indicator how the color of grapes had been affected by the operation. Ideally the objective of a process is to keep ΔE as small to keep the food's color close to original after the treatment. Figure 4.18 shows the ΔE values of grapes throughout drying.

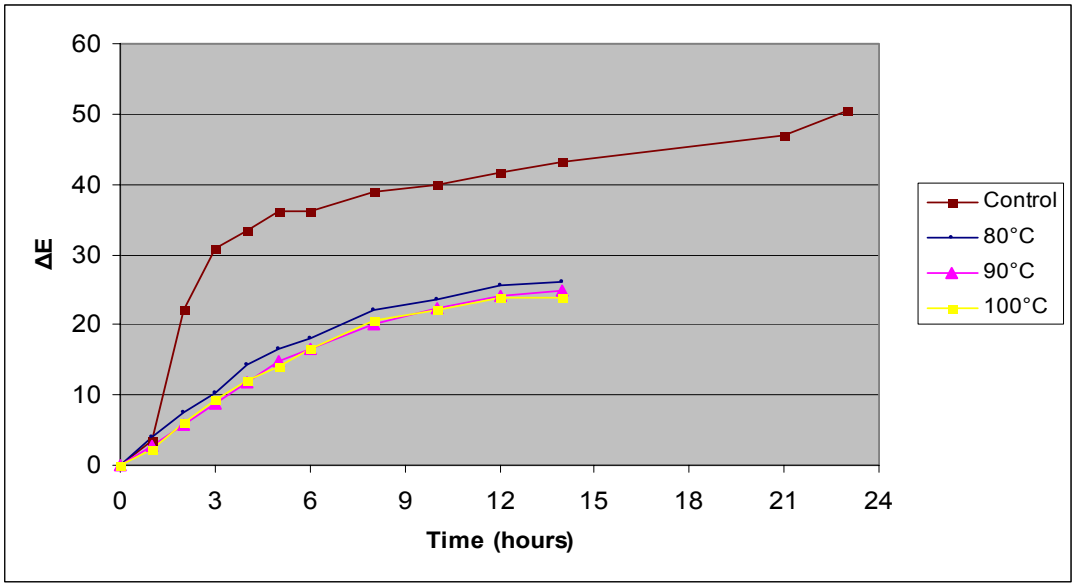

Figure 4.18: Total Color Change of Control and Steam Blanched Grapes

Figure 4.18 shows that blanched grapes had much less color change than the control. Final color of blanched grapes was "moderate yellowish brown" while control's was "grayish brown" according to color naming standards of United States Department of Commerce's National Bureau of Standards (NBS).

Equation (3.9) is used to normalize the b*, chroma and total color change values at all steam temperatures. Kinetic parameters for 80°, 90° and 100°C steam temperatures are given in Table 4.4. ΔE, chroma and b*-values followed first-order degradation kinetics. It should be noted the C_0 in equation (3.9) for ΔE is zero. The R^2 for chroma, b*-values and ΔE were greater than 0.95 at all steam temperatures. The statistics of non-linear regression analysis are given in Table C.2.

Table 4.4: Non-linear Regression Coefficients of Fractional Conversion Equation to Selected Dipping Temperatures and Color Values

Constants		**Blanching Temperature (°C)**		
		80	*90*	*100*
ΔE	C_f	26.01	24.83	23.77
	k_c (h^{-1})	0.205	0.186	0.196
Chroma	C_0	35.40	35.83	36.06
	C_f	21.47	22.59	22.99
	k_c (h^{-1})	0.207	0.186	0.193
b*	C_0	35.36	35.79	36.00
	C_f	21.15	22.23	22.77
	k_c (h^{-1})	0.206	0.181	0.189

4.2.6 PPO inactivation

Figure 4.19 shows the calculated temperature profiles at the chosen node throughout blanching and cooling. At all steam temperatures, the temperature at the node that is 1.1 mm from the skin was approximately between 78° and 85°C, which is higher than 66°C at which the D-value of PPO is 600 seconds. Therefore, although the center of the grapes experienced a lower temperature, 71°, 68° and 55°C at 80°, 90° and 100°C steam temperatures, respectively, the temperature of the node close to surface was sufficient to inactivate PPO.

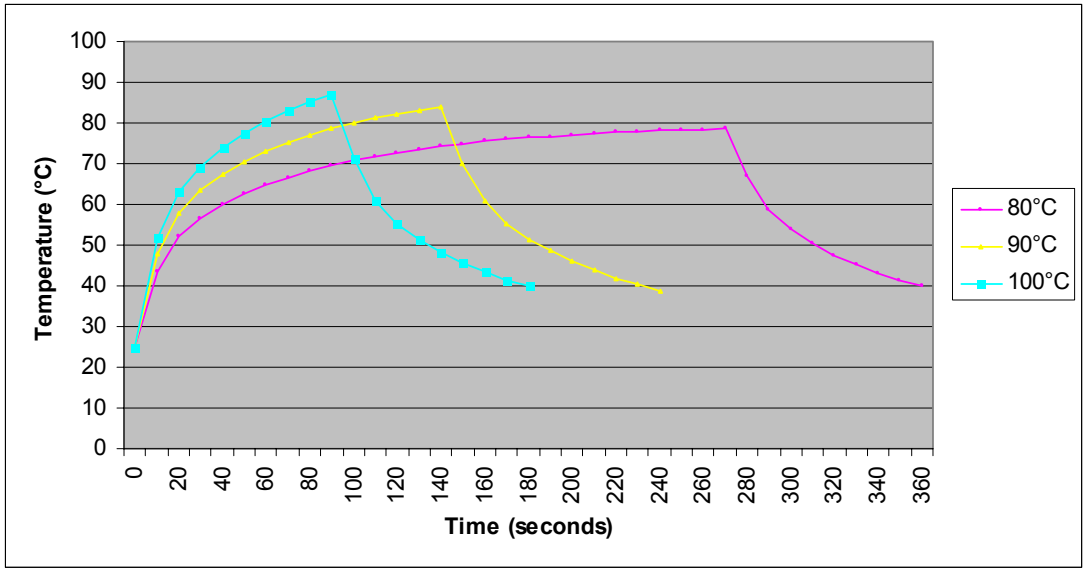

Figure 4.19: Temperature Profiles at Different Steam Temperatures at the Node, 1.1 mm from the Skin

It was seen that 99% reduction of PPO at all steam temperatures is predicted during blanching. Cooling period only reduced 0.1% of PPO, which could be ignored as seen in Figure 4.20. The actual PPO activity was not measured experimentally.

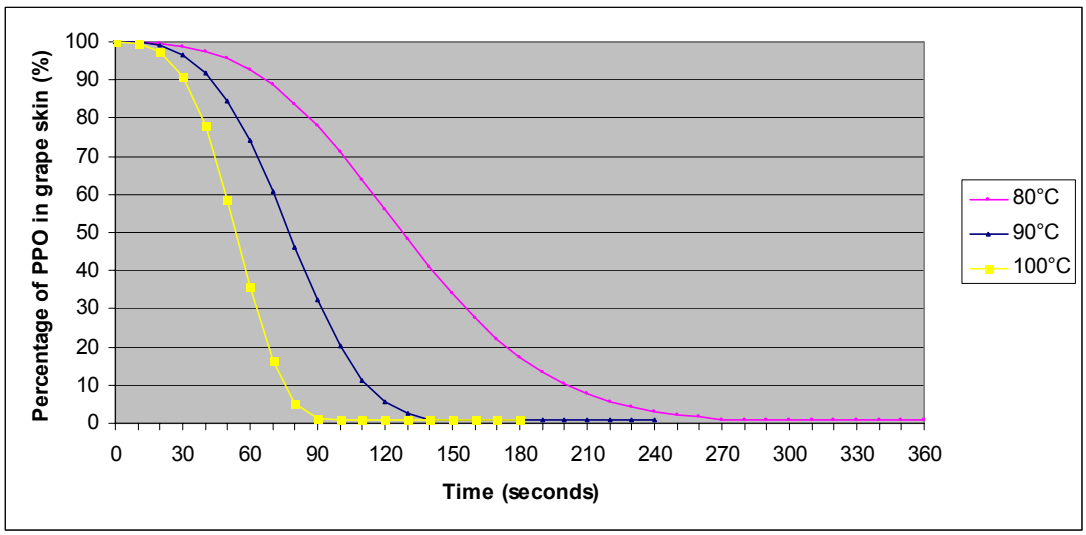

Figure 4.20: Calculated Percentage of Remaining PPO at the Node 1.1 mm from the Skin at Different Steam Temperatures

4.3 High Hydrostatic Pressure Processing

It is well known that application of high pressures (100-800 MPa) causes permeabilization of cell structure (Dornenburg and Knorr, 1993; Rastogi et al., 2000). This phenomenon is exploited here both to inactivate the browning causing enzyme, PPO, and to enhance mass transfer rates during dehydration of grapes, by pre-treating the samples at such high pressures.

4.3.1 Drying kinetics

For all applied pressure levels and holding times there was a moisture loss ranging from 1.5 to 3.4% during pressurization of grapes. Figure 4.21 shows drying rate of grapes that were pressurized at 300 and 600 MPa for 10, 20, 30 minutes and the control. It was seen that there was not much difference between the drying rate of control and pressurized grapes.

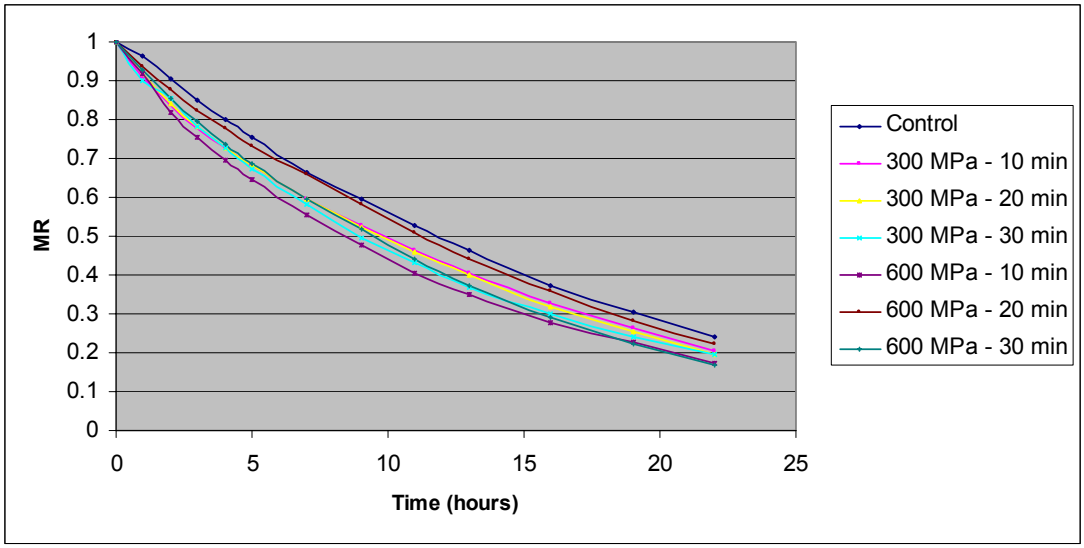

Figure 4.21: Drying Rate of Grapes at 300 and 600 MPa Pressure Level and 10, 20 and 30 minutes Holding Time

Rastogi et al. (2000) pressurized fresh potato slices at 200 and 400 MPa for 10 min and then osmotically dehydrated. They concluded that pressurization enhanced mass transfer properties of fresh potato slices thus reduced drying time. The sole reason that high pressure accelerated dehydration rate in Rastogi et al.'s experiment was that the potatoes were sliced and no other mass transfer resistant layer were present. However for grapes, although the cells were ruptured, the outermost waxy layer was not affected by HHP and was still resistant to mass transfer. The slight increase in drying rate might be caused by temperature increase from 15° to 39.4°C during compression which might have caused a mild blanching effect.

4.3.2 Thin-layer modeling

Thin-layer drying models (Table 2.2) were applied to describe the drying data. All of the applied models described the drying curves for 300 MPa (Table 4.5) and 600 MPa (Table 4.6) treatments with regression coefficient larger than 0.99 and RMSE and SSE smaller than 0.01, the statistics of which are given in Table B.1 and Table B.2. Thus for simplicity Lewis model was selected for describing the drying curves of pressure pretreated grapes. The constant of Lewis model, namely k (1/h), implies the rate of drying. It is seen from Table 4.5 that as the holding time increased the value of Lewis' constant, k, also increased which shows that holding time at 300 MPa had slightly increased the drying rate thus reduced the drying time. However at 600 MPa, holding time was not proportional to Lewis' constant. 10 minutes holding time

at 600 MPa had the highest k-value whereas 20 minutes had the lowest. It was also observed that except 20 minutes holding time at 600 MPa, increase in pressurization level increased the Lewis' constant thus the drying rate.

Table 4.5: Constants of Thin-layer Models Applied to 300 MPa Pressure Level Obtained Using Non-linear Regression Analysis

Model	10 minutes	20 minutes	30 minutes
Lewis	k=0.072	k=0.073	k=0.075
Page	k_1=0.088 n=0.917	k_1=0.083 n=0.946	k_1=0.086 n=0.951
Henderson and Pabis	a=0.974 k=0.069	a=0.982 k=0.071	a=0.985 k=0.075
Logarithmic	a=0.953 k=0.073 c=0.024	a=0.984 k=0.071 c=-0.002	a=0.955 k=0.081 c=0.037
Approximation of Diffusion	a=0.170 k=0.1 b=0.678	a=-3.866 k=0.082 b=0.979	a=-3.309 k=0.085s b=0.976
Wang and Singh	a_1=-0.066 b_1=0.001	a_1=-0.066 b_1=0.001	a_1=-0.070 b_1=0.002
Midilli et al.	a=1.002 k_1=0.095 n=0.807 b_2=-0.005	a=1.002 k_1=0.090 n=0.846 b_2=-0.005	a=0.996 k_1=0.084 n=0.957 b_2=-0.0001

Table 4.6: Constants of Thin-layer Models Applied to 600 MPa Pressure Level Obtained Using CFT

Model	10 minutes	20 minutes	30 minutes
Lewis	k=0.083	k=0.063	k=0.076
Page	k_1=0.099 n=0.920	k_1=0.057 n=1.042	k_1=0.072 n=1.024
Henderson and Pabis	a=0.979 k=0.080	a=1.003 k=0.064	a=1.003 k=0.077
Logarithmic	a=0.930 k=0.091 c=0.060	a=1.171 k=0.0485 c=-0.181	a=1.067 k=0.067 c=-0.073
Approximation of Diffusion	a=-2.424 k=0.088 b=0.982	a=-0.258 k=0.086 b=0.785	a=-0.470 k=0.086 b=0.924
Wang and Singh	a_1=-0.075 b_1=0.002	a_1=-0.0558 b_1=0.0009	a_1=-0.067 b_1=0.001
Midilli et al.	a=1.004 k_1=0.104 n=0.891 b_2=-0.001	a=0.999 k_1=0.061 n=0.911 b_2=-0.006	a=1.001 k_1=0.077 n=0.949 b_2=-0.003

4.3.3 Shrinkage

During drying, the view area of grapes shrank ranging from 27 to 36%. However it should be noted that pressurized grapes were not thoroughly dehydrated given that drying rates were close to control. The change of view area with time is seen in Figure 4.22.

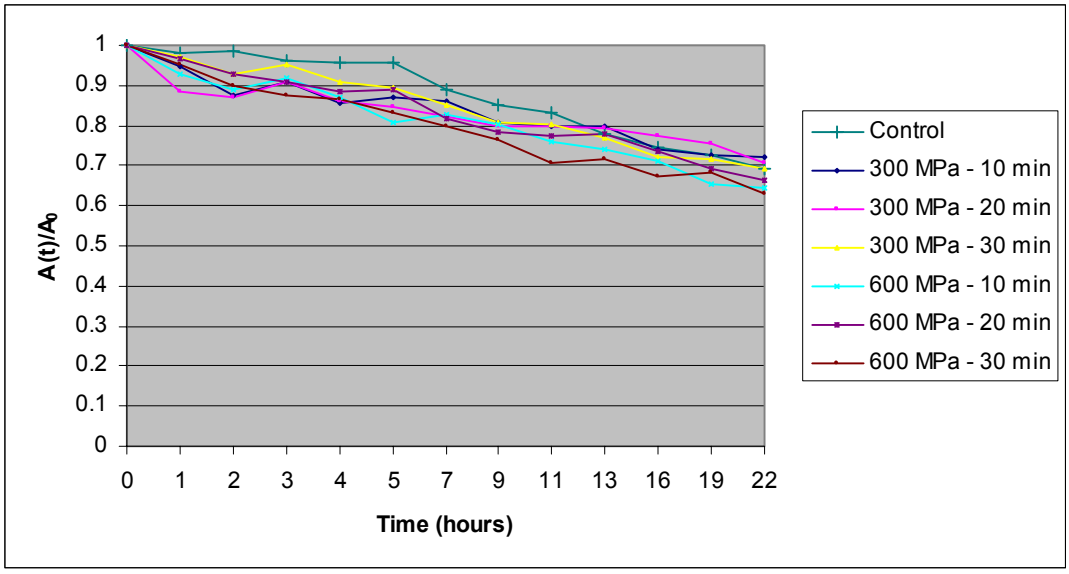

Figure 4.22: Normalized View Area of Pressurized and Control Grapes

Similar to Figure 4.7 shrinkage was linearly proportional to moisture ratio with a coefficient of determination (R^2) greater than 0.99 which is presented in Figure 4.23.

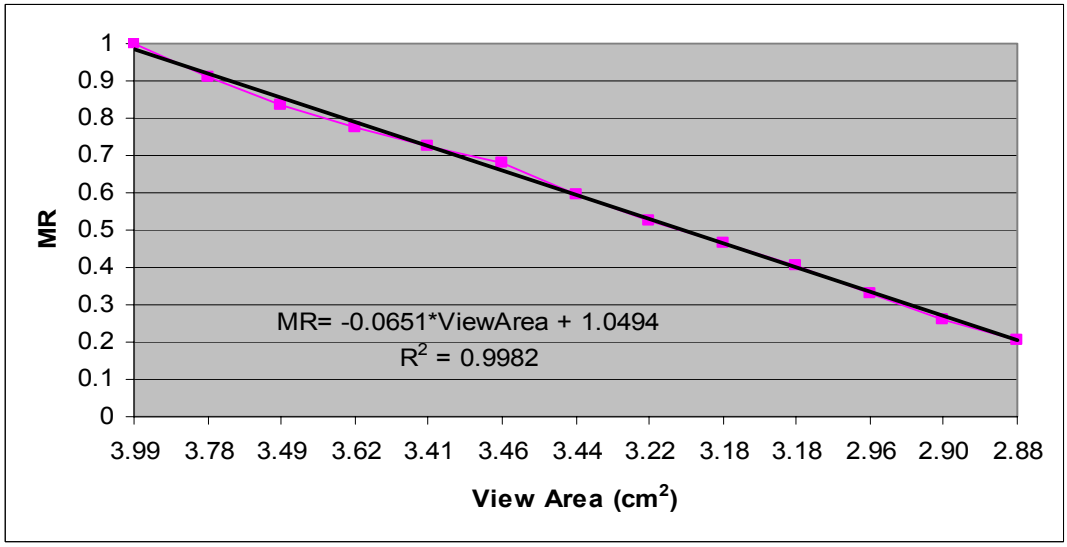

Figure 4.23: Shrinkage of 300 MPa, 10 minutes Pressurized Grapes During Drying

The collapse of grape tissue which is linear with moisture loss might be due to low radial outward pressure and also might be due to rupture of cells that was caused by pressurization.

4.3.4 Effective diffusivities

The effective moisture diffusivity was calculated using equation **(2.5)** and effective diffusivities of 300 and 600 MPa pressurized grapes and the control is given in Figure 4.24.

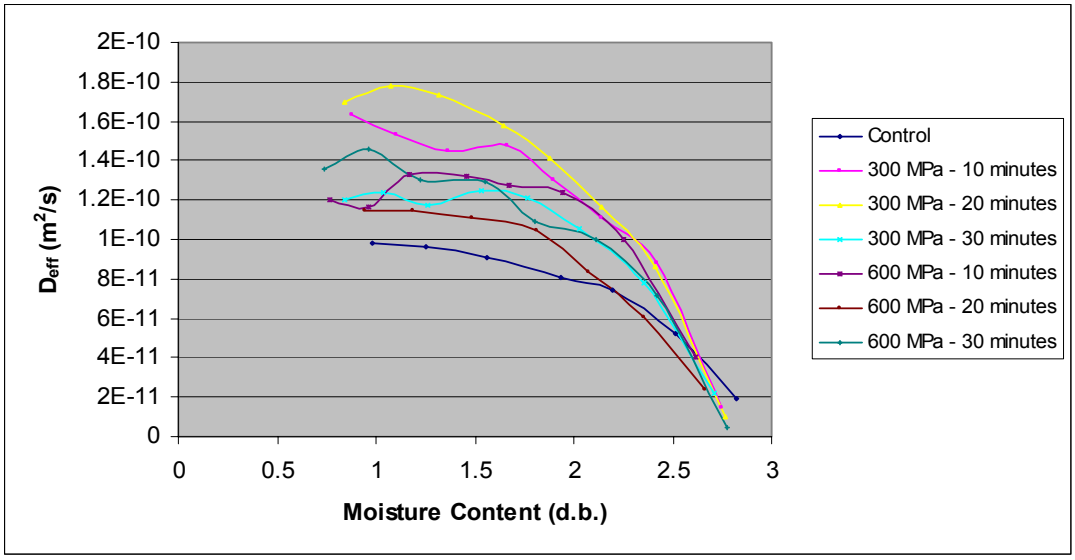

Figure 4.24: Effective Diffusivities of 300 and 600 MPa Pressurized Grapes

From Figure 4.24 it is clear that HHP changed the moisture diffusion properties of grapes. All of the treatments had higher effective diffusivity values than the untreated grapes. However, since HHP had no effect on the outermost waxy layer, drying rate was not much accelerated. Although application of 600 MPa pressure level for 10 and 20 minutes dried comparatively faster than application of 300 MPa for 10 and 20 minutes, for the effective diffusivity values it was vice versa. This was due to the fact that the values of effective diffusivity at any time were proportional with the square of radius (equation (2.5)). It was observed application of 300 MPa had higher normalized view area values than that of 600 MPa which in turn led to higher effective diffusivity values.

4.3.5 Color analysis

Cheftel (1992) states that effect of high pressure are generally marked as retention of color, flavor and fresh appearance. Immediately after pressurization grapes did not

lose their fresh green values, on the contrary, they obtained more intense bright green color on their surface which might be caused by leakage of chlorophyll into the intercellular space due to damage to the chloroplasts. This is consistent with Krebbers et al. (2002), where green beans were pressurized to 500 MPa for 60 seconds which in turn led to a decrease in a*-value from -16.1 to -16.9. However in this study it was observed that after 2 hours browning started at ambient conditions. Since PPO could exist in latent state (Matser et al., 2000), activation occurred as a result of pressurization and PPO might have caused the formation of brown pigments. This is also observed during drying of pressurized grapes. As seen in Figure 4.25, untreated grapes, namely control, changed from a negative a*-value (greenness) to a positive a*-value (redness) later than all of the pressurized grapes. This shows that pressurization accelerated the browning reactions and even 600 MPa pressure level and 30 minutes holding time did not prove to be sufficient for inactivation of grape PPO. From Figure 4.25, it may be concluded that all pressure levels and holding times had accelerated the browning reactions by activating PPO.

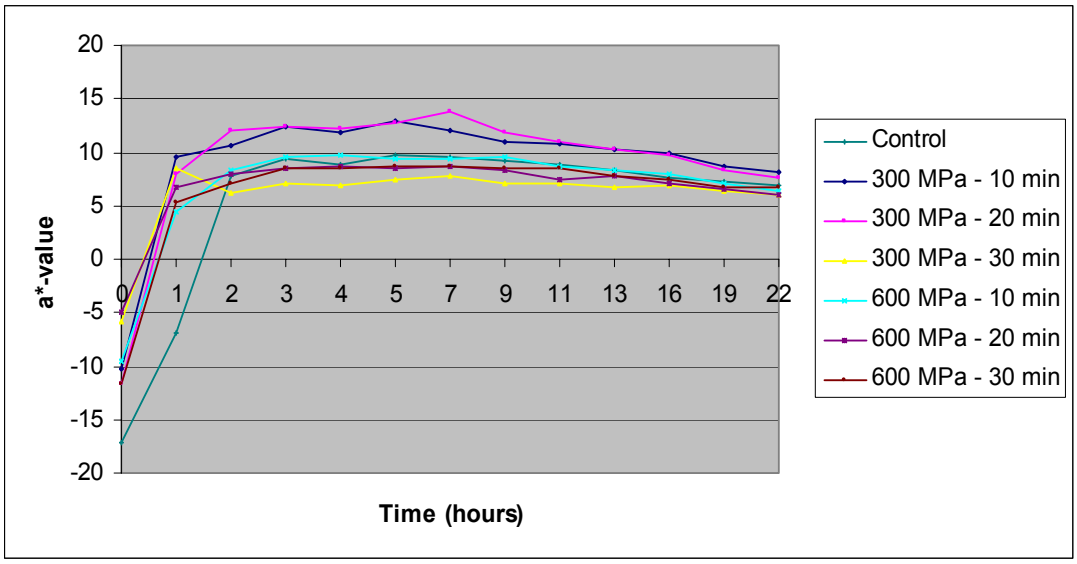

Figure 4.25: Change in a*-value of Pressurized and Untreated Grapes

Equation (3.9) is used to normalize the b*, chroma and total color change values at all pressure levels and holding times. Kinetic parameters are given in Table 4.7. ΔE, chroma and b-values followed a first-order degradation kinetics. It should be noted the C_0 in equation (3.9) for ΔE is zero. The R^2 for chroma and b*-values were around 0.94 at 300 MPa pressure level for 30 minutes and 600 MPa pressure level for 10 and 20 minutes, whereas in all other pressure levels and holding times it was

around 0.84. Total color change data fitted in equation (3.9) with an R^2 smaller than 0.80 except 600 MPa pressure level and 10 minutes holding time. Statistics of non-linear regression analysis are presented in Table C.1.

Table 4.7: Non-linear Regression Coefficients of Fractional Conversion Equation to Selected Color Values

Constants		**Pressure Level (MPa)**					
		300			*600*		
		Holding Time (min)					
		10	*20*	*30*	*10*	*20*	*30*
ΔE	C_f	45.82	47.71	30.49	38.31	34.68	48.06
	k_c (h^{-1})	0.365	0.379	0.167	0.283	0.163	0.23
Chroma	C_0	48.80	49.75	36.64	40.90	36.92	47.13
	C_f	18.46	18.31	18.27	17.26	15.99	16.75
	k_c (h^{-1})	0.22	0.217	0.137	0.199	0.147	0.232
b*	C_0	47.71	48.34	36.18	39.77	36.59	45.67
	C_f	16.58	16.62	17.22	16.05	14.84	15.37
	k_c (h^{-1})	0.251	0.252	0.142	0.217	0.163	0.228

4.4 Microwave-Assisted Drying of Grapes

Conventional drying of materials is a slow process that relies on the heat conduction from the outer layers towards the interior. When the material is thicker, the evaporation becomes slower. Microwaves, high frequency electromagnetic waves, offer an opportunity for enhancing the rate of evaporation and optimizing the overall process by its superior penetration and selective heating capability (Metaxas and Meredith, 1988). During convective drying of materials, the outer layers dry first which causes scorchy and tough product surface. Microwaves enhance the diffusion rate from interior of the material to its surface thereby, if adequately applied, eliminating the problems that are inherent to convective drying.

4.4.1 Small scale microwave drying (SSMD)

4.4.1.1 Drying kinetics

The moisture ratio versus time curves of constant microwave power and isothermal drying of grapes are shown in Figure 4.26. To describe the drying process thin-layer models (Table 2.2) were applied to the moisture ratio vs. time data. Logarithmic, Approximation of Diffusion, and Midilli et al. equations give better fit, regression

coefficient greater than 0.99 and SSE and RMSE smaller than 0.15, compared to other models, the statistics of which are presented in Table B.7.

A constant rate period was not observed during either constant power drying or isothermal drying. This result is in agreement with Sharma and Prasad's (2004) garlic drying, and Maskan's (2000) banana drying. Isothermal drying took much longer time to reach the same moisture level (Figure 4.26). In the beginning of the drying, the curves for 100 and 200 W were much steeper than that of 50 W and 70°C isothermal drying. As drying proceeded, due to moisture loss, the absorbed microwave energy decreased and for all applied power levels drying rate decreased.

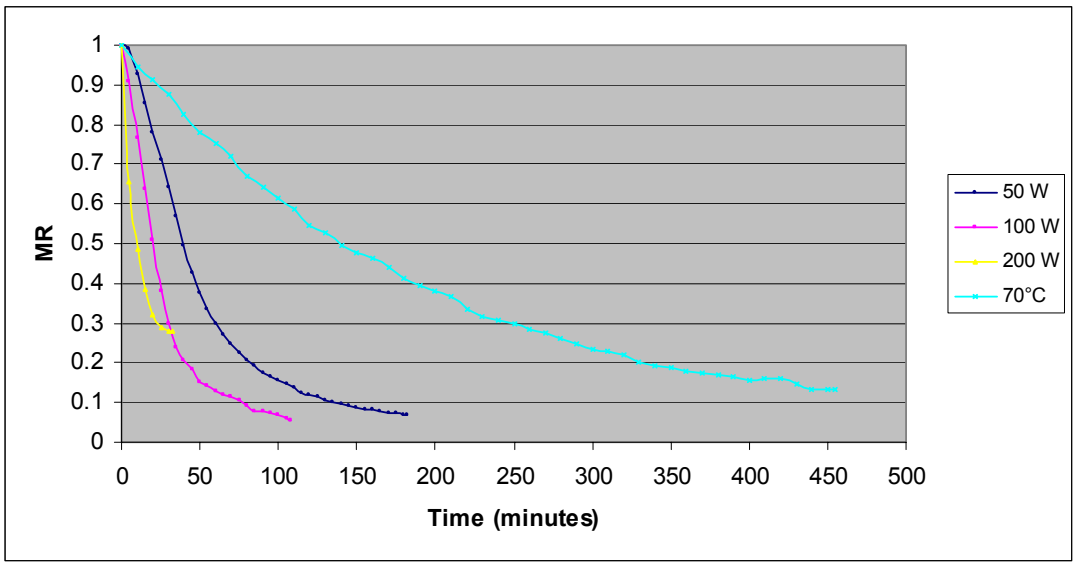

Figure 4.26: Isothermal and Constant Power Drying of Grapes

4.4.1.2 Thin-layer modeling

Constants of thin-layer models which describes microwave drying of grapes at 50, 100, 200 W and 70°C were given in Table 4.8. Logarithmic model was chosen for comparison due to its simplicity compared to Approximation of Diffusion and Midilli et al. equation. Similar descriptive model was used by Khraisheh et al. (2000) to describe the drying curves of raw potato by ignoring the c constant of logarithmic model. The drying constant k (min^{-1}) of Logarithmic model which is an indicator how fast the drying progressed, were 0.022, 0.044, 0.1186 and 0.005 (min^{-1}) for 50,100, 200 W power levels and 70°C isothermal drying, respectively. Microwave power level of 200 W has 5 times and 2.7 times higher drying constants than that of 50 W and 100 W, respectively. As the microwave power increased drying times were

significantly reduced ($P<0.01$). Similar findings were reported by Soysal (2004), and Andres et al. (2004).

Table 4.8: Results of Applied Thin-layer Models to SSMD

Model	50 W	100 W	200 W	Isothermal 70°C
Lewis	k=0.018	k=0.034	k=0.058	k=0.005
Page	k_1=0.011 n=1.118	k_1=0.031 n=1.036	k_1=0.155 n=0.646	k_1=0.006 n=0.973
Henderson and Pabis	a=1.096 k=0.019	a=1.064 k=0.037	a=0.866 k=0.047	a=0.994 k=0.005
Logarithmic	a=1.083 k=0.022 c=0.042	a=1.054 k=0.044 c=0.053	a=0.731 k=0.119 c=0.257	a=0.967 k=0.005 c=0.043
Approximation of Diffusion	a=-0.139 k=0.268 b=0.076	a=-0.085 k=0.912 b=0.041	a=0.725 k=0.125 b=0.015	a=0.007 k=2.165 b=0.002
Wang and Singh	a_1=0.000 b_1=-0.014	a_1=0.000 b_1=-0.024	a_1=0.001 b_1=-0.060	a_1=0.000 b_1=-0.004
Midilli et al.	a=1.044 k_1=0.007 n=1.256 b_2=0.000	a=1.042 k_1=0.022 n=1.182 b_2=0.000	a=1.001 k_1=0.112 n=0.884 b_2=0.006	a=0.996 k_1=0.004 n=1.048 b_2=0.000

4.4.1.3 Temperature profiles

Figure 4.27 shows temperature profile of grapes during combined-microwave isothermal drying. The sample temperature reached the desired temperature within a very short time and was maintained with little fluctuation throughout drying, which is inherent to PID controllers.

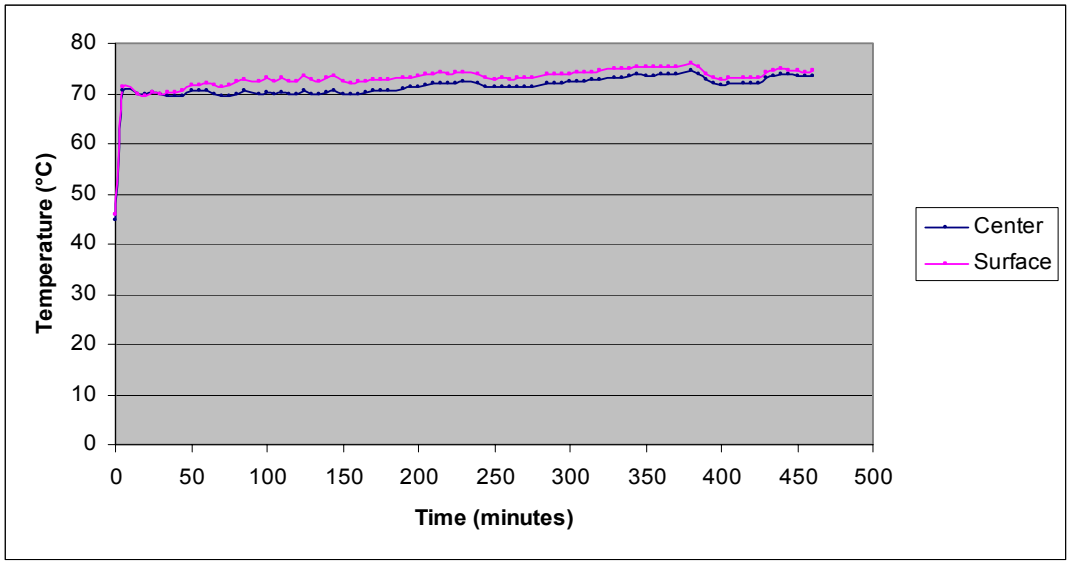

Figure 4.27: Isothermal Temperature Profile of Grapes

Although the feedback to the controller was with the fiber optic inserted in the center of the grape, the surface also maintained the same temperature as center. This is in agreement with Sirikiatden and Roberts (2005) where the authors used potato, carrot core and carrot cortex with 0.7 cm diameter and reported that the surface reached the center temperature after approximately 10 minutes. The lack of difference between center and surface temperatures in the very initial stage of drying can be attributed to the greater surface evaporation of potato, carrot core and cortex where evaporative cooling effects are higher compared to the grapes, in which the skin has resistance to moisture transfer to the surface.

Figure 4.28 shows the temperature profiles of grapes during constant microwave power drying. Similar to isothermal drying, there was no difference between center and surface temperatures for 50 W and the difference was negligible for 100 W microwave power. This is not in agreement with Bilbao-Sainz et al. (2006) where the authors used apple cylinders of 20 mm diameter, applied 3 W/g and 10 W/g microwave power, and found that in both power levels, center temperature was greater than surface temperature throughout drying. Similar to Sirikiatden and Roberts (2005), evaporative cooling might have suppressed the surface temperature.

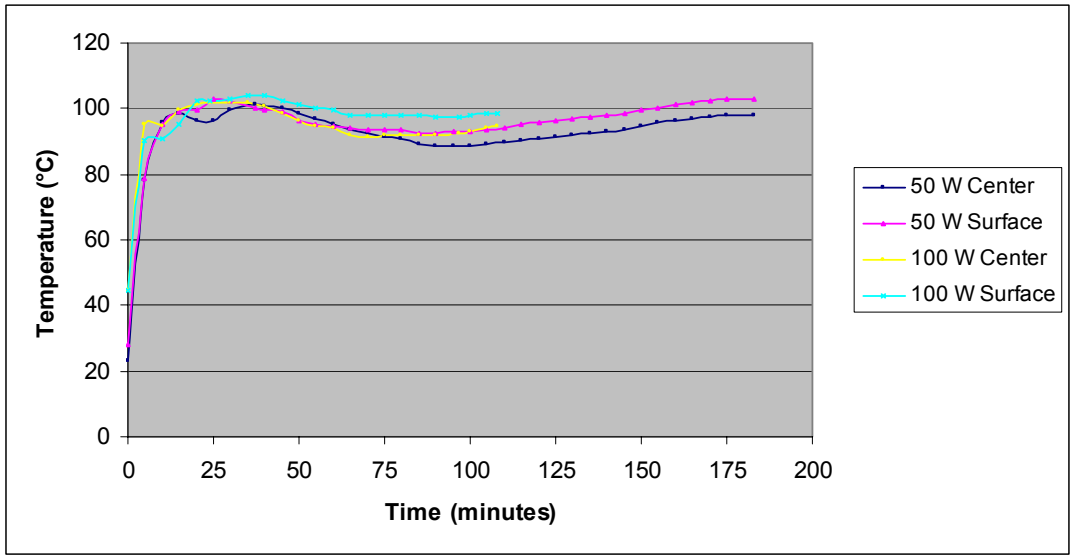

Figure 4.28: Constant Power Temperature Profile of Grapes

After 30 minutes, 200 W microwave power caused center and surface temperatures to go up to 132.77°C and 138.07°C, respectively. This was observed as charred zones in grapes.

4.4.2 Bulk scale microwave drying (BSMD)

4.4.2.1 Drying kinetics

During SSMD, the power ratio was between 1.60 and 2.75 W/g for 50 and 100 W constant microwave power applications. It was seen that 1.60 and 2.75 W/g produced raisins that were in acceptable quality both in terms of color and general appearance. However, when the sample weight was either 300 or 600 g, even 1.0 W/g power ratio was observed to be high for drying of grapes at the same microwave system. Grapes released too much juice during drying and due to juice release resulting raisins had charred zones. Close observations for microwave drying of Washington potatoes and Australian carrots were reported by Chua and Chou (2005). Although the authors did not report the mass of the products that was dried, they observed that high microwave powers of 700 and 1000 W caused charring thus they lowered the microwave power to 100, 300 and 500 W.

The drying kinetic of 1 W/g constant microwave drying at different initial powers and different air temperatures is shown in Figure 4.29.

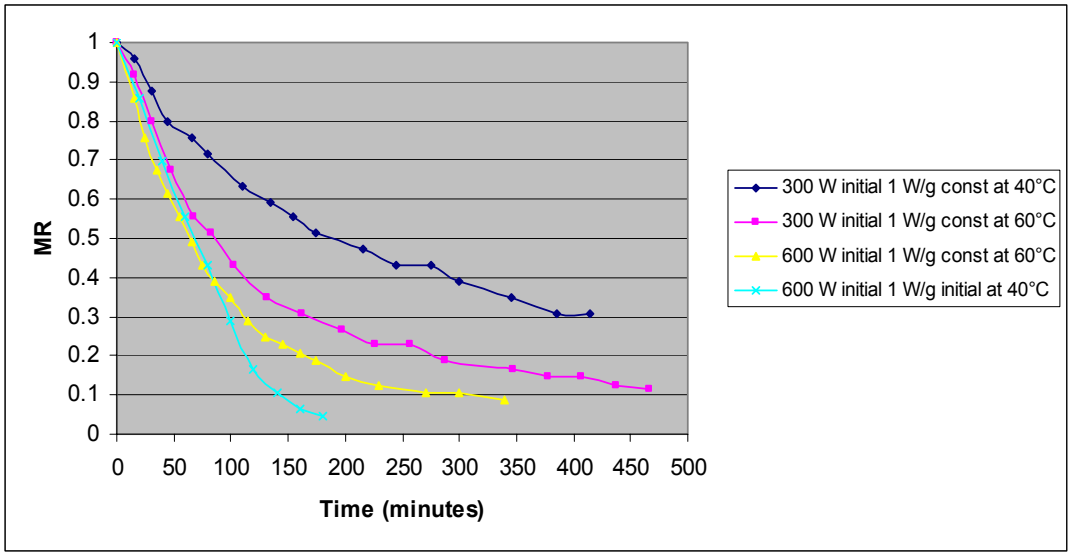

Figure 4.29: 1 W/g Initial and Constant Microwave Power Ratio Drying at 300 and 600 W Initial Powers and 40 and 60°C Convective Air Temperatures

It is seen from Figure 4.29 that although the power ratios were same, increasing the power from 300 to 600 W decreased the drying time of grapes by 25%. Increasing the temperature of the convective air from 40°C to 60°C also increased the drying rate of grapes by 166.67%. However when the power ratio was initially 1 W/g and since grapes lost mass during dehydration, power ratio gradually increased and was higher than 4 W/g at the very last stages of drying. Thus, although the air temperature was 40°C during 1 W/g initial power ratio drying, the drying rate was even higher than 60°C air temperature assisted with 1 W/g constant power ratio. This suggested that during dehydration, although the microwave power was constant, the microwave power ratio increased and the increase in power ratio had increased the drying rate.

Since the quality of the grapes produced with 1 W/g initial or constant power ratio drying was not satisfactory, the power ratio was reduced to 0.5 W/g. The drying kinetics at 50° and 60°C is shown in Figure 4.30. There was no constant rate period in both 50° and 60°C convective air temperatures. Thin-layer models (Table 2.2) were used to describe the drying curves. The drying curves at both temperatures could be accurately described by Logarithmic equation (Yaldiz et al., 2001) in Table 2.2 where for both convective air temperatures, R^2 was greater than 0.99 and RMSE and SSE was close to zero (Table B.9). From Table 4.9, the value of the constants a and k (min^{-1}) for 50 and 60°C were 1.694, 0.002 and 1.795, 0.003, respectively.

Table 4.9: Results of Applied Thin-layer Models to Selected BSMD

Model	1W/g constant at 60°C	0.5 W/g constant at 60°C	0.5 W/g initial at 50°C	0.5 W/g initial at 60°C
Lewis	k=0.007	k=0.005	k=0.004	k=0.007
Page	k_1=0.021 n=0.773	k_1=0.002 n=1.157	k_1=0.000 n=1.474	k_1=0.000 n=1.596
Henderson and Pabis	a=0.944 k=0.006	a=1.052 k=0.005	a=1.097 k=0.005	a=1.120 k=0.008
Logarithmic	a=0.884 k=0.010 c=0.132	a=1.088 k=0.005 c=-0.049	a=1.694 k=0.002 c=-0.655	a=1.795 k=0.003 c=-0.739
Approximation of Diffusion	a=0.757 k=0.011 b=0.131	a=2.166 k=0.004 b=0.858	a=2.826 k=0.002 b=0.667	a=3.655 k=0.003 b=0.719
Wang and Singh	a_1=0.000 b_1=-0.005	a_1=0.000 b_1=-0.004	a_1=0.000 b_1=-0.003	a_1=0.000 b_1=-0.005
Midilli et al.	a=1.024 k_1=0.013 n=0.903 b_2=0.000	a=1.003 k_1=0.002 n=1.204 b_2=0.000	a=0.996 k_1=0.000 n=1.386 b_2=-0.000	a=0.999 k_1=0.000 n=1.541 b_2=-0.000

Taking the time derivative of Logarithmic model gives:

$$\frac{dMR}{dt} = -a \cdot k \cdot \exp(-k \cdot t) \qquad \textbf{(4.1)}$$

It is seen from equation (4.1) that the multiplication of a and k plays the major role in the decrease of moisture ratio with time. The ratio of multiplication for 60° to 50°C was 1.59. Thus it can be concluded that increasing the temperature increased the drying rate roughly 1.59 times, since k values were close to each other and zero. This was in agreement with McMinn (2006) who reported that an increase in convective air temperature from 40 to 60°C resulted in 17% decrease in the microwave drying time of lactose powders. Silvia et al. (2006) reported a slight decrease in drying time of microwave-assisted hot air drying of macadamia nut with an increase in air temperature from 58 to 62°C where the initial microwave power ratio was reported to be 0.33 W/g to maintain product temperature below 70°C.

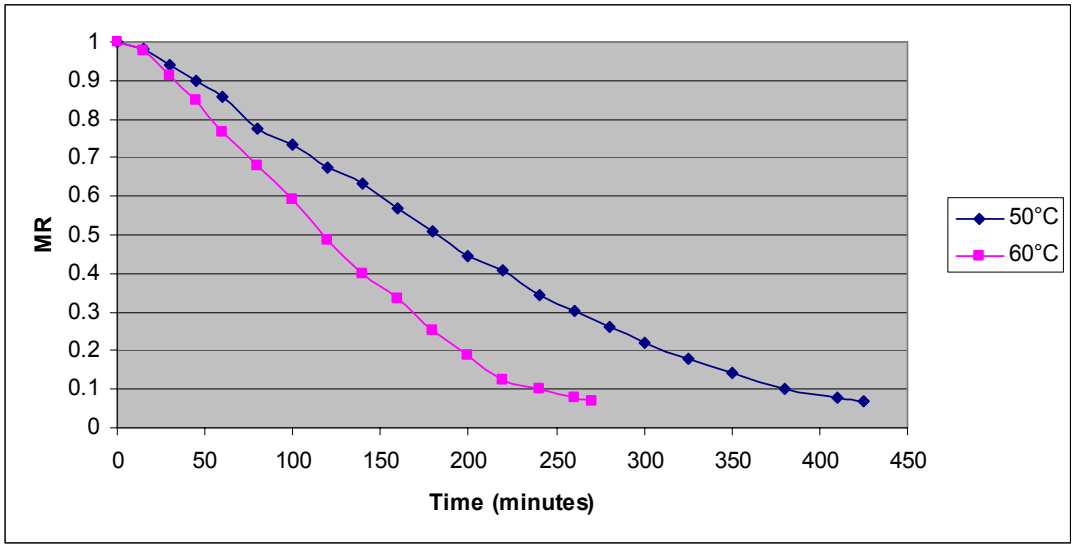

Figure 4.30: Drying Kinetics of 0.5 W/g Initial Power Ratio at 50 and 60°C Convective Air Temperatures

Grapes were also dried at constant power ratio at 0.5 W/g. Drying curves is shown in Figure 4.31. It is seen that at 40° and 50°C convective air temperatures, moisture ratio was 0.56 and 0.37 which corresponded to moisture content of 71 and 57% (wet basis), respectively, whereas for the same drying time, the moisture ratio for 60°C convective air at the same power ratio was below 0.1 which corresponded approximately to moisture content of 25% (wet basis). Thus it can be concluded that convective air temperatures below 60°C was not suitable for 0.5 W/g constant power ratio drying of grapes.

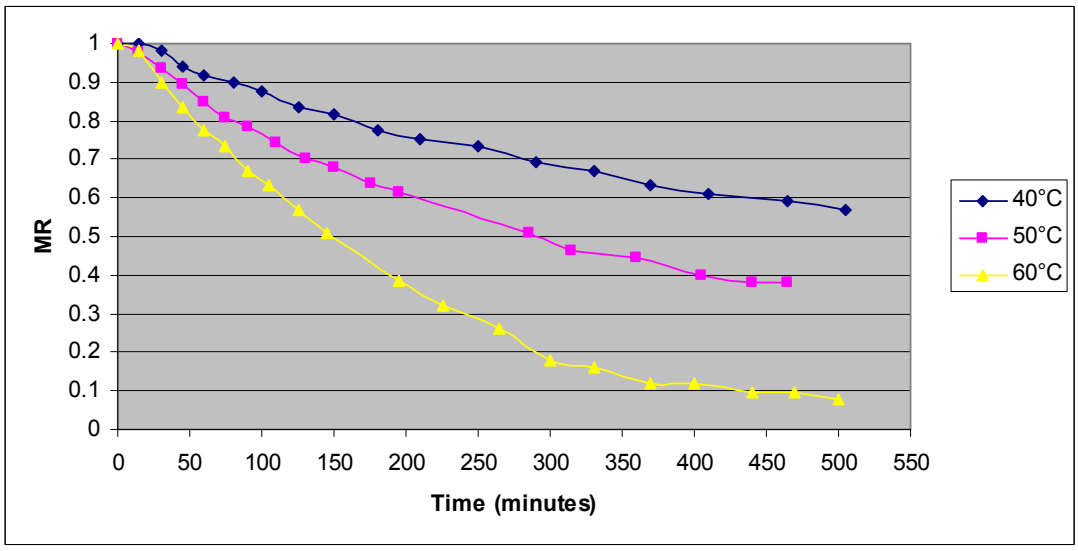

Figure 4.31: Drying Kinetics of 0.5 W/g Constant Power Ratio at 40, 50 and 60°C Convective Air Temperatures

Microwave-assisted convective drying curve of grapes at 0.5 W/g constant microwave power ratio at 60°C air temperature could be described by all of the seven thin-layer modeling equations with an R^2 greater than 0.99 and with RMSE and SSE close to zero (Table B.9). Of all the seven thin-layer models, Logarithmic model was chosen for its simplicity. To compare 0.5 W/g initial power ratio at 60°C air temperature with 0.5 W/g constant power ratio at 60°C air temperature, equation (4.1) was used to calculate change of moisture ratio with time. The ratio of initial power ratio to constant power ratio at 60°C air temperature was close to 1.63 until 250 minutes drying time. The reason that the comparison made until 250 minutes drying time, can be explained by Figure 4.32.

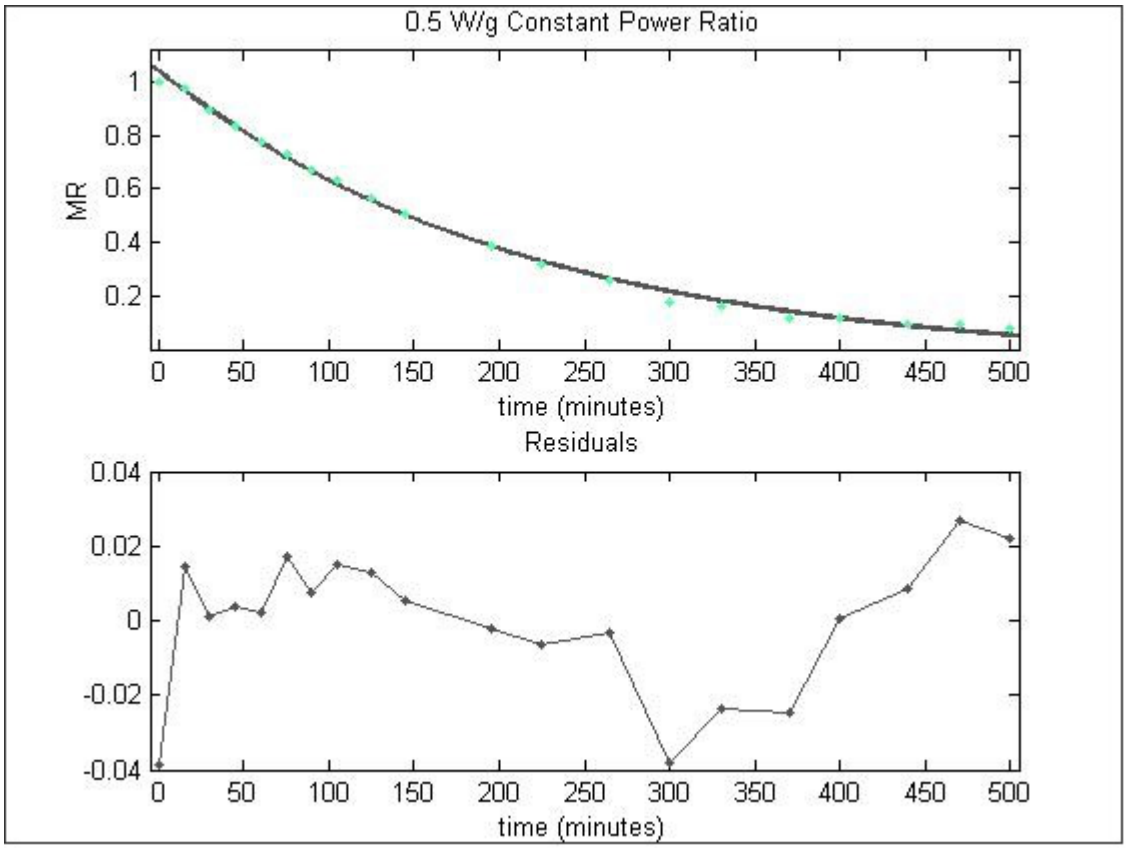

Figure 4.32: Curve Fitting and Residual Plot of 0.5 W/g Constant Power Ratio at 60°C

It is seen in Figure 4.32 that until 250 minutes, the residuals of the fit was centered around zero, except the beginning of drying, which indicates a good fit. However, as of 250 minutes of drying the residuals scatter from zero which meant that Logarithmic equation poorly described the remaining of drying. Thus the comparison was made where the Logarithmic equation gave better fit.

During 0.5 W/g constant power ratio drying of grapes, the transition from first falling rate to second falling rate was dependent on convective air temperature whereas during initial power ratio drying this was independent of convective air temperature as seen in Figure 4.33. This was around 0.4 and 0.15 for constant power ratio at 50° and 60°C, respectively, and was below 0.1 for initial power ratio for both temperatures.

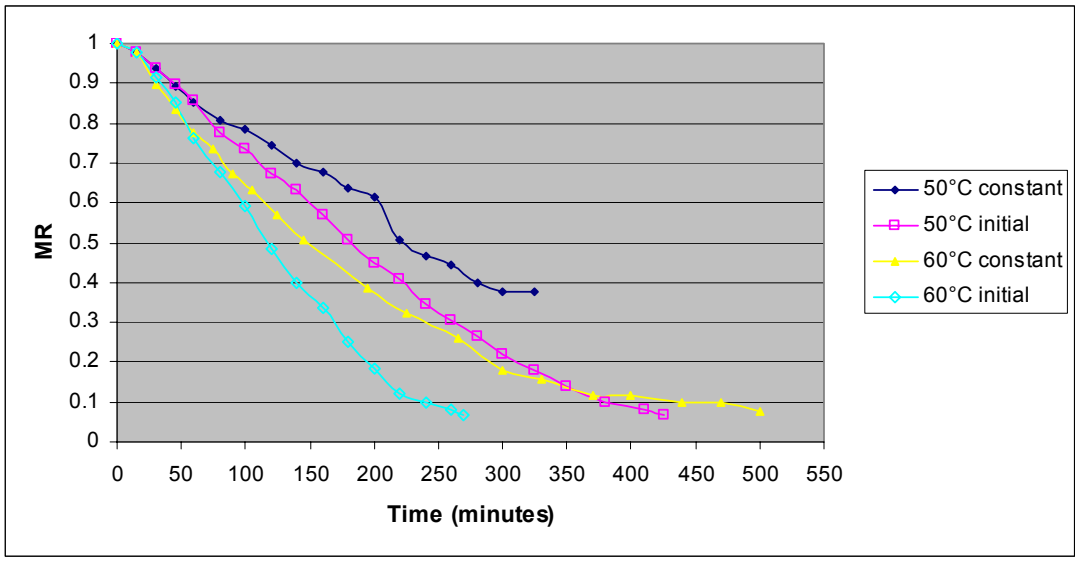

Figure 4.33: 0.5 W/g Constant and Initial Power Ratio Drying of Grapes at 50° and 60°C

A comparison between constant power ratio at 60°C air temperature and initial power ratio at 50°C air temperature drying revealed that, in the first falling rate period temperature of convective air played more important role rather than applied microwave power level in terms of drying rate however in the second falling effectiveness of microwave power increased. Moreover, it should be noted that at the same convective air temperature, an increase in microwave power ratio increased the drying rate which is in agreement with McMinn et al. (2003) and Soysal (2004).

The drying kinetics of untreated and pretreated grapes is shown in Figure 4.34. It is seen that contrary to convective drying, drying rate was not improved by 40°C and 3 minutes dipping treatment during microwave-assisted convective drying. It might be concluded that mild pretreatments did not affect drying rate of microwave-assisted drying of grapes as it did in convective drying. However, steam blanching, which considerably reduced drying time of convective drying of grapes also significantly

reduced drying time of microwave-assisted convective drying of grapes where the reduction was 75 and 36%, respectively.

Drying curves of microwave-assisted drying at 0.25 W/g inital power ratio and 60°C convective air temperature for both untreated and pretreated grapes could be accurately described by the thin-layer models given in Table 2.2. R^2 and RMSE and SSE values are given in Table B.8 and the constants are presented in Table 4.10.

The constants a and k (min^{-1}) of Logarithmic model for untreated and dipped grapes can be considered to be same which reveals itself as an overlapped curve in Figure 4.34.

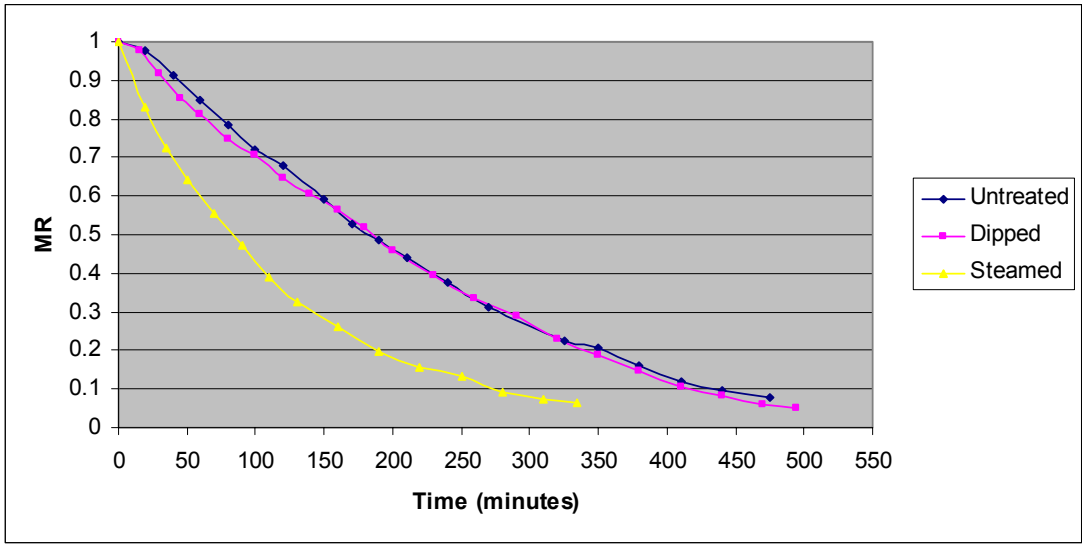

Figure 4.34: 0.25 W/g Initial Power Ratio Drying of Untreated and Pretreated Grapes at 60°C

Table 4.10: Results of Applied Thin-layer Models to Untreated and Pretreated Grapes at 0.25 W/g Initial Power Rate and 60°C Convective Air Temperature

Model	Untreated	Steam Blanched	Dipped
Lewis	k=0.004	k=0.008	k=0.004
Page	k_1=0.000 n=1.331	k_1=0.009 n=0.968	k_1=0.001 n=1.281
Henderson and Pabis	a=1.084 k=0.005	a=0.989 k=0.008	a=1.062 k=0.005
Logarithmic	a=1.346 k=0.003 c=-0.304	a=0.983 k=0.008 c=0.007	a=1.347 k=0.003 c=-0.330
Approximation of Diffusion	a=4.291 k=0.002 b=0.671	a=0.024 k=0.114 b=0.072	a=3.179 k=0.002 b=0.617
Wang and Singh	a_1=0.000 b_1=-0.003	a_1=0.000 b_1=-0.006	a_1=0.000 b_1=-0.003
Midilli et al.	a=1.009 k_1=0.001 n=1.260 b_2=-0.000	a=0.998 k_1=0.010 n=0.961 b_2=-0.000	a=1.001 k_1=0.002 n=1.119 b_2=-0.000

To compare the moisture loss with time equation (4.1) was used to calculate the change of moisture ratio of steam blanched and dipped grapes with time and the ratio of change of moisture ratio of steam blanched and dipped grapes with time was found to be 2.30 until 300 minutes drying. This clearly showed that drying of steam blanched grapes was 2.30 times faster than dipped grapes until 300 minutes of drying.

4.4.2.2 Temperature profiles

Temperature profiles of 1 W/g constant and initial power ratio microwave-assisted convective drying of grapes is given in Figure 4.35. It is seen that initial temperature rise both at 40° and 60°C was very close both at center and near surface of grapes during both constant (CPR) and initial (IPR) power ratio drying. Except IPR at 60°C air temperature, convective hot air suppressed the near surface temperature at initial stages of drying where a lower convective temperature resulted in a lower near surface temperature. The suppression of near surface temperature at 40°C air temperature for both CPR and IPR continued throughout drying where the temperature difference between center and near surface for CPR gradually decreased.

This suggested that lowering the input microwave power reduced the temperature gradient within the grapes.

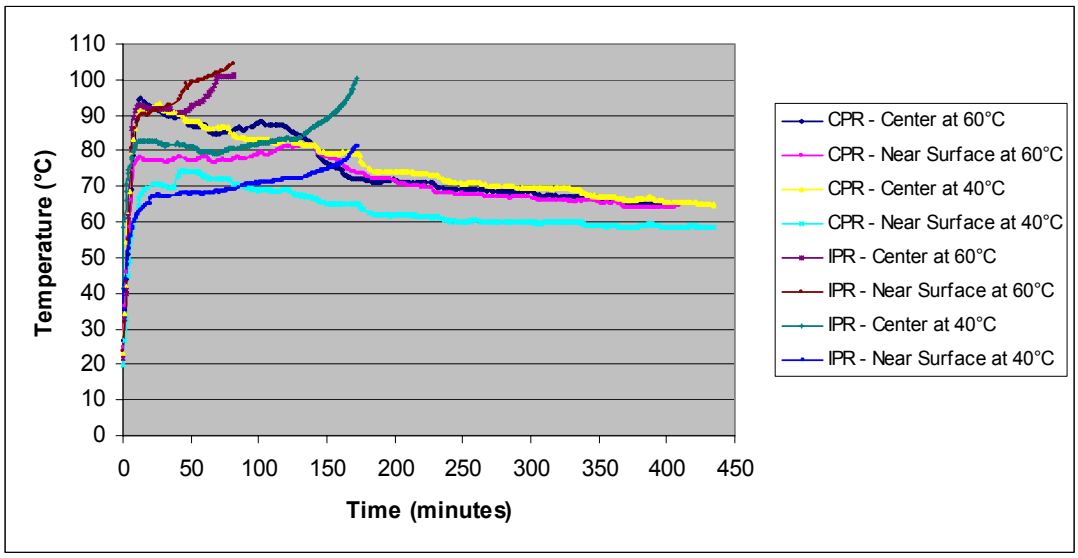

Figure 4.35: Temperature Profiles at Center and Near Surface during 1 W/g Constant (CPR) and Initial (IPR) Power Ratio Drying of Grapes

After an initial temperature rise of grapes at 40° and 60°C air temperatures, temperature of grapes during IPR drying continued to increase, whereas during CPR drying temperature gradually decreased. The decrease in temperature during CPR drying might be due to a decrease in the microwave power input proportional to weight loss.

The temperature profiles of 0.5 W/g CPR drying is given in Figure D.1. The temperature profile during 0.5 W/g CPR drying was much the same as 1 W/g CPR drying except the initial rise of center temperature, which was 22 and 16°C less for 40 and 60°C air temperatures, respectively. However the difference in initial rise of near surface temperature for 1 W/g and 0.5 W/g CPR drying at 40 and 60°C air temperatures was 8 and 2°C for , respectively.

The temperature profile of 0.5 W/g IPR drying is shown in Figure 4.36. Unlike 1 W/g IPR drying at 60°C air temperature, the temperature remained constant for a short period of time and then started to increase. It is seen that between 0.2 and 0.3 moisture ratios, the temperature of center made a maximum and then started to decrease. At this point grape might have changed state that might have affected its dielectric properties.

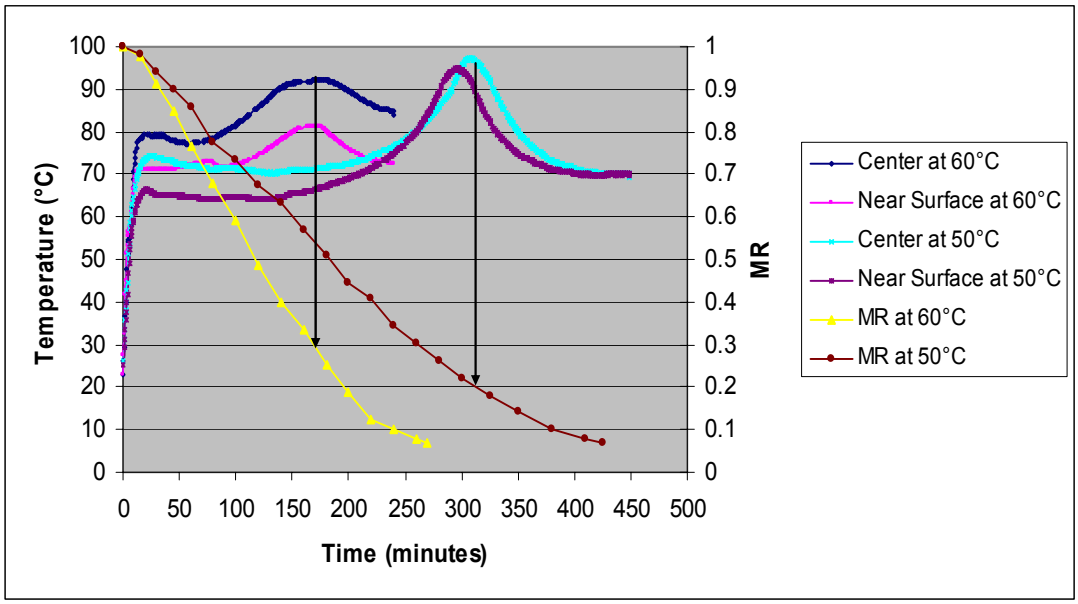

Figure 4.36: Temperature Profiles at Center and Near Surface during 0.5 W/g Initial Power Ratio Drying of Grapes

Microwave initial power ratio was lowered to 0.25 W/g and also grapes were pretreated either by dipping in chemical solutions or by blanching with steam. Temperature profiles of untreated and pretreated grapes are given in Figure 4.37. The initial temperature rise (indicated by red arrow) of dipped and untreated grapes was higher than steamed grapes. This was due to higher moisture loss of steamed grapes during drying (Figure 4.34) which led to higher evaporative cooling effect. As was observed in 0.5 W/g IPR drying at 60°C air temperature, the temperature of pretreated grapes made a maximum at a moisture ratio very close to 0.4, which might be due to changes in dielectric properties. Thus from Figure 4.36 and Figure 4.37 it might be inferred that depending on the applied microwave power there was a sudden change in dielectric properties of grapes on the last stages of microwave-assisted convective drying.

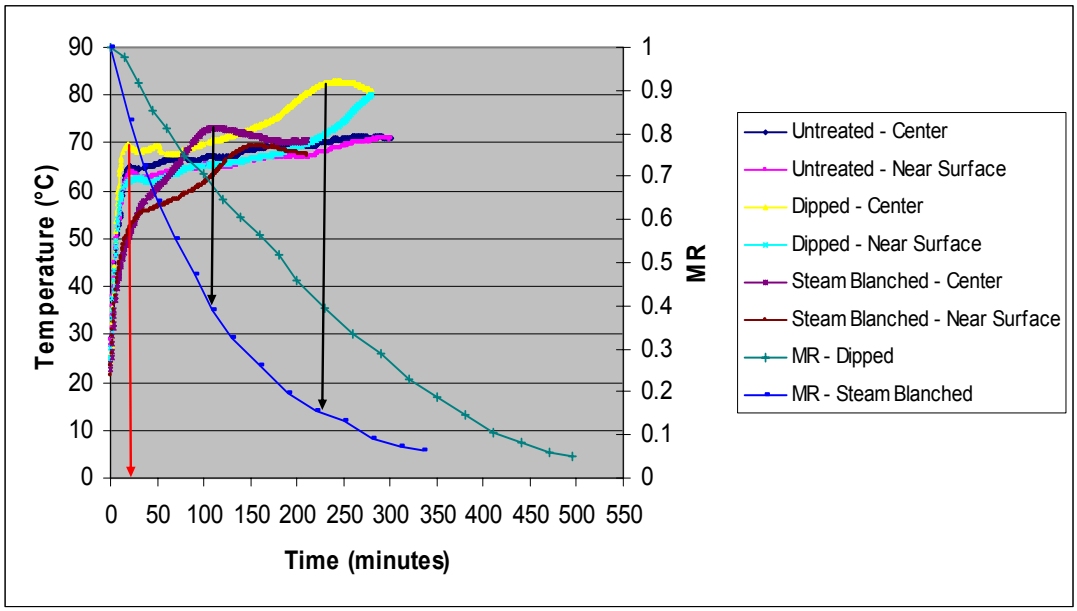

Figure 4.37: Temperature Profiles at Center and Near Surface during 0.25 W/g Initial Power Ratio Drying of Grapes

4.4.2.3 Color profiles

Final color values of selected microwave-assisted drying of grapes are shown in Table 4.11. The chroma value indicates the degree of saturation of color and is proportional to the strength of the color. The chroma values of produced raisins were approximately half the chroma values of fresh grapes and these values were very much close to b*-values. This might indicate the strength of yellow color in grapes and that the color forming pigments were heat labile (Maskan, 2001).

Table 4.11: Final Color Values of Microwave-assisted Dried Grapes

Drying Method	L*	a*	b*	Chroma
1 W/g IPR, Untreated, 40°C Convective Air Temperature	41.41	2.65	19.62	19.80
0.5 W/g IPR, Untreated, 50°C Convective Air Temperature	38.03	5.25	22.51	23.12
0.5 W/g IPR Untreated,60°C Convective Air Temperature	38.03	5.28	22.61	23.22
0.25 W/g IPR Untreated, 60°C Convective Air Temperature	38.86	6.11	23.64	24.41
0.25 W/g IPR, DIPPED, 60°C Convective Air Temperature	34.71	5.74	20.86	21.64
0.25 W/g IPR, STEAMED, 60°C Convective Air Temperature	40.68	4.39	27.35	27.70

Initial a*-values of grapes were negative, indicating greenness and from Table 4.11 it was observed that regardless of the drying methods the final a*-value were positive which indicated a shift to redness. According to Clydesdale (1997) during heat

treatment the bright green chlorophylls generally degrade to a dull olive-brown which might be the cause of the shift from a negative to a positive a*-value.

It is seen that 1 W/g IPR at 40°C convective air temperature has the highest L*- and lowest a*-value. The reason might be that drying did not last for a long time (lasted for 180 minutes) and grapes lost excessive juice due to mainly high microwave power ratio and insufficient air temperature to remove excessive juice loss. Since the drying was not carried out for a long time a*-values did not increase very much. The higher L*-value might be due to the leakage of juice onto the surface of grape and might also be due to shorter drying time. Thus grapes that were steam blanched at 90°C for 140 seconds prior to drying could be considered to have the highest L*- and lowest a*-value which meant they were the shiniest and the least browned.

It was observed that at 0.5 W/g IPR, the temperature of convective air had negligible effect on L*-, a*- and b*-values. The difference between the values of L*, a* and b* were 0, 0.03 and 0.1, respectively. Also at the same convective air temperature decreasing the microwave power ratio from 0.5 to 0.25 W/g had slightly affected the L*, a* and b*-values. The difference between L*-, a*- and b*-values of 0.5 and 0.25 W/g initial microwave power ratio was -0.83, -0.83 and -1.03, respectively. The results were similar to Dev et al. (2007) who observed that pretreating grapes with different microwave power ratios did not significantly affect the L*-values of resulting raisins.

4.5 Numerical Simulations of Temperature Profiles

4.5.1 Convective drying of untreated grapes

Calculation procedure of convective heat transfer coefficient is given in Appendix (E.1). Since the center temperature of the grape reached the air temperature after 2 hours, simulation was run for 2 hours. Equation (3.13) was solved numerically with Matlab assuming no internal heat generation and since grapes lost approximately 5% of their moisture within the first 1 hour, heat loss due to evaporation was also neglected. Thus besides the constant a, the constant f was also taken as zero in equation (3.12). The constants d and c was defined as $\rho \cdot C$, $k \cdot r$ where ρ, C and k was found with equation (3.1), (3.2) and (3.3). The temperature profile of both experimental and simulation temperatures is seen in Figure 4.38.

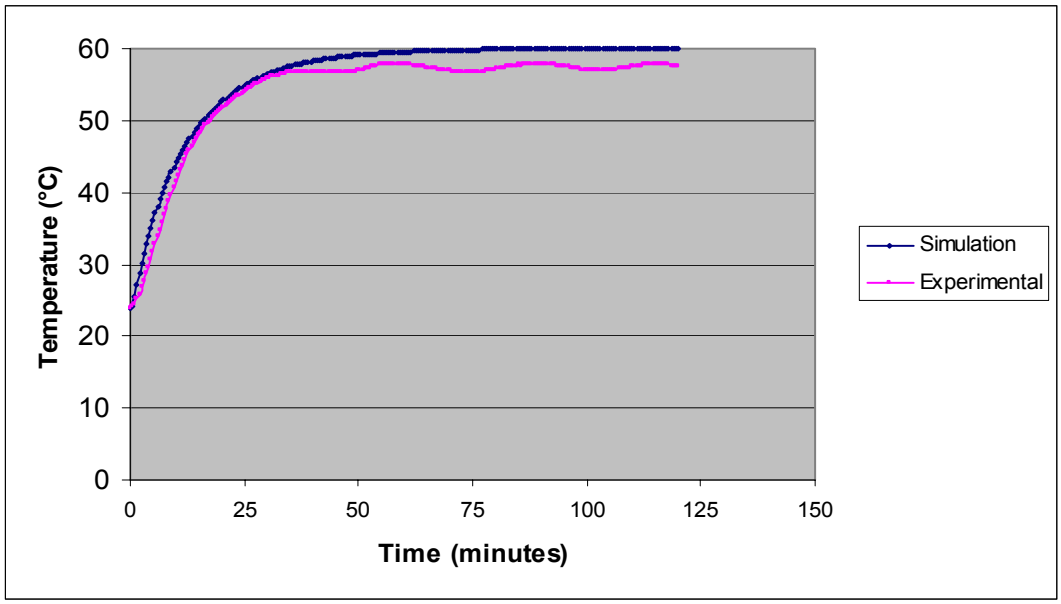

Figure 4.38: Experimental and Simulation Center Temperature Profile of Untreated Grapes

A paired t-test revealed that the difference greater than 2.21°C between experimental and simulation temperatures was statistically insignificant (P>0.05 and Confidence interval of means at 95% confidence level was between 1.99 and 2.21, df=240). The frequency of differences between experimental and simulation temperatures that were more than 3°C were less than 10. As seen from Figure 4.38 the experimental temperature values did not reach 60°C due to oscillation in air temperature between 58° and 61°C, which was generally close to 58°C.

4.5.2 Convective drying of steam blanched grapes

When capillary-porous bodies that contains moisture are exposed to heat, migration of moisture takes place and therefore, to describe mathematically the process of drying it is necessary to determine both temperature and moisture-content distribution within the material. A corresponding system of differential equations of coupled heat and moisture transfer, provided the change in the moisture content of the body occurs as a result of moisture transfer and conversion of the liquid into the vapor phase:

$$\frac{\partial T}{\partial t} = \frac{1}{C \cdot \rho} \cdot \frac{\partial}{\partial x}\left(k \cdot \frac{\partial T}{\partial x} \right) + \frac{\sum \Delta h_v}{C} \cdot \frac{\partial u}{\partial t} \quad \textbf{(4.2)}$$

where k is thermal conductivity, Δh_v is specific heat of evaporation, u is moisture content (Luikov and Mikhailov, 1959; Martynenko et al., 1980).

In cylindrical coordinates, equation (4.2) could be written similar to equation (3.13) where $\dot{q}$ was equal to the evaporative heat loss term in equation (4.2). Time dependent moisture transfer during convective drying of steam blanched grapes was represented by the logarithmic thin-layer model. Since the initial center temperature of grapes was close to 20°C and air temperature was 60°C, enthalpy of vaporization was calculated at 40°C. Calculation procedures of both convective heat transfer coefficient and evaporative heat loss is given in Appendix (E.2).

Using Matlab equation (4.2) was numerically solved using equation (3.13) in cylindrical coordinates. The constants a and f in equation (3.12) was taken as zero and as the rate of evaporative heat loss (grapes lost approximately 45% of their moisture within the first 1 hour), respectively. The constants d and c was defined as ρ·C, k·r where ρ and C was found with equation (3.1) and (3.2), respectively. Equation (3.3) was not used to calculate the thermal conductivity since steam blanching removes the air on the surface and softens the texture of fruits and vegetables. Thus it was assumed that steam blanched grapes had slightly higher thermal conductivity than untreated grapes and thermal conductivity was found by trial and error method. The temperature profile of both experimental and simulation temperatures is seen in Figure 4.39.

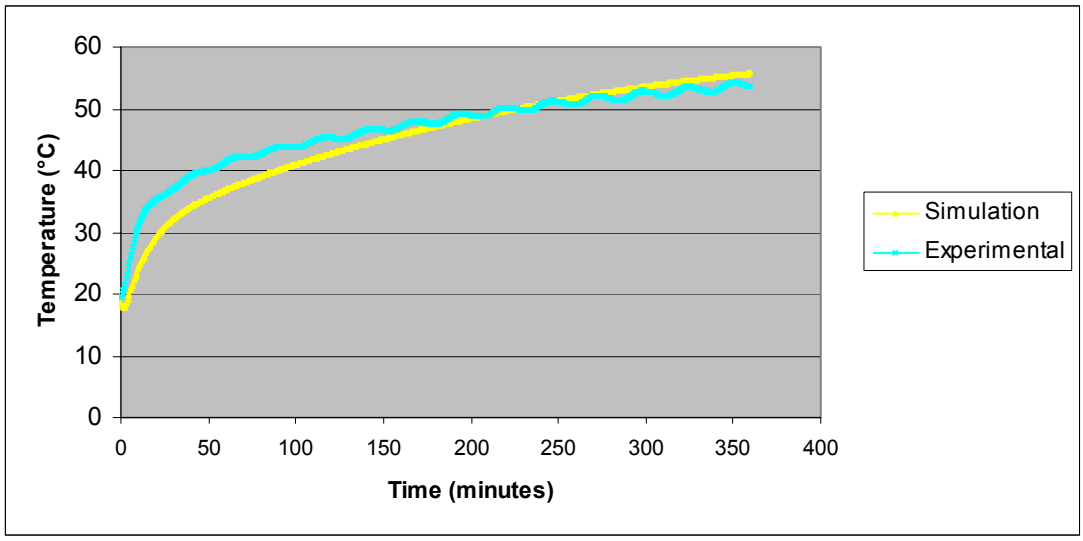

Figure 4.39: Simulation of Convective Center Temperature Profile of Steam Blanched Grapes

Contrary to untreated grapes whose temperature rised over 50°C within 30 minutes, temperature of steam blanched grapes rised over 50°C after more than 250 minutes due to evaporative heat loss which suppressed the temperature rise. The average difference between simulation and experimental temperature was 0.27°C. However within 120 minutes the average difference was 1.29°C. The high difference might be due to the fitting of experimental drying data to Logarithmic thin-layer equation where the residuals of the fit had higher values within 120 minutes. This might mean that logarithmic model might not have represented the drying curve very well, which in turn caused weak estimation of the evaporative heat loss within 120 minutes.

4.5.3 Heating of grapes during steam blanching

Calculation procedure of convective heat transfer coefficient is given in Appendix (E.3). Grapes were assumed to be horizontal cylinders which were exposed to steam at 80°, 90° and 100°C. Steam was assumed to condense filmwise on the grape. Since there was no internal heat generation, the constant f in equation (3.12) was taken as zero. The constants d and c was defined as ρ·C, k·r where ρ and C was found with equation (3.1) and (3.2), respectively. Equation (3.3) was not used to calculate the thermal conductivity of grape, since steam blanching removes the air on the surface and softens the texture of fruits and vegetables. It was assumed that during steam blanching the thermal conductivity of grapes increased and was taken as 0.7 W/m·°C. This assumption was based on the fact that steam blanching ruptures the

skin and tissue, and removes the air within the product. Simulation was run for 270, 140 and 90 seconds for 80°, 90° and 100°C, respectively. The experimental and simulation heating curves for 80°, 90° and 100°C is seen in Figure 4.40. There was 1, 7 and 10°C difference between the means of experimental and simulation heating values of 80°, 90° and 100°C, respectively. From the mean difference values and Figure 4.40 it was observed that the maximum error occurred in 100°C steam heating of grapes.

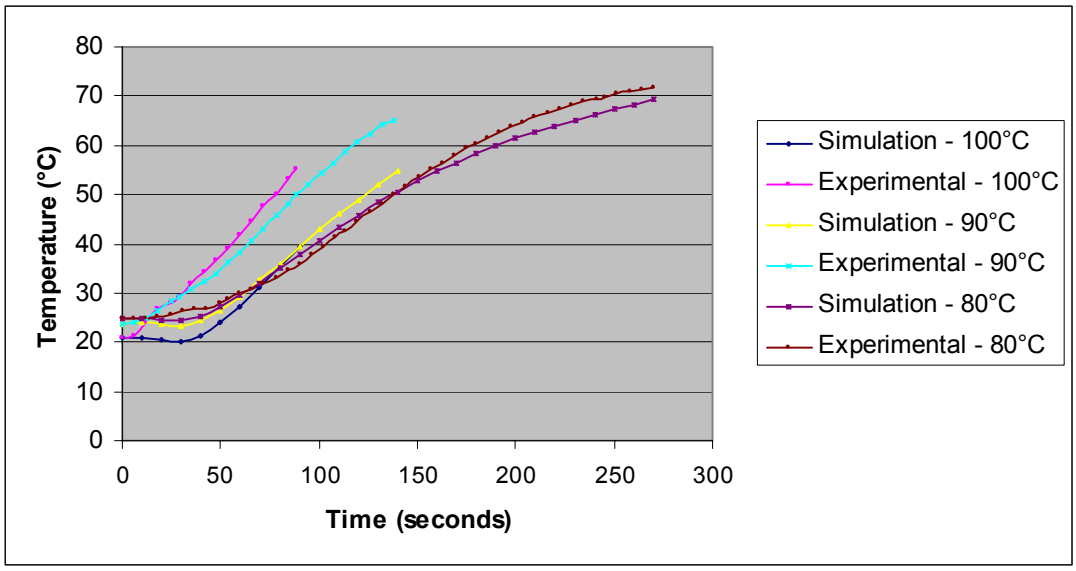

Figure 4.40: Simulation and Experimental Center Temperature of Grapes during Steam Blanching

One of the reasons for the error in 90° and 100°C steam heating of grapes was that the simulation temperature values was nearly constant within 50 seconds of heating where actual heating was a steep curve in this time frame. Also grapes thermal properties played an important role in the simulation data. Table 4.12 shows the effect of thermal conductivity on the simulation final center temperature of grapes.

Table 4.12: Effect of Thermal Conductivity on the Final Center Temperature of Grapes

	Steam Temperature (°C)		
Thermal conductivity (W/m·°C)	*80*	*90*	*100*
0.6	65.518	49.133	34.206
0.7	69.175	54.676	39.391
0.8	71.879	59.522	44.420
0.9	74.048	63.721	49.179
1.0	75.571	67.342	53.605

From Table 4.12 it can be inferred that thermal conductivity of grapes played an important role in the simulation of steam heating of grapes. If thermal conductivity is taken as 0.98 instead of 0.7 W/m·°C it was observed that the average mean difference between simulation and experimental temperature values for 90° and 100°C was 0.4° and 4.5°C. The experimental and simulation heating curves for 90° and 100°C is seen in Figure 4.41.

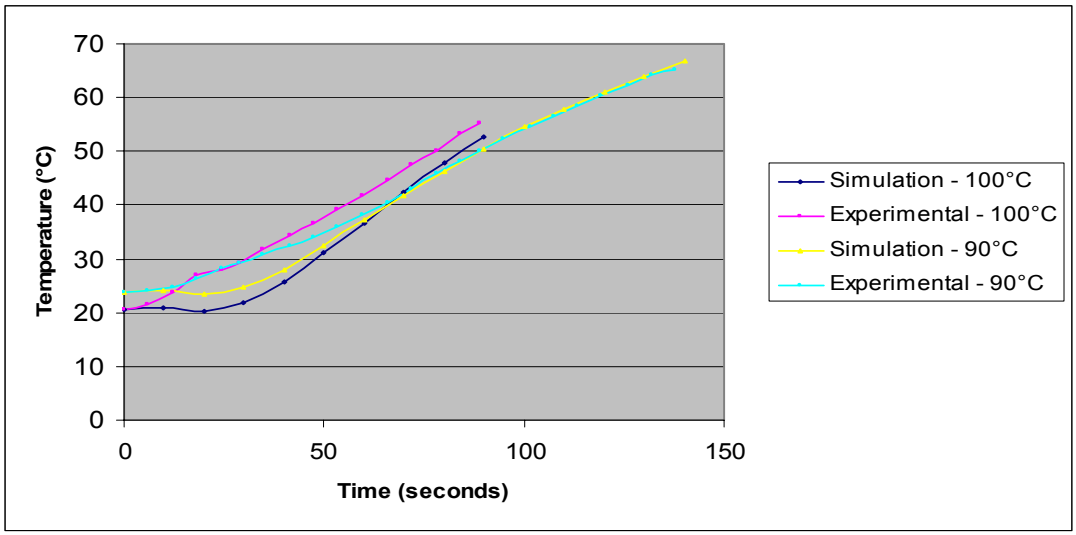

Figure 4.41: Simulation and Experimental Steam Heating Curves for 90 and 100°C of Grapes (Thermal Conductivity was taken as 0.98 W/m°C).

From Figure 4.41 it can be observed that the error between simulation and experimental values lessened compared to Figure 4.40. The main reason for this was the decrease in the thermal resistance of grapes by increased thermal conductivity where heat could more easily penetrate into the center. It is also worth observing the effects of heat transfer coefficient of steam on the final center temperature of grapes for 80°C steam heating.

From Table 4.13 it was observed that the heat transfer coefficient of steam had negligible effect on the final center temperature of grapes compared to grapes' thermal conductivity. For all values of heat transfer coefficient of steam, center temperature of grape was closely gathered around a mean value which meant that the effect of heat transfer coefficient of steam was negligible. Therefore, to simulate steam heating of grapes one should focus on precise measurement of thermal properties of grape rather than thermal properties of steam. From Figure 4.40 it is seen that as the temperature of the steam increased, the error in simulation increased. This might be due to the fact that as the temperature of the steam increased, grapes

experienced a harsher treatment, which might have resulted in a more rapid change of thermal properties of grapes during blanching. Also, steam blanching caused observable cracks on the surface of grapes which might ease the penetration of the heat to center more rapid than expected.

Table 4.13: Effect of Different Heat Transfer Coefficients of Steam and Thermal Conductivity of Grapes on the Final Center Temperature of Grapes

	k (W/m·°C)			
h (W/m^2·°C)	*0.6*	*0.8*	*1.0*	***Standard Deviation***
7272	65.518	71.879	75.571	5.085
15000	65.745	72.232	75.777	5.087
30000	65.784	72.328	75.840	5.103
Standard Deviation	0.143	0.236	0.140	

As shown in Figure 3.2, using curve fitting method to calculate thermal properties of both steam and grape, the inactivation time for polyphenol oxidase (PPO) enzyme, which resides within the skin of grape, was found to be 270, 140 and 90 seconds for 80°, 90° and 100°C steam temperatures. Using descriptive equations to calculate thermal properties of grapes, and equations to calculate thermal properties of steam, the inactivation time for PPO was found to be 290, 130 and 90 seconds for 80°, 90° and 100°C steam temperatures. Although there was considerable error between experimental and simulation center temperature when descriptive equations were used, steam heating of grapes had high Biot number which meant that the process within a short time frame was used for surface heating purposes. Thus the near surface temperature difference between curve fitting method and the method that used descriptive equations was negligible which then resulted in negligible time difference for inactivation of PPO.

4.5.4 Microwave-assisted drying of grapes

0.25 W/g initial power ratio was selected for temperature profile simulation of grapes. This was based on the fact that the final quality of raisins obtained using 0.25 W/g power ratio at 60°C convective air was superior to other power ratios at other air temperatures.

The electric field is the prime parameter in microwave heating which offers an intangible link between the electromagnetic energy and the material to be treated. It is often difficult to predict the magnitude of the electric field developed in the

material since its introduction into the cavity or applicator alters the absolute value of the field. One way to determine the absolute value of effective electric field is through calorimetry (Metaxas and Meredith, 1988) and equation (2.12) was used to calculate the effective electric field. The left side of equation (2.12) assumes bulk heating of the material. It was observed that within 10 minutes of microwave-assisted drying of grapes the maximum difference between center and near surface temperature was less than 1°C which could be assumed as bulk heating. Equation (2.12) assumes that the electric field within the material is constant. Since the electric field within the grape was not constant (radius of grape was 10.31 mm and penetration depth was 9.25 mm) using equation (2.9) integral average of the electric field was calculated . The descriptive figure is shown in Figure 4.42.

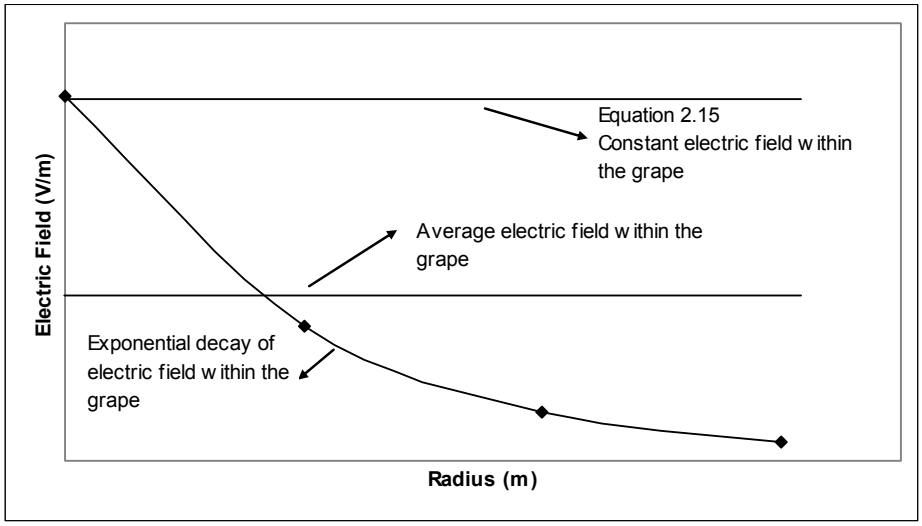

Figure 4.42: Constant and Exponential Variation of Electric Field within the Grape

According to Lyons et al., (1972) during initial heating period when the solid material contains very high proportions of water, some moisture may be removed from the solid as liquid, due to filtrational flow driven by the total pressure gradient. This phase of drying precedes the constant or falling rate period of drying and is termed 'liquid movement period' (Metaxas and Meredith, 1988). It was observed that during 'liquid movement period' moisture content of grapes fell from 77.6 to 77.22% (wet basis). Thus it was assumed that for the first 20 minutes, the initial heating period or in other words 'liquid movement period', evaporative heat loss was negligible. This assumption was also in agreement with Boldor et al., (2005).

Equation (2.13) was used to calculate time dependent center temperature profile of grapes during microwave-assisted convective drying. Convective energy flow term

in equation (2.13) was neglected and was used as a boundary condition. Moisture dependent internal heat generation was used since the dielectric loss term in equation (2.12) was moisture dependent. Moisture loss was found using Lewis equation and by this way the rate of evaporative heat loss was calculated. The constant f in equation (3.12) was taken as the difference of internal heat generation and evaporative heat loss. The constants d and c was defined as ρ·C, k·r where ρ,C and k was found with equation (3.1), (3.2) and (3.3). The experimental and simulation temperature profile of grapes is shown in Figure 4.43.

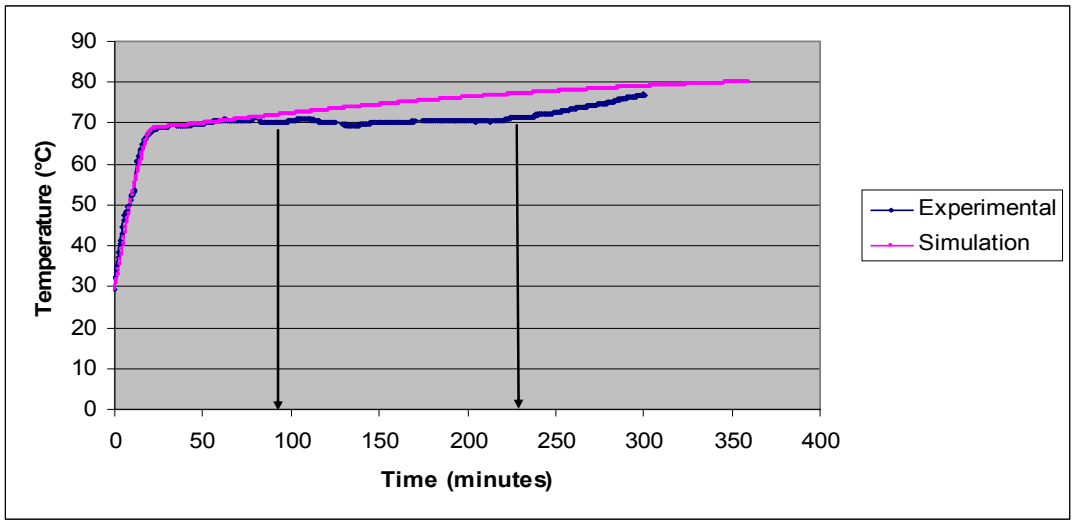

Figure 4.43: Experimental and Simulation Center Temperature Profiles of Grapes during 0.25 W/g Initial Microwave Power Ratio and 60°C Convective Air Drying

Maximum temperature difference between simulation and experimental temperature was during initial heating up period and was approximately 4°C. However after initial heating up period the difference was less than 1°C. It was also observed that after 110 minutes of drying the difference was slightly over 1°C and gradually increased. This might be due to lack of evaporative heat loss term due to errors in curve fitting of Lewis equation. Also it was observed that after 56% moisture content (w.b.) the experimental temperature values showed a sudden increase which is shown by an arrow.

4.6 General Evaluation

Several methods have been developed to reduce the drying time of grapes and to enhance the quality of raisins in terms of color and appearance. In most of the pretreatment methods, the grapes are first fumigated with sulphur dioxide to attain a

concentration of about 900 ppm. This sulphuring treatment is mainly aimed at obtaining a bright yellow color in the finished product (Tulasidas et al., 1995). The fumigated fruits are then dipped in dipping solutions to make the outer skin more permeable to water for rapid drying. The dipping solutions may range from ethyl oleate and potassium carbonate mixtures, to alkaline solutions and even the use of honey mixture was reported by McLellan et al., (1995). Grapes are then, either dried by sun or by convective air. It is reported that air temperature should not exceed 74°C for drying prunes and grapes (Petrucci and Clary, 2002). Figure 4.44 shows the drying kinetics of untreated and peeled grapes at different air temperatures that are considered to be in safe region for grape drying.

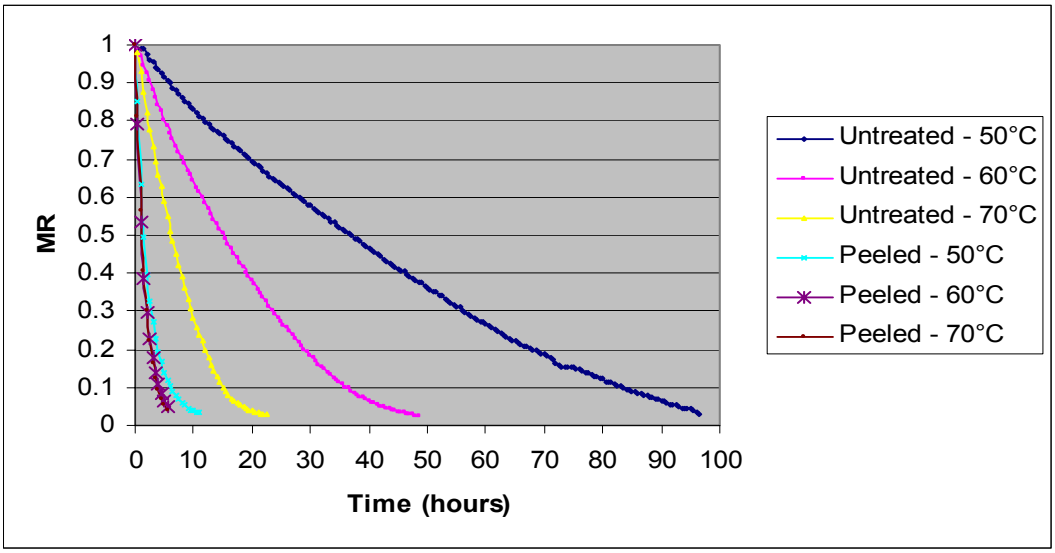

Figure 4.44: Drying Kinetics of Untreated and Peeled Grapes at Different Air Temperatures

It is seen from Figure 4.44 that even at 50°C drying temperature, peeled grapes had higher drying rate than 70°C drying temperature of untreated grapes. It was observed that as the temperature of the air increases the drying rate also increases. An increase of 10°C in air temperature approximately halved the drying time of untreated grapes but the same effect was not observed on peeled grapes. The overall drying rate of peeled grapes at 50, 60 and 70°C drying temperature were 8, 9 and 4 times, respectively, higher than untreated grapes. Final color values of the raisins of untreated and peeled grapes is given in Table 4.14.

Table 4.14: L*a*b* Values and Hue Angles of Untreated and Peeled Grapes at Different Temperatures

		50°C	*60°C*	*70°C*
Untreated	*L**	28.57	29.80	31.57
	*a**	5.03	9.16	9.67
	*b**	12.33	18.10	20.12
	Hue°	67.78	63.16	64.341
Peeled	*L**	49.87	48.62	45.20
	*a**	0.01	-0.52	0.78
	*b**	31.52	31.00	27.14
	Hue°	89.97	90.95	88.36

The hue angle (h°) represents color by a positive number between 0° and 360°, where 0° is red-purple, 90° is yellow, 180° is bluish-green and 270° is blue. It is seen that raisins that were produced from peeled grapes had a hue angle of approximately between 90° and an L*-value of 48 which indicated a moderately light yellow. However raisins that were produced from untreated grapes had hue angles of approximately 64° and an L*-value of 28 which would be dark orange and be perceived as brown (Bartleson, 1976). Although the L*, a* and b*-values and hue angles of raisins produced from untreated grapes were very close at 60 and 70°C and drying rate of 70°C is much greater than 60°C, it was visually observed that the raisins produced at 60°C had a better appearance in terms of color and texture. Thus in this study 60°C convective air temperature was used.

It should be noted that pretreatment methods such as dipping in chemical solutions or steam blanching removes the waxy layer or forms cracks on the grape surface however peeling the grapes in other words by completely removing the skin that is resistant to moisture transfer, drying rate should be the highest. Thus it can be hypothesized that the drying of grapes pretreated chemically or non-chemically should be faster than untreated grapes but could not be faster than peeled grapes.

It is seen from Figure 4.45 that this hypothesis was true for this study and that the peeled grape had the highest drying rate whereas untreated grapes had the lowest. Drying rate of steam blanched grapes were close to peeled grapes. Compared to untreated grapes, drying time was slightly reduced by dipping grapes at 40°C for 3 minutes.

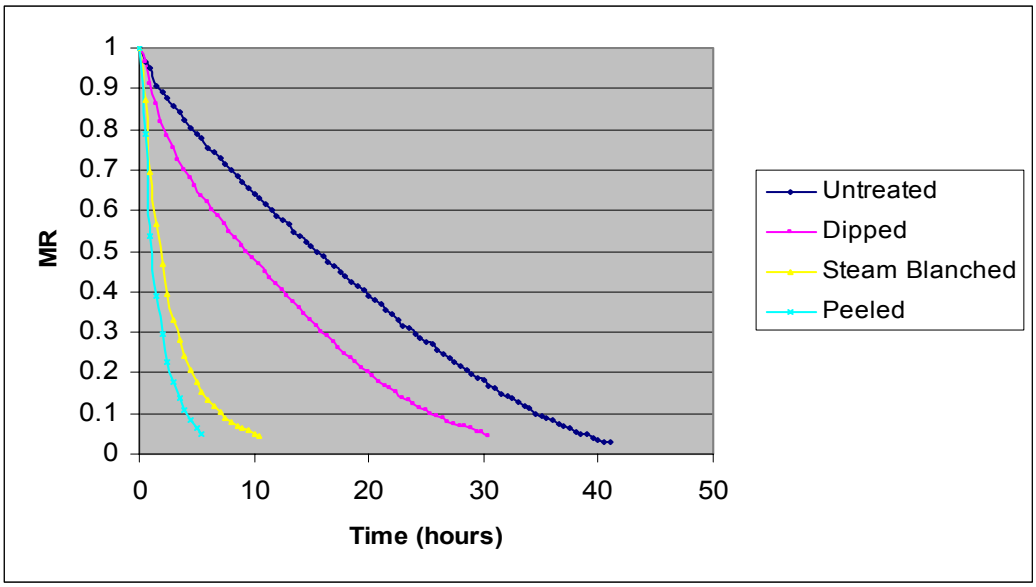

Figure 4.45: Drying Kinetics of Untreated, Dipped (40°C, 3 minutes), Steam Blanched (90°C) and Peeled Grapes at 60°C Convective Air Temperature

Final color values of the raisins produced by no-treatment, dipping in ethyl oleate and potassium carbonate at 40°C for 3 minutes, 90°C steam blanching or peeling is given in Table 4.15.

Table 4.15: L*a*b* Values and Hue Angles of Raisins Produced by Different Pretreatment Mehods at 60°C Convective Air Temperature

	Untreated	*Dipped*	*Steamed*	*Peeled*
*L**	29.80	26.67	40.15	48.62
*a**	9.16	7.02	5.83	-0.52
*b**	18.10	15.51	24.47	31.00
Hue°	63.16	65.64	76.60	90.95

It is seen from Figure 4.45 and Table 4.15 that as the drying rate increased by a pretreatment method the hue angle increased and a*-values were decreased. Therefore it can be inferred that as the effectiveness of the pretreatment method on the grape skin increased, proportionally the browning decreased and yellowness increased.

Pretreatment methods like chemical dipping or steam blanching mainly has external effects on the grapes' skin by either dissolving waxy layer or by forming cracks. However pretreatments like pressurization, pulsed electric field or freezing have internal effects that cause irreversible cell permeabilization. Comparison of external and internal effect on grape drying is shown in Figure 4.46.

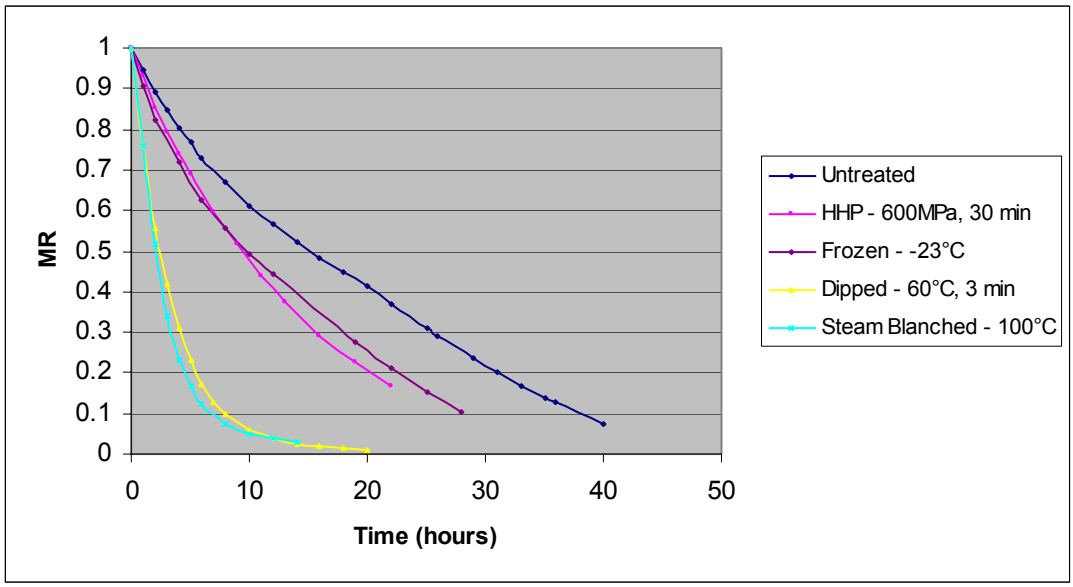

Figure 4.46: Effect of Different Pretreatment Methods on the Drying Rate of Grapes

It is seen from Figure 4.46 that pretreatments that both had internal and external effects on grapes, accelerated the drying rate compared to untreated grapes. Figure 4.46 revealed that pretreatment methods that externally affected grapes accelerated the drying rate far more than pretreatment methods that internally affected. This is in agreement with Dev et al. (2007) who also found that dipping grapes in 0.5% sodium hydroxide with 2% ethyl oleate at 80°C for 3 minutes had accelerated the drying rate much more than applying electric field at 1 kV/cm with exponential decay waveform with 100 pulses. It is also seen from Figure 4.46 that the drying rate of grapes that were dipped in 2% ethyl oleate and 5% potassium carbonate at 60°C for 3 minutes were the same as the drying rate of grapes that were steam blanched at 100°C for 90 seconds.

The L*-, a*- and b*-values revealed that the final color of raisins were affected by drying regardless of pretreatment method applied. Initial values of grapes had a negative a*-value indicating greenness and from Figure 4.47 it was observed that at the end of drying regardless of the pretreatment method all of the raisins had a positive a*-value indicating a shift to redness to some extent.

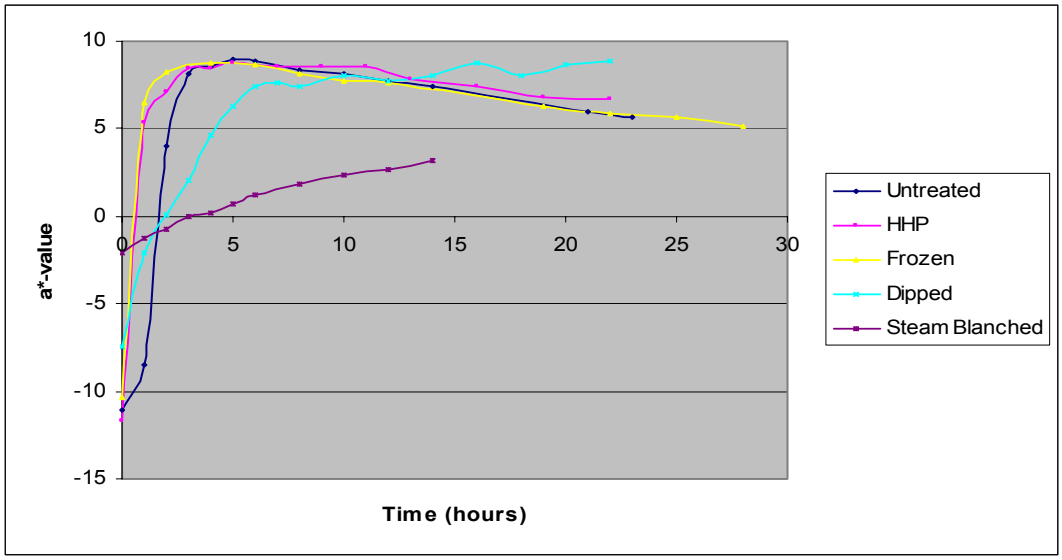

Figure 4.47: Change of a*-value of Untreated and Pretreated Grapes During Drying

It is seen from Figure 4.47 that pressurized and frozen grapes shifted to positive a*-value within the first hour of drying whereas untreated and dipped grapes shifted to positive a*-value after 2 hours. The reason for this could be that like pressurization, freezing might have activated polyphenol oxidase which in turn accelerated the browning reactions. The slowest shift to positive a*-value was observed for grapes that were steam blanched which had light yellowish final appearance. Irrespective of the pretreatment method, within 5 hours there was a shift from a negative a*-value to a positive a*-value which might be due to the heat treatment which degraded the bright green chlorophylls to a dull olive-brown (Clydesdale, 1997). It should be noted that although the final a*-value of raisin that were produced from steam blanched grapes were positive, their Hue value was 82.04° and L*-value was 53.65 wherefore they were perceived as a light yellowish color.

Conventional drying of relatively thick materials is a slow process relying on heat conduction from the outer layers towards the interior. High frequency electromagnetic energy, with its vastly superior penetration, offers a unique opportunity for enhancing the rate of evaporation and optimizing the overall drying process (Metaxas and Meredith, 1988). This is shown in Figure 4.48.

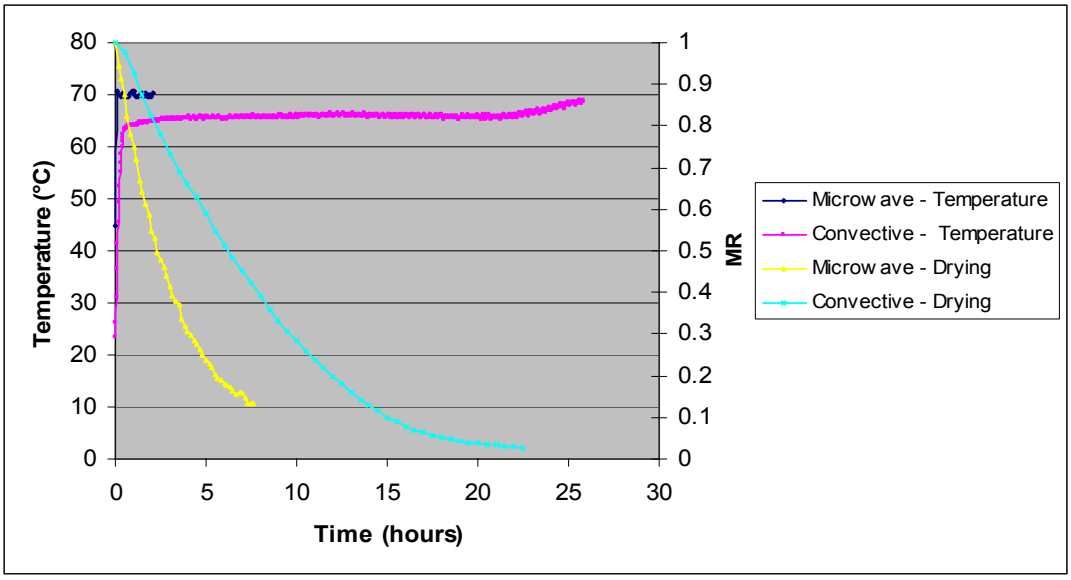

Figure 4.48: Microwave and Convective Heating Profiles (Primary Axis) and Drying Curves of Grapes (Secondary Axis)

It is seen from Figure 4.48 that microwave heated grapes reached the target temperature of 70°C within 10 minutes whereas convective heated grapes reached close proximity of target temperature in 2 hours however they reached the target temperature in approximately 25 hours. It is also seen that the drying time to reach a moisture ratio of 0.1 for microwave-assisted convective dried grapes was approximately the half of only convective dried grapes. This could be mainly due to the average temperature difference of 4.81°C and could be due to less case hardening and less tissue collapse which is in agreement with Srikiatden and Roberts (2005) where the first stages of microwave drying might be limited to liquid diffusion and as drying proceeds, moisture content decreases and a porous structure is formed and vapor diffusion through spaces may be the dominant moisture transfer mechanism. Giri and Prasad (2007) reported that in air-dried mushrooms there was very less open structure and pores as compared to microwave vacuum dried samples which indicated severe tissue shrinkage and collapse during air drying.

It is also seen from Figure 4.49 (a) and (b) that microwave dried grapes had much openings on the skin whereas convective dried grapes the skin was firmer which might impede moisture loss thus delay the drying.

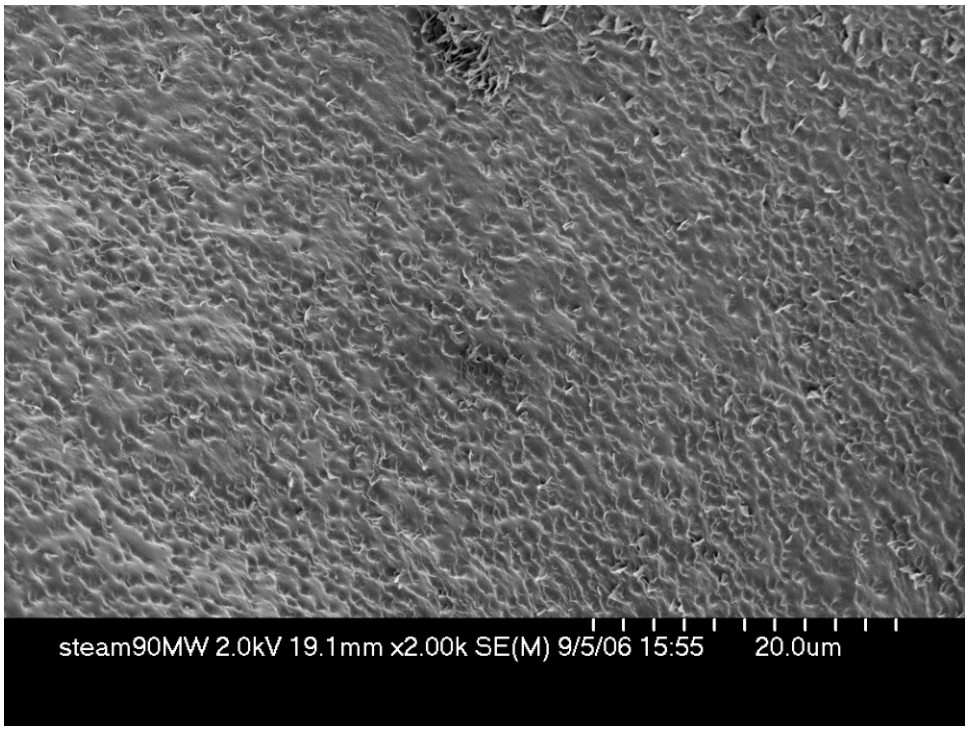

(a)

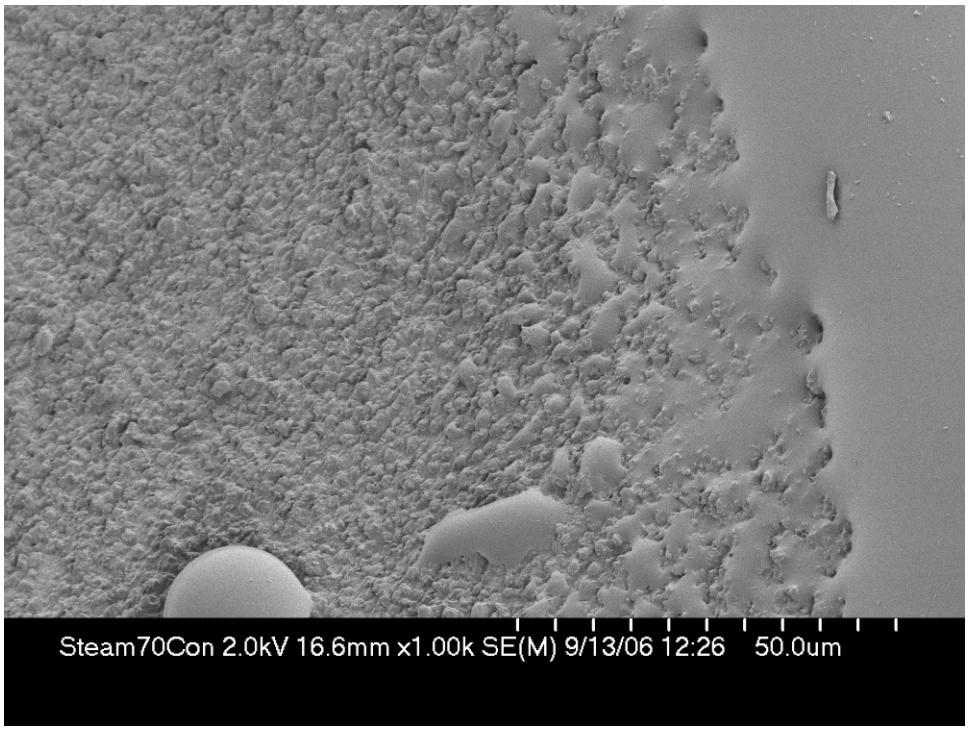

(b)

Figure 4.49: Scanning Electron Microscopy Images of Steam Blanched Grapes: (a) Microwave-assisted Dried, (b) Convective Dried

5. CONCLUSIONS

In this study, prior to drying of important export product of Turkey, namely raisins, effect of pretreatment methods, such as dipping grapes into a solution or application of high hydrostatic pressure (HHP) or steam blanching, with or without convective drying or microwave-assisted convective drying was investigated. Pretreatment solutions such as ethyl oleate and potassium carbonate decreased convective drying time by removing wax on grape surface and increased final color properties. HHP, which causes membrane permeabilisation by forming pores in biological cells and improves mass transfer properties, increased convective drying rate slightly. Steam blanching at different steam temperatures increased drying rate by removing waxy layer and by forming visual cracks on skin and improved final color properties by 2-log presumable inactivation of polyphenol oxidase enzyme. Thin-layer models were used to investigate the drying kinetics of both convective and microwave-assisted convective drying of grapes. Mathematical models investigating the temperature profiles for steam, convective and microwave heating were developed.

Although increasing the temperature of the convective air increased the drying rate, it was found that temperatures above 60°C did not give visually satisfactory end-product thus for drying of Thompson seedless grapes 60°C air temperature was more suitable in terms of both quality of produced raisins and drying rate.

Drying of grapes pretreated with dipping solutions and dried at 60°C air temperature with a 0.6 m/s air velocity could be best described with Midilli equation. As the temperature of dipping solution increased to 50° and 60°C there was no noticeable difference on drying rate of grapes between 2 and 3 minutes dipping time. However dipping time played more important role on drying rate at 30° and 40°C. Color data, normalized using fractional conversion, followed first order degradation kinetics. Chroma and b*-values showed no significant difference during drying. At all temperatures browning occurred, however as the dipping temperature increased above 40°C, the final color of raisins were light brown or light yellowish brown.

Shrinkage of grapes pretreated with dipping solutions at 30° and 40°C was linearly proportional with moisture loss whereas this relationship was exponential for the shrinkage of grapes preatreated with dipping at 50° and 60°C.

Steam blanching is an easy and relatively inexpensive pretreatment method prior to grape drying. Since there is no chemical involved during the process the only waste is condensed water. In this study steam blanching of grapes prior to drying greatly reduced the drying time. Normalized total color change, chroma and b*-values of steam blanched grapes followed first order degredation kinetics during drying. Since grapes did not brown during drying and had a golden yellow color, the use of sulfite, which has undesirable side effects, was thus prevented. It was found that steam blanching grapes at 100°C for 90 seconds was better in terms of lower center temperature and slightly higher near skin temperature compared to other time temperature combinations. The added advantage of steam blanching was to reduce the drying time, under identical drying conditions, to about one third of that of controls. The reduction in drying time may have desirable economic benefits. Except the Wang and Singh equation, drying of steam blanched grapes at 60°C air temperature with a 0.6 m/s air velocity can be described with all thin-layer equations. Shrinkage of steam blanched grapes during drying was linearly proportional to moisture loss.

Unlike dipping and steam blanching pretreatments, HHP causes membrane permeabilization rather than removing the waxy layer of grapes. It was found that application of HHP slightly increased the drying rate of grapes. All of the thin-layer equations accurately described (R^2 was greated than 0.99 and SSE and RMSE was close to zero) the drying curves of grapes pretreated with HHP. It was observed that pressurization of grapes at 600 MPa for 30 minutes was not enough to inactivate grape PPO. On the contrary, all of the applied pressures levels activated grape PPO which accelerated browning reactions. Shrinkage of pressurized grapes during drying were linearly proportional with moisture loss.

It was proved that as the microwave power increased the drying rate and temperature within the grapes increased. It was found that 0.25 W/g initial power ratio combined with 60°C convective air temperature produced better raisins compared to 1 W/g and 0.5 W/g power ratios combined with 40° and 50°C convective air temperature. Microwave assisted convective drying of grape data is best described with the Midilli

and Logarithmic models. It was observed that applied microwave power ratio did not significantly affected L*, a* and b*-values of raisins. Microwave energy heated the grapes quickly and presumably inactivated polyphenol oxidase enzyme, and prevented browning of raisins. This method could be a safe and economical substitute for sulfite use.

Except 90° and 100°C steam heating of grapes, the proposed mathematical models and their simulations for temperature profiles of convective and microwave-assisted convective drying of untreated grapes, convective drying of steam blanched grapes and steam heating of grapes were in close agreement with experimental data.

It can be concluded that for a better end-product, the pretreatment method and drying technique and their parameters should be selected carefully according to physical properties of the raw material.

REFERENCES

Ade-Omowaye, B.I.O., Rastogi, N.K., Angersbach, A. and Knorr, D., 2001. Effects of high hydrostatic pressure of high intensity electrical field pulse pre-treatment on dehydration characteristics of red paprika, *Innovative Food Science & Emerging Technologies*, **2**, 1-7.

Anon., 2004. Available: http://www.fas.usda.gov/htp/Hort_Circular/2003/9-12-03%20Web%20Art%20Updates/Raisins%20Situation%20Report%209-2-03.pdf

Anon., 2005a Available: http://www.leopold.iastate.edu/pubs/staff/grapes/grape.htm

Anon., 2005b Available: http://www.wholehealthmd.com/refshelf/foods_view/1,1523,67,00.html

Anon., 2005c Available: http://www.nutritiondata.com/facts-001-02s01hc.html

Anon., 2006. Available: http://www.gallawa.com/microtech/history.html

Anon., 2007a. Available: http://www.reference.com/browse/wiki/Sultana_%28grape%29

Anon., 2007b. Available: http://www.calwinexport.com/content/Stats&Research/world_vineyard%20Grape%20Wine%20Report%202003.htm

Azzouz, S., Guizani, A., Jomaa, W. and Belghith, A., 2002. Moisture diffusivity and drying kinetic equation of convective drying of grapes, *Journal of Food Engineering*, **55**, 323-330.

Babalis, S.J., Papanicolau, E., Kyriakis, N. and Belessiotis, V.G., 2006. Evaluation of thin-layer drying models for describing drying kinetics of figs (Ficus carica), *Journal of Food Engineering*, 75(**2**), 205-214.

Barbosa-Canovas, G.V. and Vega-Mercado, H., 1996. Dehydration of Foods, Eds. Barbosa-Canovas, G.V, Chapman & Hall, NY.

Barbosa, R.D., 2003. High pressure and temperature dependence of thermodynamic properties of model food solutions obtained from in situ ultrasonic measurements. *Ph.D. Dissertation*, University of Florida, Florida.

Barreiro, J.A., Milano, M. and Sandoval, A.J., 1997. Kinetics of colour change of double concentrated tomato paste during thermal treatment, *Journal of Food Engineering*, **33**, 359-371.

Bartleson, C.J., 1976. Brown, *Color Research and Application*, **1(4)**, 181-191.

Baydar, N.G., Özkan, G. and Sağdıç, O., 2004. Total phenolic contents and antibacterial activities of grape (Vitis vinifera L.) extracts. *Food Control*, **15**, 335-339.

Berg, R.W.,Hoogland, B.H., Lelieveld, H.L.M. and Schepdael, L., 2001. High pressure equipment designs for food processing applications, in *Ultra High Pressure Treatments of Foods*, pp. 297-313, Eds Hendrickx, M.E.G., Knorr, D., Kluwer Academic, New York.

Bilbao-Sainz, C., Andres, A., Chiralt, A. and Fito, P., 2006. Microwaves phenomena during drying of apple cylinders, *Journal of Food Engineering*, 74, 160-167.

Boldor, D., Sanders, T.H., Swartzel, K.R. and Farkas, B.E., 2005. A model for temperature and moisture distribution during continuous microwave drying, *Journal of Food Process Engineering*, **28**, 68-87.

Brimelow, C.J.B. and Joshi, P., 2001. Color measurement of foods by color reflectance in *Instrumentation and sensors for the food industry*, pp. 85-113, Eds. Rogers, E.K, Brimelow, C.J.B., Woodhead Publishing Ltd. And CRC Press LLC.

Busch, J.M., 1999. Enzymatic browning in potatoes: a simple assay for polyphenol oxidase catalyzed reaction, *Biochemical Education*, **27**, 171-173.

Castellari, M., Matricardi, L., Arfelli, G., Rovere, P. and Amati, A., 1997. Effects of high pressure processing on polyphenoloxidase enzyme activity of grape musts, *Food Chem*., **60**, 647-649.

Cheftel, J. C., 1992. Effects of high hydrostatic pressure on food constituents: an overview, in *High pressure and biotechnology*, pp. 195–209, Eds. C. Balny, R. Hayashi, K. Heremans, Masson, P., Editions John Libbey Euro-text, Montrouge.

Chen, C.R. and Ramaswamy, H.S., 2002. Color and texture change kinetics in ripening bananas, *Lebensm.-Wiss. u.-Technol.*, **25**, 415-419.

Chua, K.J., Chou, S.K., 2005. A comparative study between intermittent microwave and infrared drying of bioproducts, *International Journal of Food Science and Technology*, **40**, 23-39.

Clydesdale, E.M. 1998. Color: origin, stability, measurement, and quality, in *Food Storage Stability*, pp. 175-191 Eds. Taub, I.A., Singh, R.P., CRC Press LLC.

Cohen, J.S. and Yang, T.C.S., 1995. Progress in food dehydration, *Trends in Food Science and Technology*, **6**, 20-25.

Cui, Z.W., Xu, S.Y. and Sun, D.W., 2004. Microwave-vacuum drying kinetics of carrot slices, *Journal of Food Engineering*, **65**, 157-164.

Çengel, Y. A., 1998. Heat Transfer: A practical approach, McGraw-Hill, Inc. New Jersey, USA.

Datta, A.K., 2001. Fundamentals of Heat and Moisture Transport for Microwaveable Food Product and Process Development, in *Handbook of Microwave Technology for Food Applications*, pp.115-172, Eds. Datta, A.K., Anantheswaran, R.C., Marcel Dekker, Inc., New York.

Datta, A.K., and Ni, H., 2002. Infrared and hot-air-assisted microwave heating of foods for control of surface moisture, *Journal of Food Engineering*, 51, 355-364.

Datta, A.K., Geedipalli, S.S.R. and Almeida, M.F., 2005. Microwave Combination Heating, *Food Technology*, **59**, 36-40.

Delgado, A.E., Sun, D.W and Rubiolo, A.C., 2006. Thermal Physical Properties of Foods, in Thermal Food Processing: New Technologies and Quality Issues, pp. 3-34, Eds. Sun, D.W., CRC Press Taylor & Francis Group, Florida.

Dev, R.S.S., Padmini, T., Adedeji, A., Raghavan, G.S.V. and Gariepy, Y., 2007. Effect of chemical, microwave and pulsed electric field pretreatments on convective drying of grape, *ASAE Annual Meeting*, Paper number 072323.

Dibben, D., 2001. Electromagnetics: Fundamental Aspects and Numerical Modelling, in *Handbook of Microwave Technology for Food Applications*, pp.1-28, Eds. Datta, A.K., Anantheswaran, R.C., Marcel Dekker Inc., New York.

Dornenburg, H. and Knorr, D., 1993. Cellular permeabilisation of cultured plant tissue by high electric field pulse and ultra high pressure for recovery of secondary metabolites, *Food Biotechnology*, **7**, 35-48.

Doymaz, I., 2004. Effect of dipping treatment on air drying of plums. *Journal of Food Engineering*, **64**, 465-470.

Doymaz, I. and Pala, M. 2002. The effects of dipping pretreatments on air-drying rates of the seedless grapes, *Journal of Food Engineering*, **52**, 413-417.

Ehlerman, D.A.E., 2002. Microwave processing, in *The Nutrition Handbook for Food Processors*, pp. 396-407, Eds. Henry, C.J.K., Chapman, C., CRC Press LLC.

Ertekin, F.K. and Gedik, A., 2004. Sorption isotherms and isosteric heat of sorption for grapes, apricots, apples and potatoes, *Lebensm. Wiss. u. Technol*., 429-438.

Fellows, P., 2000. Blanching in Food Processing Technology: Principles and Practice, Second Edition, Midway Technology Limited, Cambridge, United Kingdom.

Fortes, M. and Okos, M.R., 1980. Drying Theories: Their Bases and Limitations as Applied to Foods and Grains, in *Advances in Drying Vol.1*, pp. 119-154, Eds. Mujumdar, A.S., McGraw-Hill, NY.

Francis, F.J., 2005. Colorimetric properties of foods, in *Engineering Properties of Foods*, pp. 495-524, Eds. Rao, M.A., Rizvi, S.S.H., Taylor and Francis Group, Florida.

Garcia, A., Torres, J.L., De Blas, M., De Francisco, A. and Illanes, R., 2004. Dielectric Characteristics of Grape Juice and Wine, *Biosystems Engineering*, **88** (3), 343-349.

Geankoplis, C.J., 1993. Transport Processes and Unit Operations, 3rd Ed., Prentice Hall, Englewood Cliffs, New Jersey.

Gentry, T.S. and Roberts, J.S., 2005. Design and evaluation of a continuous flow microwave pasteurization system for apple cider, *Lebensmittel-Wissenschaft und Technologie*, **38**, 227-238.

Giri, S.K. and Prasad, S., 2007. Drying kinetics and rehydration characteristics of microwave-vacuum and convective hot-air dried mushrooms. *Journal of Food Engineering*, **78**, 512-521.

Glenn, G.M., Chiou, B.S., Imam, S.H., Wood, D.F. and Orts, W.J., 2005. Role of cuticles in produce quality and preservation, in *Produce degradation: pathways and prevention*, pp. 19-53, Eds. Lamikanra, O., Imam, S.H., Ukuku, D.O., CRC Press. LLC.

Gomez-Lopez, V.M., 2002. Some biochemical properties of polyphenol oxidase from two varieties of avocado, *Food Chemistry*, **77**, 163-169.

Gould, G.W., 2000. New and emerging physical methods of preservation, in *The Microbiological Safety and Quality of Food*, pp. 277-293, Eds Lund, B.M., Bard-Parker, T.C., Gould, G.W., Aspen Publishers Inc., Gaitheesburg, Maryland.

Gould, G.W., 2001. The evolution of high pressure processing of foods, in *Ultra High Pressure Treatments of Foods*, pp. 3-21, Eds. Hendrickx, M.E.G., Knorr, D., Kluwer Academic, New York.

Gowen, A.A., Abu-Ghannam, N., Frias, J.M. and Oliveira, J.C., 2007. Characteristics of cooked chickpeas and soybeans during combined microwave-convective hot air drying, *Journal of Food Processing and Preservation*, **31**, 433-453.

Grabowski, S. and Marcotte, M., 2003. Pretreatment efficiency in osmotic dehydration of cranberries, in *Transport Phenomena in Food Processing*, pp.83-95, Eds. Welti-Chanes, J., Velez-Ruiz, J.F., Barbosa-Canovas, G.V., CRC Press LLC, Florida

Grncarevic, M., 1963. Effect of various dipping treatments on the drying rate of grapes for raisins, *Am. J. Enol. Viticult*, **14**, 230.

Henderson, S. M. and Pabis, S., 1961. Grain drying theory I: Temperature effect on drying coefficient, *Journal of Agriculture Research Engineering*, **6**, 169–174.

Hite, B.H., 1899. The effect of pressure in the preservation of milk, *Bull. of the West Virg. Univ. Agric. Exp. Station*, **58**, 15-35.

Hu, Q., Zhang, M., Mujumdar, A.S., Xiao, G. and Sun, J., 2006. Drying of edamames by hot air and vacuum microwave combination, *Journal of Food Engineering*, **4**, 977-982.

HunterLab, 2000. What is color and how is measured?, *HunterLab Applications Note*, **12**(5), http://www.hunterlab.com/appnotes/an05_00.pdf

HunterLab, 2001. The basics of color perception and measurement, *HunterLab*, http://www.hunterlab.com/pdf/color.pdf

Karabulut, I., Topcu, A., Duran, A., Turan, S. and Ozturk, B., 2007. Effect of hot air drying and sun drying on color values and β-carotene content

of apricot (Prunes armenica L.), *LWT - Food Science and Technology*, **40(5)**, 753-758.

Kim, M.J., Kim, C.Y., Park, I., 2005. Prevention of enzymatic browning of pear by onion extract, *Food Chemistry*, **89**, 181-184.

Kismali, I. and Altindisli, A., 2007. Cekirdeksiz kuru uzum uretimi, Available: http://www.agr.ege.edu.tr/~tuam/dergi/dergi1/uzumuretim.htm

Krebbers, B., Matser, A.M., Koets, M. and Van den Berg, R.W., 2002. Quality and storage stability of high-pressure preserved green beans, *Journal of Food Engineering*, **54**, 27-33.

Leblebici, F. and Koksel, H., 1999. Inactivation of sugar beet polyphenoloxidase by steam blanching, *Zuckerindustrie*, 124 (**3**), 213-216.

Lewis, W. K., 1921. The rate of drying of solid materials, *Industrial Engineering Chemistry*, **13**, 427–443.

Ludikhuyze, L., Loey, A.V., Denys, I.S. and Hendrickx, M.E.G., 2001. Effects of high pressure on enzymes related to food quality, in *Ultra High Pressure Treatments of Foods*, pp. 115-166, Eds. Hendrickx, M.E.G., Knorr, D., Kluwer Academic, New York.

Luikov, A.V. and Mikhailov, Yu.A., 1959. Theory of Energy and Mass Transfer, AN BSSR, Minsk.

Luzuriaga, D.A., Balaban, M.O. and Yeralan, S., 1997. Analysis of visual quality attributes of white shrimp by machine vision. *Journal of Food Science*, **62**, 113-118.

Lyons, D.W., Hatcher, J.D. and Sunderland, J.E., 1972. Drying of a porous medium with internal heat generation, *International Journal of Heat and Mass Transfer*, **15**, 897.

MacDougall, D.B., 2001. Principles of colour measurement for food, in *Instrumentation and sensors for the food industry*, pp. 63-82, Eds. Rogers, E.K, Brimelow, C.J.B., Woodhead Publishing Ltd. And CRC Press LLC.

Martinez, M.V. and Whitaker, J.R., 1995. The biochemisty and control of enzymatic browning, *Trends in Food Science & Technology*, **6**, 195-200.

Martynenko, O.G., Pavlyukevich, N.V. and Rudin, G.I., 1980. Mathematical methods and kinetics of heat and mass transfer with phase change in porous media, in *Advances in Drying Volume 1*, pp. 101-118, Eds. Mujumdar, A.S.,Hemisphere Publishing Corporation with McGraw-Hill International Book Company, Washington, USA.

Maskan, M., 2000. Microwave/air and microwave finish drying of banana, *Journal of Food Engineering*, **44**, 71-78.

Maskan, M., 2001. Kinetics of colour change of kiwifruits during hot air and microwave drying, *Journal of Food Engineering*, **48**, 169-175.

Matser, A.M., Knott, E.R., Teunissen, P.G.M. and Bartels, P.V., 2000. Effects of high isostatic pressure on mushrooms, *Journal of Food Engineering*, **45**, 11-16.

Matteo, M.D., Cinquanta, L., Galiero, G. and Crescitelli, S., 2000. Effect of a novel physical pretreatment process on the drying kinetics of seedless grapes. *Journal of Food Engineering*, **46**, 83-89.

Mazliak, P., 1970. Lipids, in *The Biochemistry of Fruits and Their Products*, pp. 209-221, Eds. Hulme, A.C., Elsevier, Amsterdam.

McLellan, M.R., Kime, R.W., Lee, C.Y. and Long, T.M., 1995. Effect of honey as an antibrowning agent in light raisin processing, *Journal of Food Process Engineering*, **19**, 1-8.

McMinn, W.A.M., Khraisheh, M.A.M. and Magee, T.R.A., 2003. Modelling the mass transfer during convective, microwave and combined microwave-convective drying of solid slabs and cylinder, *Food Research International*, **36**, 977-983.

McMinn, W.A.M., 2006. Thin-layer modelling of the convective, microwave, microwave-convective and microwave-vacuum drying of lactose powder. Journal of Food Engineering, **72**, 113-123.

Metaxas, A.C. and Meredith, R.J., 1998. Industrial microwave heating, Eds Johns, A.T., Ratcliff, G., Platss, J.R., Peter Peregrinus Ltd, London, United Kingdom.

Midilli, A., Kucuk, H. and Yapar, Z., 2002. A new model for single-layer drying. *Drying Technology*, 20**(7)**, 1503-1513.

Nelson, S.O., 1996. Review and assessment of radio-frequency and microwave energy for stored-grain insect control, *Trans ASAE*, **39**, 1475-1484.

Nijhuis, H.H., Torringa, H.M., Muresan, S., Yuksel, D., Leguijt, C. and Kloek, W., 1998. Approaches to improving the quality of dried fruit and vegetables, *Trends in Food Science & Technology*, **9**, 13-20.

Nisha, P., Singhal, R.S. and Pandit, A.B., 2004. A study on the degradation kinetics of visual green color in spinach (Spinacea oleracea L.) and the effect of salt therein, *Journal of Food Engineering*, **64**, 135-142.

Ochoa, M.R., Kesseler, A.G., Michelis, A., Mugridge, A. and Chaves, A.R., 2001. Kinetics of colour change of raspberry, sweet (Prunus avium) and sour (Prunus cerasus) cherries preserves packed in glass containers: light and room temperature effects, *Journal of Food Engineering*, **49**, 55-62.

Ozden, C., 2007. Kuru Üzüm, Available: http://www.igeme.org.tr/tur/rapor/sektor/Kuru_uzum.pdf

Page, G.E., 1949. Factors influencing the maximum rates of air drying shelled corn in thin layers, *M. Sc. Thesis*, Purdue University.

Palou, E., Lopez-Malo, A., Barbosa Canovas, G.V., Welti Chanes, J. and Swanson, B.G., 1999. Polyphenoloxidase activity and color of blanched and high hydrostatic pressure treated banana puree. *Journal of Food Science*, 64(**1**), 42-45.

Pangavhane, D.R., Sawhney, R.L. and Sarsavadia, P.N., 1999. Effect of various dipping pretreatment on drying kinetics of Thompson seedless grapes, *Journal of Food Engineering*, **39**, 211-216.

Patterson, D., 1987. Instruments for the measurement of the color of transparent and opaque objects, in *Color Physics for Industry*, pp. 35-62, Eds. McDonald, R., Society of Dyers and Colorists, Bradford.

Pedreschi, F., Moyano, P., Kaack, K. and Granby, K., 2005. Color changes and acrylamide formation in fried potato slices, *Food Research International*, **38**, 1-9.

Perkin, R.M., 1979. Prospects of drying with radio frequency and microwave electromagnetic fields, *Journal of Separation Process Technology*, **1(2)**, 14.

Petrucci, V.E. and Clary, C.D., 2002. A Treatise on Raisin Production, Processing and Marketing, Malcolm Media Press, Clovis, California, USA.

Piga, A., Poiana, M., Pinna, I., Agabbio, M. and Mincione, A., 2004. Drying performance of five Italian apricot cultivars, *Sciences des Aliments*, 24(**3**), 247-259.

Ponting, J.D. and McBean, D.M., 1970. Temperature and dipping treatment effects on drying rates and drying times of grapes, prunes and other waxy fruits, *Food Techn*, 24(12), 1403-1406.

Radler, F., 1964. The prevention of browning during drying by the cold dipping treatment of Sultana grapes, *Journal Science Food Agriculture*, **15**, 864.

Ramaswamy, H.S., 2004. Thermal Processing of Fruits, in *Processing Fruits Science and Technology*, pp. 173-200, Eds. Barrett D.M., Somogyi, L., Ramaswamy, H.M., CRC Press LLC, Florida.

Rastogi, N.K., Angersbach, A., Knorr, D., 2000. Synergistic effect of high hydrostatic pressure pretreatment and osmotic stress on mass transfer during osmotic dehydration, *Journal of Food Engineering*, **45**, 25-31.

Regier, M. and Schubert, H., 2005. Introducing microwave processing of food: principles and technologies, in *The microwave processing of foods*, pp. 3-20, Eds Schubert, H., Regier, M., CRC Press, Woodhead Publishing Limited, Cambridge, England.

Ren, G. and Chen, F., 1998. Drying of American Ginseng (Panax quinquefolium) Roots by Microwave-Hot Air Combination, *Journal of Food Engineering*, **35**, 433-443.

Robert, C., Richard-Forget, F., Rouch, C., Pabion, M. and Cadet, F., 1996. A Kinetic Study of the Inhibition of Palmito Polyphenol Oxidase by L-cysteine, *Int. J. Biochem. Cell Biol.*, **28**, 457-463.

Roberts, J. S. and Tong, C. H., 2003. The development of an isothermal drying apparatus and the evaluation of the diffusion model on hygroscopic porous material, *International Journal of Food Properties*, **6**, 165–180.

Ryynanen, S., 2002. Microwave heating uniformity of multi-component prepared foods, PhD thesis, University of Helsinki, Finland.

Saltiel, C. and Datta, A.K., 1998. Heat and Mass Transfer in Microwave Processing, *Advances in Heat Transfer*, **32**,1-94.

Sanga, E.C.M., Mujumdar, A.S. and Raghavan, G.S.V., 2002. Simulation of convection-microwave drying for a shrinking material, *Chemical Engineering and Processing*, **41**, 487-499.

Saravacos, G.D. and Marousis, S.N., 1988. Effect of ethyl oleate on the rate of air-drying of foods, *Journal of Food Engineering*, **7**, 263-270.

Schiffmann, R.F., 1986. Food product development for microwave processing, *Food Technology*, 40(**6**), 94-98.

Schiffmann, R.F., 2001. Microwave Processes for the Food Industry, in, *Handbook of Microwave Technology for Food Applications* pp. 299-337, Eds. Datta A.K. and Anantheswaran R.C., New York, Marcel Dekker, Inc.

Sharaf-Eldeen, Y. I., and Hamdy, M. Y., 1979. Falling rate drying of fully exposed biological materials: A review of mathematical models, **ASAE Paper**, No. **79-6622**, 1979 Winter Meeting of ASAE.

Silvia, F.A., Marsaioli, A., Maximo, G.J., Silva, M.A.A.P. and Goncalves, L.A.G., 2006. Microwave assisted drying of macadamia nuts, *Journal of Food Engineering*, **77**, 550-558.

Smelt, J.P.P.M., 1998. Recent advances in the microbiology of high-pressure processing, *Trends in Food Science & Technology*, **9**, 152-158.

Soysal, Y., 2004. Microwave drying characteristics of parsley, *Biosystems Engineering*, 89(**2**), 167-173.

Srikiatden, J. and Roberts, J.S., 2005. Moisture Loss Kinetics of Apple During Convective Hor Air and Isothermal Drying, *International Journal of Food Properties*, **8**, 493-512.

Srikiatden, J. and Roberts, J.S., 2006. Measuring moisture diffusivity of potato and carrot (core and cortex) during convective hot air and isothermal drying, *Journal of Food Engineering*, **74**, 143-152.

Suarez, C., Loncin, M. and Cherife, J.A., 1984. A preliminary study of the ethyl oleate dipping treatment on drying rate of grain corn, *Journal of Food Science*, **49**, 236-238.

Tang, J., 2005. Dielectric properties of foods, in *The microwave processing of foods*, pp. 3-20, Eds Schubert, H., Regier, M., CRC Press, Woodhead Publishing Limited, Cambridge, England.

Tang, J., Hao, F. and Lau, M., 2002. Microwave Heating in Food Processing, in *Advances in Bioprocess Engineering (Advances in Agricultural Science and Technology)*, pp. 1-44, Eds Yang, H., Tang, J., World Scientific Publishing, London, United Kingdom.

Tarhan, S., 2007. Selection of chemical and thermal pretreatment combination for plum drying at low and moderate drying air temperatures, *Journal of Food Engineering*, **79**, 255-260.

Thomas, P.P. and Gopalakrishnan, N., 1991. Green colour retention in enzyme inactivated dried pepper, *Indian Spices*, 28(**1**), 6-10.

Thuery, J., 1992. Electromagnetism and Radiation, in *Microwaves: Industrial, Scientific, and Medical Applications*, pp. 3-19, Eds Grant, H.E., Artech House, Inc., London, United Kingdom.

Togrul, I.T. and Pehlivan, D., 2003. Modeling of drying kinetics of single apricot, *Journal of Food Engineering*, **58**, 23-32.

Tong, C.H., 1998. Microwave Heating of Bakes Dough Products With Simultaneous Heat and Moisture Transfer. Ph.D. Dissertation, University of Wisconsin-Madison.

Tulasidas, T., 1995. Combined convective and microwave drying of grapes, *Drying Technology*, 13(**4**), 1029-1031.

Tulasidas, T., Raghavan, G.S.V. and Norris, E.R., 1995. Effects of dipping and washing pre-treatments on microwave drying of grapes, *Journal of Food Process Engineering*, **19**, 15-25.

Umbaugh, S.E., 1998. Computer Vision and Image Processing: A Practical Approach Using CVIPtools, Prentice Hall PTR, New Jersey.

Verboven, P., Datta, A.K., Anh, N.T., Scheerlinck, N. and Nicolai, B.M., 2003. Computation of airflow effects on heat and mass transfer in a microwave oven, *Journal of Food Engineering*, **59**, 181-190.

Vollmer, M., 2004. Physics of the microwave oven, *Physics Education*, 39:1, 74-81.

Von Hippel, A., 1954. *Dielectrics and waves*, Wiley, New York.

Warner, C.R., Diachenko, G.W. and Bailey, C.J., 2000. Sulfites: An Important Food Safety Issue, *Available: http://www.cfsan.fda.gov/~dms/fssulfit.html*

Wang, J. and Sheng, K., 2006. Far-infrared and microwave drying of peach, *LWT-Food Science and Technology*, **39**, 247-255.

Wang, C. N. and Singh, R. P., 1978. A single layer drying equation for rough rice, *ASAE Paper,* 78-3001.

Wang, Y., Wig, T.D., Tang, J. and Hallberg, L.M., 2003. Dielectric properties of foods relevant to radio frequency and microwave pasteurization and sterilization, *Journal of Food Engineering*, **57**, 257-268.

Wang, J. and Xi, Y.S., 2005. Drying characteristics and drying quality of carrot using a two-stage microwave process, *Journal of Food Engineering*, **68**, 505-511.

Weemaes, C.A., Ludikhuyze, L.R., Broeck, I.V. and Hendrickx, M.E., 1998. High pressure inactivation of polyphenoloxidases, *Journal of Food Science*, **63**, 873-877.

Weemaes, C.A., Ludikhuyze, L.R., Broeck, I.V., Hendrickx, M.E. and Tobback, P.P., 1998. Activity, Electrophoretic Characteristics and Heat Inactivation of PPOs from Apples, Avocados, Grapes, Pears and Plums, *Lebensm. Wiss. u. Technol*., **31**, 44-49.

Yaldiz, O. and Ertekin, C., 2001. Thin layer solar drying of some vegetables, *Drying Technology*, **19**, 583–597.

Yaldiz, O., Ertekin, C. and Uzun, H.I., 2001. Mathematical modeling of thin layer solar drying of sultana grapes, *Energy*, **26**, 457-465.

Yam, K.L. and Papadakis, S.E., 2004. A simple digital imaging method for measuring and analyzing color of food surfaces, *Journal of Food Engineering*, **61**, 137-142.

Yemencioglu, A., 2002. Control of polyphenol oxidase in whole potatoes by low temperature blanching, *European Food Research and Technology*, 214(**4**), 313-319.

Zhang, H. and Datta, A.K., 2001. Electromagnetics of Microwave Heating: Magnitude and Uniformity of Energy Absorption in an Oven, in *Handbook of Microwave Technology for Food Applications*, pp.33-67, Eds Datta, A.K., Anantheswaran, R.C., Marcel Dekker, Inc., New York.

Zhang, M., Tang, J., Mujumdar, A.S. and Wang, S., 2006. Trends in microwave-related drying of fruits and vegetables, *Trends in Food Science & Technology*, **17**, 524-534.

APPENDIX

A. DRYING KINETICS

A.1 High-Hydrostatic Pressure Processing of Grapes

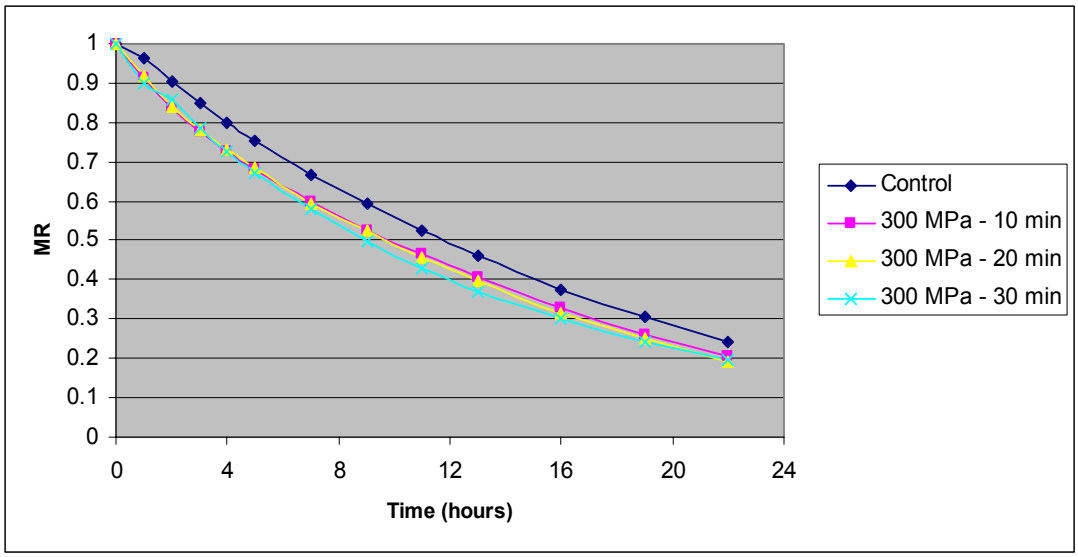

Figure A.1: Drying rate of grapes pressurized at 300 MPa for 10, 20, 30 minutes

A.2 Dipping of Grapes

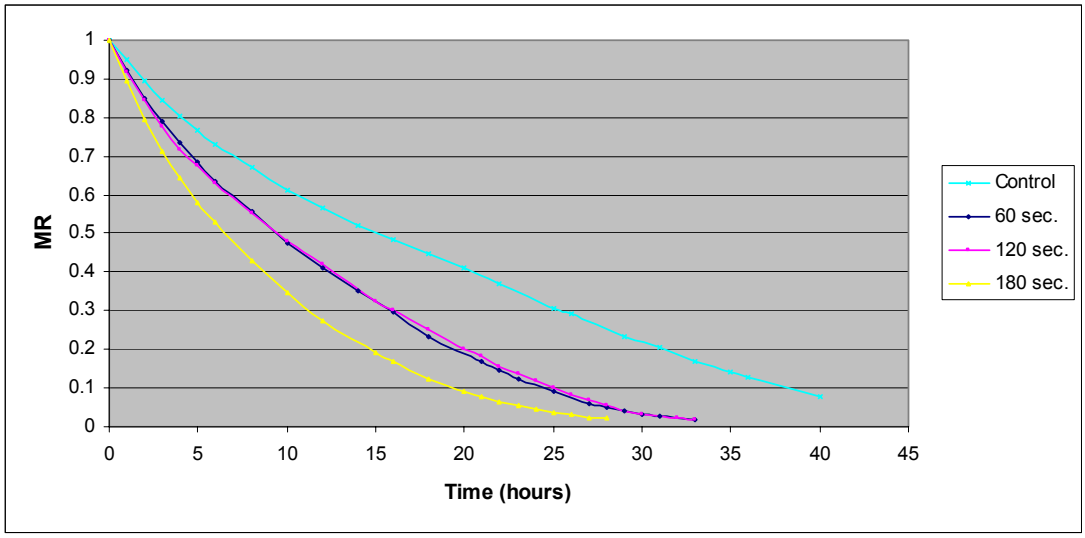

Figure A.2: Effect of Dipping at 40°C for 60, 120 and 180 seconds on Drying Rate of Grapes

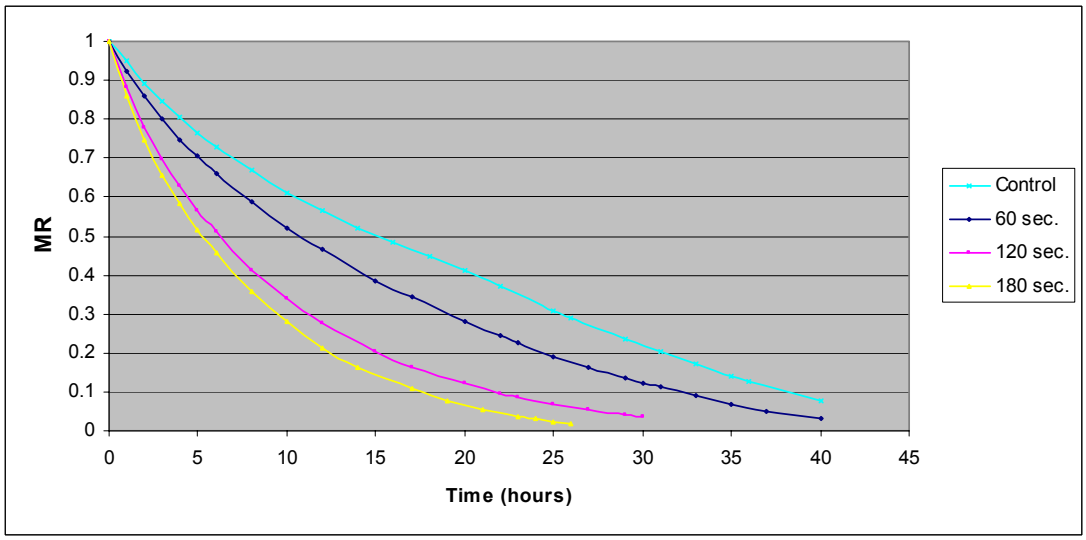

Figure A.3: Effect of Dipping at 50°C for 60, 120 and 180 seconds on Drying Rate of Grapes

B. THIN-LAYER MODELING

B.1 High-Hydrostatic Pressure Processing of Grapes

Table B.1: Statistics of thin-layer models applied to 300 MPa pressure level obtained using non-linear regression analysis.

Model	10 minutes	20 minutes	30 minutes
Lewis	R^2=0.999 RMSE=0.003 SSE=0.000	R^2=0.998 RMSE=0.013 SSE=0.002	R^2=0.999 RMSE=0.010 SSE=0.001
Page	R^2=0.998 RMSE=0.010 SSE=0.001	R^2=0.999 RMSE=0.009 SSE=0.001	R^2=0.999 RMSE=0.006 SSE=0.000
Henderson and Pabis	R^2=0.998 RMSE=0.012 SSE=0.002	R^2=0.999 RMSE=0.001 SSE=0.001	R^2=0.999 RMSE=0.008 SSE=0.001
Logarithmic	R^2=0.998 RMSE=0.012 SSE=0.002	R^2=0.998 RMSE=0.010 SSE=0.001	R^2=0.999 RMSE=0.007 SSE=0.001
Approximation of Diffusion	R^2=0.995 RMSE=0.018 SSE=0.003	R^2=0.997 RMSE=0.014 SSE=0.002	R^2=0.998 RMSE=0.011 SSE=0.001
Wang and Singh	R^2=0.990 RMSE=0.026 SSE=0.008	R^2=0.992 RMSE=0.022 SSE=0.006	R^2=0.995 RMSE=0.018 SSE=0.004
Midilli et al.	R^2=0.999 RMSE=0.003 SSE=0.000	R^2=0.999 RMSE=0.003 SSE=0.000	R^2=0.999 RMSE=0.007 SSE=0.000

Table B.2: Statistics of thin-layer models applied to 600 MPa pressure level obtained using non-linear regression analysis.

Model	10 minutes	20 minutes	30 minutes
Lewis	R^2=0.997 RMSE=0.017 SSE=0.003	R^2=0.998 RMSE=0.012 SSE=0.002	R^2=0.999 RMSE=0.009 SSE=0.001
Page	R^2=0.999 RMSE=0.006 SSE=0.000	R^2=0.998 RMSE=0.011 SSE=0.001	R^2=0.999 RMSE=0.008 SSE=0.001
Henderson and Pabis	R^2=0.998 RMSE=0.013 SSE=0.002	R^2=0.998 RMSE=0.013 SSE=0.002	R^2=0.999 RMSE=0.009 SSE=0.001
Logarithmic	R^2=0.999 RMSE=0.001 SSE=0.001	R^2=0.999 RMSE=0.006 SSE=0.000	R^2=0.999 RMSE=0.005 SSE=0.000
Approximation of Diffusion	R^2=0.996 RMSE=0.017 SSE=0.003	R^2=0.997 RMSE=0.013 SSE=0.002	R^2=0.999 RMSE=0.009 SSE=0.001
Wang and Singh	R^2=0.991 RMSE=0.026 SSE=0.007	R^2=0.998 RMSE=0.011 SSE=0.001	R^2=0.998 RMSE=0.014 SSE=0.002
Midilli et al.	R^2=0.999 RMSE=0.007 SSE=0.000	R^2=0.999 RMSE=0.004 SSE=0.000	R^2=0.999 RMSE=0.004 SSE=0.000

B.2 Steam Blanching of Grapes

Table B.3: Statistics of thin-layer models applied to steam blanched grapes obtained using non-linear regression analysis.

Model	$80^{\circ}C$	$90^{\circ}C$	$100^{\circ}C$
Lewis	R^2=0.998 RMSE=0.013 SSE=0.002	R^2=0.998 RMSE=0.016 SSE=0.003	R^2=0.995 RMSE=0.022 SSE=0.005
Page	R^2=0.999 RMSE=0.012 SSE=0.001	R^2=0.997 RMSE=0.017 SSE=0.003	R^2=0.996 RMSE=0.021 SSE=0.004
Henderson and Pabis	R^2=0.998 RMSE=0.013 SSE=0.002	R^2=0.997 RMSE=0.167 SSE=0.017	R^2=0.995 RMSE=0.022 SSE=0.005
Logarithmic	R^2=0.999 RMSE=0.006 SSE=0.000	R^2=0.998 RMSE=0.013 SSE=0.001	R^2=0.996 RMSE=0.022 SSE=0.004
Approximation of Diffusion	R^2=0.999 RMSE=0.006 SSE=0.000	R^2=0.999 RMSE=0.012 SSE=0.001	R^2=0.995 RMSE=0.023 SSE=0.004
Wang and Singh	R^2=0.938 RMSE=0.079 SSE=0.056	R^2=0.937 RMSE=0.080 SSE=0.058	R^2=0.933 RMSE=0.084 SSE=0.064
Midilli et al.	R^2=0.999 RMSE=0.006 SSE=0.000	R^2=0.999 RMSE=0.001 SSE=0.001	R^2=0.999 RMSE=0.012 SSE=0.001

B.3 Dipping of Grapes

Table B.4: Constant of thin-layer models applied to 40° and 50°C dipping temperatures obtained by using non-linear regression analysis.

Model	Dipping Temperature					
	40°C			50°C		
	Holding Time					
	60 sec.	120 sec.	180 sec.	60 sec.	120 sec.	180 sec.
Lewis	k=0.083	k=0.082	k=0.112	k=0.067	k=0.110	k=0.133
Page	k_1=0.057 n=1.138	k_1=0.063 n=1.096	k_1=0.098 n=1.057	k_1=0.066 n=1.004	k_1=0.124 n=0.948	k_1=0.139 n=0.980
Henderson and Pabis	a=1.027 k=0.085	a=1.014 k=0.083	a=1.010 k=0.114	a=0.990 k=0.066	a=0.980 k=0.108	a=0.986 k=0.131
Logarithmic	a=1.142 k=0.060 c=-0.155	a=1.144 k=0.057 c=-0.172	a=1.041 k=0.098 c=-0.052	a=1.045 k=0.056 c=-0.073	a=0.976 k=0.110 c=0.007	a=0.996 k=0.125 c=-0.017
Approximation of Diffusion	a=-9.926 k=0.131 b=0..953	a=-6.698 k=0.123 b=0.942	a=-8.256 k=0.155 b=0.963	a=-1.111 k=0.084 b=0.896	a=0.007 k=-0.016 b=-6.795	a=0.025 k=4.558 b=0.028
Wang and Singh	a_1=0.001 b_1=-0.061	a_1=0.001 b_1=-0.060	a_1=-0.002 b_1=-0.081	a_1=0.001 b_1=-0.051	a_1=0.001 b_1=-0.081	a_1=0.002 b_1=-0.095
Midilli et al.	a=0.994 k_1=0.071 n=0.979 b_2=-0.003	a=0.999 k_1=0.085 n=0.879 b_2=-0.005	a=0.997 k_1=0.110 n=0.971 b_2=-0.002	a=0.999 k_1=0.081 n=0.871 b_2=-0.003	a=1.001 k_1=0.129 n=0.919 b_2=-0.001	a=0.998 k_1=0.149 n=0.917 b_2=-0.001

Table B.5: Statistics thin-layer models applied to 30°C and 40°C dipping temperatures obtained using non-linear regression analysis.

Model	Dipping Temperature					
	30°C			40°C		
	Holding Time					
	60 sec.	120 sec.	180 sec.	60 sec.	120 sec.	180 sec.
Lewis	R^2=0.990 RMSE=0.028 SSE=0.017	R^2=0.993 RMSE=0.025 SSE=0.013	R^2=0.994 RMSE=0.026 SSE=0.015	R^2=0.989 RMSE=0.033 SSE=0.024	R^2=0.990 RMSE=0.031 SSE=0.023	R^2=0.997 RMSE=0.017 SSE=0.006
Page	R^2=0.994 RMSE=0.022 SSE=0.010	R^2=0.994 RMSE=0.023 SSE=0.010	R^2=0.996 RMSE=0.021 SSE=0.009	R^2=0.994 RMSE=0.024 SSE=0.013	R^2=0.993 RMSE=0.027 SSE=0.017	R^2=0.998 RMSE=0.014 SSE=0.004
Henderson and Pabis	R^2=0.994 RMSE=0.023 SSE=0.011	R^2=0.994 RMSE=0.022 SSE=0.010	R^2=0.994 RMSE=0.026 SSE=0.014	R^2=0.990 RMSE=0.033 SSE=0.022	R^2=0.990 RMSE=0.031 SSE=0.022	R^2=0.997 RMSE=0.017 SSE=0.006
Logarithmic	R^2=0.994 RMSE=0.023 SSE=0.010	R^2=0.995 RMSE=0.020 SSE=0.008	R^2=0.999 RMSE=0.008 SSE=0.001	R^2=0.999 RMSE=0.009 SSE=0.002	R^2=0.999 RMSE=0.011 SSE=0.003	R^2=0.999 RMSE=0.006 SSE=0.001
Approximation of Diffusion	R^2=0.996 RMSE=0.020 SSE=0.007	R^2=0.995 RMSE=0.021 SSE=0.008	R^2=0.997 RMSE=0.019 SSE=0.0075	R^2=0.995 RMSE=0.023 SSE=0.011	R^2=0.993 RMSE=0.026 SSE=0.015	R^2=0.998 RMSE=0.013 SSE=0.003
Wang and Singh	R^2=0.970 RMSE=0.051 SSE=0.051	R^2=0.978 RMSE=0.043 SSE=0.037	R^2=0.992 RMSE=0.028 SSE=0.017	R^2=0.996 RMSE=0.021 SSE=0.009	R^2=0.992 RMSE=0.028 SSE=0.018	R^2=0.988 RMSE=0.035 SSE=0.024
Midilli et al.	R^2=0.999 RMSE=0.010 SSE=0.002	R^2=0.999 RMSE=0.009 SSE=0.001	R^2=0.999 RMSE=0.009 SSE=0.001	R^2=0.999 RMSE=0.009 SSE=0.002	R^2=0.999 RMSE=0.007 SSE=0.001	R^2=0.999 RMSE=0.006 SSE=0.001

Table B.6: Statistics of thin-layer models applied to 50° and 60°C dipping temperatures obtained by using non-linear regression analysis.

Model	Dipping Temperature					
	50°C			60°C		
	Holding Time					
	60 sec.	120 sec.	180 sec.	60 sec.	120 sec.	180 sec.
Lewis	R^2=0.997 RMSE=0.018 SSE=0.007	R^2=0.999 RMSE=0.011 SSE=0.002	R^2=0.999 RMSE=0.011 SSE=0.002	R^2=0.999 RMSE=0.009 SSE=0.002	R^2=0.999 RMSE=0.009 SSE=0.001	R^2=0.999 RMSE=0.006 SSE=0.000
Page	R^2=0.997 RMSE=0.018 SSE=0.007	R^2=0.999 RMSE=0.005 SSE=0.000	R^2=0.999 RMSE=0.011 SSE=0.002	R^2=0.999 RMSE=0.008 SSE=0.001	R^2=0.999 RMSE=0.007 SSE=0.001	R^2=0.999 RMSE=0.006 SSE=0.000
Henderson and Pabis	R^2=0.997 RMSE=0.017 SSE=0.007	R^2=0.999 RMSE=0.008 SSE=0.001	R^2=0.999 RMSE=0.011 SSE=0.002	R^2=0.999 RMSE=0.008 SSE=0.001	R^2=0.999 RMSE=0.009 SSE=0.001	R^2=0.999 RMSE=0.006 SSE=0.000
Logarithmic	R^2=0.999 RMSE=0.011 SSE=0.002	R^2=0.999 RMSE=0.008 SSE=0.001	R^2=0.999 RMSE=0.009 SSE=0.001	R^2=0.999 RMSE=0.008 SSE=0.001	R^2=1.000 RMSE=0.002 SSE=0.000	R^2=0.999 RMSE=0.004 SSE=0.000
Approximation of Diffusion	R^2=0.997 RMSE=0.018 SSE=0.007	R^2=0.999 RMSE=0.010 SSE=0.002	R^2=0.999 RMSE=0.010 SSE=0.002	R^2=0.999 RMSE=0.011 SSE=0.002	R^2=1.000 RMSE=0.002 SSE=0.000	R^2=0.999 RMSE=0.004 SSE=0.000
Wang and Singh	R^2=0.987 RMSE=0.036 SSE=0.028	R^2=0.971 RMSE=0.053 SSE=0.048	R^2=0.973 RMSE=0.052 SSE=0.044	R^2=0.974 RMSE=0.051 SSE=0.044	R^2=0.907 RMSE=0.092 SSE=0.110	R^2=0.876 RMSE=0.107 SSE=0.149
Midilli et al.	R^2=0.999 RMSE=0.003 SSE=0.000	R^2=0.999 RMSE=0.002 SSE=0.000	R^2=0.999 RMSE=0.003 SSE=0.000	R^2=0.999 RMSE=0.003 SSE=0.000	R^2=0.999 RMSE=0.002 SSE=0.000	R^2=0.999 RMSE=0.003 SSE=0.000

B.4 Microwave Drying

B.4.1 Small scale microwave drying (SSMD)

Table B.7: Statistics of applied thin-layer models to SSMD obtained using non-linear regression analysis.

Model	50 W	100 W	200 W	Isothermal 70°C
Lewis	R^2=0.981 RMSE=0.040 SSE=0.279	R^2=0.981 RMSE=0.037 SSE=0.150	R^2=0.872 RMSE=0.072 SSE=0.170	R^2=0.998 RMSE=0.010 SSE=0.045
Page	R^2=0.984 RMSE=0.035 SSE=0.221	R^2=0.981 RMSE=0.037 SSE=0.147	R^2=0.983 RMSE=0.026 SSE=0.021	R^2=0.999 RMSE=0.010 SSE=0.037
Henderson and Pabis	R^2=0.990 RMSE=0.030 SSE=0.157	R^2=0.985 RMSE=0.033 SSE=0.120	R^2=0.929 RMSE=0.054 SSE=0.100	R^2=0.998 RMSE=0.010 SSE=0.045
Logarithmic	R^2=0.992 RMSE=0.025 SSE=0.109	R^2=0.993 RMSE=0.023 SSE=0.057	R^2=0.999 RMSE=0.001 SSE=0.006	R^2=0.999 RMSE=0.006 SSE=0.020
Approximation of Diffusion	R^2=0.991 RMSE=0.027 SSE=0.128	R^2=0.985 RMSE=0.033 SSE=0.114	R^2=0.999 RMSE=0.007 SSE=0.001	R^2=0.998 RMSE=0.009 SSE=0.045
Wang and Singh	R^2=0.979 RMSE=0.040 SSE=0.302	R^2=0.955 RMSE=0.057 SSE=0.351	R^2=0.958 RMSE=0.042 SSE=0.056	R^2=0.995 RMSE=0.017 SSE=0.133
Midilli et al.	R^2=0.997 RMSE=0.016 SSE=0.038	R^2=0.997 RMSE=0.018 SSE=0.033	R^2=0.999 RMSE=0.004 SSE=0	R^2=0.999 RMSE=0.006 SSE=0.016

B.4.2 Microwave bulk scale drying (BSMD)

Table B.8: Statistics of applied thin-layer models to untreated and pretreated grapes at 0.25 W/g initial power ratio and 60°C convective air temperature using non-linear regression analysis.

Model	Untreated	Steam Blanched	Dipped
Lewis	R^2=0.973 RMSE=0.050 SSE=0.046	R^2=0.999 RMSE=0.008 SSE=0.001	R^2=0.97 RMSE=0.047 SSE=0.047
Page	R^2=0.999 RMSE=0.008 SSE=0.001	R^2=0.999 RMSE=0.006 SSE=0.000	R^2=0.996 RMSE=0.020 SSE=0.008
Henderson and Pabis	R^2=0.985 RMSE=0.038 SSE=0.024	R^2=0.999 RMSE=0.007 SSE=0.000	R^2=0.983 RMSE=0.040 SSE=0.033
Logarithmic	R^2=0.997 RMSE=0.016 SSE=0.004	R^2=0.999 RMSE=0.007 SSE=0.000	R^2=0.998 RMSE=0.012 SSE=0.002
Approximation of Diffusion	R^2=0.994 RMSE=0.022 SSE=0.008	R^2=0.999 RMSE=0.006 SSE=0.000	R^2=0.998 RMSE=0.013 SSE=0.003
Wang and Singh	R^2=0.996 RMSE=0.018 SSE=0.005	R^2=0.983 RMSE=0.038 SSE=0.019	R^2=0.999 RMSE=0.009 SSE=0.001
Midilli et al.	R^2=0.999 RMSE=0.006 SSE=0.000	R^2=0.999 RMSE=0.007 SSE=0.000	R^2=0.998 RMSE=0.011 SSE=0.002

Table B.9: Statistics of applied thin-layer models to selected BSMD using non-linear regression analysis.

Model	1W/g constant at 60°C	0.5 W/g constant at 60°C	0.5 W/g initial at 50°C	0.5 W/g initial at 60°C
Lewis	R^2=0.959 RMSE=0.056 SSE=0.054	R^2=0.991 RMSE=0.030 SSE=0.017	R^2=0.956 RMSE=0.066 SSE=0.091	R^2=0.942 RMSE=0.081 SSE=0.100
Page	R^2=0.985 RMSE=0.034 SSE=0.019	R^2=0.998 RMSE=0.013 SSE=0.003	R^2=0.998 RMSE=0.014 SSE=0.004	R^2=0.998 RMSE=0.012 SSE=0.002
Henderson and Pabis	R^2=0.963 RMSE=0.054 SSE=0.047	R^2=0.995 RMSE=0.021 SSE=0.008	R^2=0.971 RMSE=0.053 SSE=0.057	R^2=0.961 RMSE=0.066 SSE=0.062
Logarithmic	R^2=0.996 RMSE=0.017 SSE=0.004	R^2=0.996 RMSE=0.019 SSE=0.006	R^2=0.996 RMSE=0.019 SSE=0.007	R^2=0.992 RMSE=0.030 SSE=0.011
Approximation of Diffusion	R^2=0.996 RMSE=0.016 SSE=0.004	R^2=0.992 RMSE=0.028 SSE=0.014	R^2=0.979 RMSE=0.045 SSE=0.038	R^2=0.982 RMSE=0.045 SSE=0.024
Wang and Singh	R^2=0.930 RMSE=0.074 SSE=0.089	R^2=0.998 RMSE=0.012 SSE=0.002	R^2=0.994 RMSE=0.022 SSE=0.010	R^2=0.989 RMSE=0.035 SSE=0.017
Midilli et al.	R^2=0.994 RMSE=0.021 SSE=0.006	R^2=0.998 RMSE=0.012 SSE=0.002	R^2=0.999 RMSE=0.009 SSE=0.001	R^2=0.998 RMSE=0.011 SSE=0.001

C. COLOR KINETICS

C.1 High Hydrostatic Pressure Processing of Grapes

Table C.1: Statistics of Fitting of Fractional Conversion Equation Using Non-Linear Regression Analysis

Constants		**Pressure Level (MPa)**					
		300			**600**		
		Holding time (min)					
		10	*20*	*30*	*10*	*20*	*30*
ΔE	R^2	0.763	0.783	0.767	0.877	0.795	0.787
	SSE	0.181	0.169	0.187	0.107	0.162	0.166
	RMSE	0.123	0.118	0.125	0.094	0.116	0.117
Chroma	R^2	0.799	0.794	0.985	0.943	0.943	0.877
	SSE	0.160	0.167	0.016	0.056	0.054	0.107
	RMSE	0.116	0.118	0.037	0.068	0.067	0.094
b*	R^2	0.831	0.843	0.981	0.964	0.943	0.907
	SSE	0.138	0.132	0.021	0.038	0.055	0.084
	RMSE	0.107	0.105	0.042	0.056	0.068	0.084

C.2 Steam Blanching of Grapes

Table C.2: Statistics of Fitting of Fractional Conversion Equation Using Non-Linear Regression Analysis

Constants		**Blanching Temperature (°C)**		
		80	*90*	*100*
ΔE	R^2	0.983	0.961	0.969
	SSE	0.020	0.051	0.040
	RMSE	0.044	0.071	0.063
Chroma	R^2	0.978	0.961	0.959
	SSE	0.027	0.051	0.055
	RMSE	0.052	0.071	0.074
b*	R^2	0.978	0.960	0.958
	SSE	0.027	0.052	0.056
	RMSE	0.052	0.072	0.075

C.3 Dipping of Grapes

Table C.3: Non-linear regression coefficients of fractional conversion equation to selected color values.

Constants		**Temperature**					
		40°C			**50°C**		
		Holding time (min)					
		1	*2*	*3*	*1*	*2*	*3*
ΔE	C_f	60.25	56.73	57.99	63.98	56.41	60.23
	k_c (h^{-1})	-0.11	-0.10	-0.10	-0.10	-0.12	-0.14
Chroma	C_0	51.33	48.86	48.12	51.02	49.19	49.41
	C_f	13.29	12.83	12.38	10.03	13.66	11.33
	k_c (h^{-1})	-0.10	-0.09	-0.10	-0.10	-0.12	-0.15
b*	C_0	49.05	46.18	46.13	48.35	46.49	46.51
	C_f	12.05	11.91	11.34	9.27	12.40	10.41
	k_c (h^{-1})	-0.10	-0.09	-0.10	-0.10	-0.12	-0.14

Table C.4: Statistics of Fitting of Fractional Conversion Equation Using Non-Linear Regression Analysis

Constants		**Temperature**					
		30°C			**60°C**		
		Holding time (min)					
		1	*2*	*3*	*1*	*2*	*3*
ΔE	R^2	0.935	0.957	0.950	0.944	0.984	0.988
	SSE	0.144	0.102	0.119	0.126	0.027	0.017
	RMSE	0.089	0.075	0.083	0.089	0.042	0.034
Chroma	R^2	0.873	0.961	0.944	0.951	0.992	0.982
	SSE	0.358	0.092	0.143	0.109	0.013	0.024
	RMSE	0.141	0.071	0.091	0.082	0.029	0.040
b*	R^2	0.850	0.951	0.930	0.942	0.985	0.986
	SSE	0.459	0.124	0.192	0.137	0.024	0.019
	RMSE	0.160	0.083	0.106	0.093	0.040	0.036

Table C.5: Statistics of Fitting of Fractional Conversion Equation Using Non-Linear Regression Analysis

Constants		**Temperature**					
		40°C			**50°C**		
		Holding time (min)					
		1	*2*	*3*	*1*	*2*	*3*
ΔE	R^2	0.956	0.972	0.946	0.958	0.943	0.949
	SSE	0.094	0.050	0.118	0.099	0.149	0.112
	RMSE	0.074	0.054	0.089	0.074	0.094	0.087
Chroma	R^2	0.962	0.979	0.948	0.964	0.947	0.956
	SSE	0.080	0.039	0.114	0.086	0.139	0.096
	RMSE	0.069	0.048	0.087	0.069	0.090	0.079
b*	R^2	0.951	0.974	0.931	0.951	0.928	0.944
	SSE	0.114	0.053	0.163	0.125	0.202	0.125
	RMSE	0.081	0.056	0.104	0.083	0.109	0.091

Table C.6: Visual Color Change of Grapes According to NBS Names

Temperature / time	**60 seconds**	**120 seconds**	**180 seconds**
30°C	Brownish gray	Grayish brown	Grayish brown
40°C	Grayish brown	Grayish yellowish brown	Grayish yellowish brown
50°C	Dark grayish yellowish brown	Grayish brown	Grayish yellowish brown
60°C	Dark grayish yellowish brown	Moderate brown	Light brown

D. TEMPERATURE PROFILES

D.1 Microwave

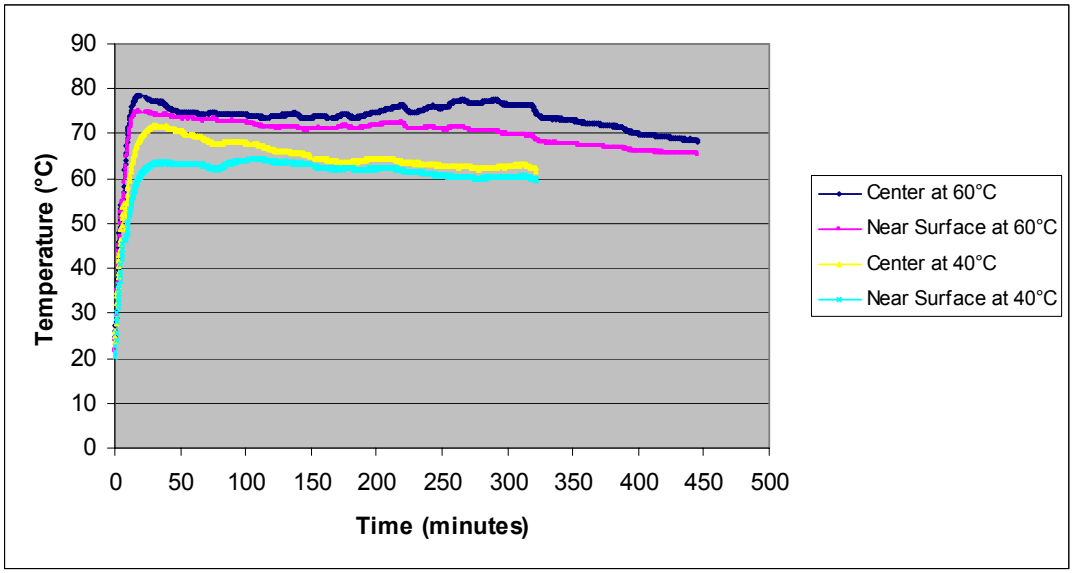

Figure D.1: Temperature Profiles at Center and Near Surface during 0.5 W/g Constant Power Ratio Drying of Grapes.

E. CALCULATIONS PROCEDURES IN SIMULATION

E.1 Convective Drying of Untreated Grapes

T_{air}=60°C, v_{air}=1.8 m/s
$T_{surface}$=29°C
D_{grape}=20 mm = 20×10^{-3} m

Film temperature of air was calculated as follows:

$$T_f = \frac{T_{air} + T_{surface}}{2} = \frac{60+29}{2} = 44.5°C$$

Properties of air at 44.5°C:

ρ=1.1140 kg/m^3
C_p=1006.8 J/kg°C
μ=1.926×10^{-5} kg/ms
k=0.0275 W/m·°C
Pr=0.7041

$$\mathrm{Re} = \frac{\rho \cdot v \cdot D}{\mu} = \frac{1.1140\left(\frac{kg}{m^3}\right)\cdot 1.8\left(\frac{m}{s}\right)\cdot 20\cdot10^{-3}(m)}{1.926\cdot10^{-5}\left(\frac{kg}{ms}\right)} = 2082.242$$

$Nu=C\cdot Re^m\cdot Pr^n$
For 40<Re<4000 m=0.466, n=1/3 and C=0.683 (Çengel, 1998)

$$Nu = \frac{h\cdot D}{k} = 0.683\,\mathrm{Re}^{0.466}\cdot \mathrm{Pr}^{1/3}\,(\text{Çengel},1998)$$

$$\frac{h\cdot 20\cdot10^{-3}(m)}{0.0275\left(\frac{W}{m°\cdot C}\right)} = 0.683\cdot(2082.242)^{0.466}(0.7041)^{1/3}$$

$$h = 29.401\,W/m^2\cdot°C$$

If Churchill and Bernstein equation was used to calculate Nusselt number h would be equal to 31.909 W/m^2·°C

E.2 Convective Drying of Steam Blanched Grapes

The change of moisture ratio with time is defined in Logarithmic model as:

$$MR = \frac{M(t) - Me}{M_0 - M_e} = a \cdot e^{-k \cdot t} + c \quad \textbf{(E.1)}$$

Taking the time derivative of equation (E.1) and replacing M(t) with $m_w(t)/m_s$ where $m_w(t)$ is the water content of grape with respect to time and m_s is the solid mass content gives:

$$\frac{dm_w(t)}{dt} = -a \cdot k \cdot e^{-k \cdot t} \cdot (M_0 - M_e) \cdot m_s \quad \textbf{(E.2)}$$

Both $m_w(t)$ and m_s were in kilogram units. The value of coefficient a and k was 0.9771 and 0.3952 (1/h), respectively. The R^2 of fitting was 0.998 and SSE and RMSE was 0.0017 and 0.0097.

The length of the grape was L=28.60 mm and diameter D=19.63 mm. With cylinder approximation the initial volume was calculated as $8.655.10^{-6}$ m^3.

The average initial radius of dried steam blanched grapes (subscript e is used) was 18.0 mm. The view area of grapes was known and this data was used to calculate average initial length assuming that the 2-D top view of grapes could be approximated to view of an ellipsoid. It was assumed that average length did not change during drying. Then time dependent radius of grapes thus time-dependent area was found by fitting the area data to a second degree polynomial with a regression coefficient of 0.99:

$$A_e(t) = 4 \cdot 10^{-6} t^2 - 5 \cdot 10^{-5} t + 0.0003 \ (m^2) \quad \textbf{(E.3)}$$

Enthalpy of vaporization of water vapor at 40°C is h_{fg}=2406000 J/kg°C.

Evaporative heat loss was calculated as follows:

$$\dot{Q}_{evaporation} = \frac{\left|\frac{dm_w(t)}{dt}\right| \cdot h_{fg}}{V_0 \cdot \frac{A_e(t)}{A_{0,e}}} \left(\frac{W}{m^3}\right) \quad \textbf{(E.4)}$$

Convective Heating at the boundary was calculated as follows:

T_{air}=60°C, v_{air}=1.8 m/s
$T_{surface}$=25.37°C
D_{grape}=19.63 mm = 19.63×10^{-3} m

$$T_f = \frac{T_{air} + T_{surface}}{2} = \frac{60 + 25.37}{2} = 42.69°C$$

Properties of air at 42.69°C:

ρ=1.1205 kg/m^3
C_p=1006.7 J/kg°C
μ=1.91×10^{-5} kg/ms
k=0.0274 W/m·°C
Pr=0.704

$$\mathrm{Re} = \frac{\rho \cdot v \cdot D}{\mu} = \frac{1.1205\left(\frac{kg}{m^3}\right) \cdot 1.8\left(\frac{m}{s}\right) \cdot 19.63 \cdot 10^{-3}(m)}{1.91 \cdot 10^{-5}\left(\frac{kg}{m \cdot s}\right)} = 2072.86$$

$Nu=C\cdot Re^m\cdot Pr^n$

For 40<Re<4000 m=0.466, n=1/3 and C=0.683 (Çengel, 1998)

$$Nu = \frac{h \cdot D}{k} = 0.683\,\mathrm{Re}^{0.466} \cdot \mathrm{Pr}^{1/3} \text{ (Çengel, 1998)}$$

$$\frac{h \cdot 19.63 \cdot 10^{-3}(m)}{0.0274\left(\frac{W}{m° \cdot C}\right)} = 0.683 \cdot (2072.86)^{0.466}(0.704)^{1/3}$$

$$h = 29.782\,W/m^2 \cdot °C$$

E.3 Steam Blanching of Grapes

Heat of vaporization at 100°C is $h_{fg}=2257\times10^3$ J/kg°C
Density of vapor at 100°C is $\rho_v=0.60$ kg/m^3
Diameter of grape subjected to steam was D=19.6 mm
Surface temperature of grape was initially $T_s=25$°C
Steam temperature was $T_{steam}=100$°C.

$$Tf = \frac{T_{steam} + T_s}{2} = 62.5°C$$

Properties of water at 62.5°C:

$\rho_l=981.94$ kg/m^3
$C_{pl}=4180$ J/kg°C
$\mu_l=4.525\times10^{-4}$ kg/ms
$k_l=0.656$ W/m·°C
$Pr_l=2.883$
Modified heat of vaporization is (Çengel, 1998):

$$h_{fg}^* = h_{fg} + 0.68 \cdot C_{pl} \cdot (T_{steam} - T_s) = 2257 \cdot 10^3 \left(\frac{J}{kg°C}\right) + 0.68 \cdot 4180 \left(\frac{J}{kg°C}\right) \cdot (100-25)°C$$

$$h_{fg}^* = 2470 \cdot 10^3 \left(\frac{J}{kg°C}\right)$$

It was assumed that filmwise condensation occurred during steam blanching of grapes. Thus for horizontal cylinders the following formula was used (Çengel, 1998):

$$h_{horizontal} = 0.729 \cdot \left[\frac{g \cdot \rho_l \cdot (\rho_l - \rho_v) \cdot h_{fg}^* \cdot k_l^3}{\mu_l \cdot (T_{steam} - T_s) \cdot D}\right]$$

$$h_{horizontal} = 0.729 \cdot \left[\frac{9.81\left(\frac{m}{s^2}\right) \cdot 981.94\left(\frac{kg}{m^3}\right) \cdot (981.94-0.60)\left(\frac{kg}{m^3}\right) \cdot 2470 \cdot 10^3 \left(\frac{J}{kg}\right) \cdot 0.656\left(\frac{W}{m \cdot °C}\right)}{4.525 \cdot 10^{-4}\left(\frac{kg}{m \cdot s}\right) \cdot (100-25)°C \cdot 19.6 \cdot 10^{-3}(m)}\right]$$

$$h_{horizontal} = 7272.42\left(\frac{W}{m^2 \cdot °C}\right)$$

E.4 Microwave-assisted Drying of Grapes

Diameter of grape was D=20.62 mm
Length of grape was L=28.5 mm
With cylinder approximation volume of grape was $V_{grape}=9.517.10^{-6}$ m^3
Predictive equations for dielectric properties of fruits and vegetables at 2450 MHz is given as follows (Delgado et al., 2006):

$$\varepsilon' = 2.14 - 0.104 \cdot T + 0.808 \cdot X_w$$
$$\varepsilon'' = 3.09 - 0.0638 \cdot T + 0.213 \cdot X_w \quad \textbf{(E.5)}$$

where ε' and ε" is dielectric constant and dielectric loss factor, respectively, T is temperature (°C) and X_w is the percentage of moisture in wet basis. The initial moisture content of grapes was 77.6%.

The root mean square electric field was calculated using equation (E.6) (Metaxas and Meredith, 1988) :

$$E_{rms} = \left(\frac{\rho \cdot Cp \cdot (T - T_0)/t}{0.556 \cdot 10^{-10} \cdot f \cdot \varepsilon''} \right)^{1/2} \left(\frac{V}{m} \right) \quad \textbf{(E.6)}$$

where f was 2450.10^6 Hz and ρ and C_p was calculated using equation (3.1) and (3.2). Initial temperature of grape was T_0=29.4°C and temperature after 10 minutes, T, rised to 52.4°C. Until 10 minutes the heating of grapes was approximately isothermal hence T in equation (E.6) was equal to the temperature of 10 minutes heating. ε" was calculated using equation (E.5) assuming that the temperature had negligible effect on the value of dielectric loss factor in the heating rate of this study. Using equation (E.6), E_{rms} was found to be 250.09 (V/m).

It was assumed that the electric field within the grape had an average value different than that of E_{rms} thus the average electric field value within the grape was calculated using the integral average:

$$E_{average} = \frac{\int_0^{D/2} E_{\max} \cdot e^{-\alpha z}}{\frac{D}{2} - 0} = \frac{\int_0^{D/2} E_{rms} \cdot e^{-\alpha z}}{\frac{D}{2} - 0} \quad \textbf{(E.7)}$$

where D was the diameter of grape, α is the attenuation factor and z is the distance which electromagnetic wave traveled. Attenuation factor can be found using equation **(2.10)**. Using equation **(E.7)** average electric field was found 194.07 V/m.

The change of moisture ratio with time is defined in Lewis model as:

$$MR = \frac{M(t) - Me}{M_0 - M_e} = e^{-k \cdot t} \quad \textbf{(E.8)}$$

Taking the time derivative of equation (E.8) and replacing M(t) with $m_w(t)/m_s$ where $m_w(t)$ is the water content of grape with respect to time and m_s is the solid mass content gives:

$$\frac{dm_w(t)}{dt} = -k \cdot e^{-k \cdot t} \cdot (M_0 - M_e) \cdot m_s \quad \textbf{(E.9)}$$

Thus the change of moisture percentage with time was:

$$\frac{dX_w}{dt} = \frac{m_{w,i} - \left|\frac{dm_w(t)}{dt}\right|}{m_i - \left|\frac{dm_w(t)}{dt}\right|} \times 100 \quad \textbf{(E.10)}$$

where m_i and $m_{w,i}$ was the initial weight of grape and initial weight of moisture, respectively.

Replacing the right part of equation (2.12) with the known values yields:

$$P_{abs} = 1092.87 \cdot \frac{dX_w}{dt} \quad \textbf{(E.11)}$$

Boundary Condition:

T_{air}=60°C, v_{air}=1.9 m/s
$T_{surface}$=27.5°C

Film temperature of air was calculated as follows:

$$T_f = \frac{T_{air} + T_{surface}}{2} = \frac{60 + 27.5}{2} = 43.75°C$$

Properties of air at 43.75°C:

ρ=1.1160 kg/m^3
C_p=1006.81 J/kg·°C
μ=1.92×10^{-5} kg/m·s
k=0.0275 W/m·°C
Pr=0.7042

$$\mathrm{Re} = \frac{\rho \cdot v \cdot D}{\mu} = \frac{1.1160\left(\frac{kg}{m^3}\right) \cdot 1.9\left(\frac{m}{s}\right) \cdot 20.62 \cdot 10^{-3}(m)}{1.92 \cdot 10^{-5}\left(\frac{kg}{m \cdot s}\right)} = 2277.22$$

$Nu=C\cdot Re^m\cdot Pr^n$
For 40<Re<4000 m=0.466, n=1/3 and C=0.683 (Çengel, 1998)

$$Nu = \frac{h \cdot D}{k} = 0.683 \cdot \mathrm{Re}^{0.466} \cdot \mathrm{Pr}^{1/3} \text{(Çengel, 1998)}$$

$$\frac{h \cdot 20.62 \cdot 10^{-3}(m)}{0.0275\left(\frac{W}{m \cdot °C}\right)} = 0.683(2277.22)^{0.466}(0.7042)^{1/3}$$

$$h = 29.73\, W/m^2 \cdot °C$$

BACKGROUND

Gökhan BİNGÖL was born in 1975 in Adiyaman, Turkey. He graduated from Private Tercuman Middle and High School. In 1995, he enrolled to Istanbul Technical University Food Engineering Deparment's undergraduate program. In 1999 he registered to Istanbul Technical University Institute of Science and Technology, Food Engineering Program and was awarded with M.Sc. degree in 2001. Since then, he is a Ph.D. candidate and a Research Assistant at the same university. He joined several international and national conferences. This dissertation received an award from Istanbul Chamber of Industry in 2007.